Blood pressure variability in neonates : with a special focus on signal acquisition and signal processing

Blood Pressure Variability in Neonates

with a special focus on signal acquisition and signal processing

Wim de Jong

CIP-DATA LIBRARY TECHNISCHE UNIVERSITEIT EINDHOVEN

Jong, Wim de

Blood pressure variability in neonates : with a special focus on signal acquisition and signal processing / by Wim de Jong. – Eindhoven : Technische Universiteit Eindhoven, 2000. – Proefschrift. –
ISBN 90-386-0977-9
NUGI 743
Trefw.: klinische informatiesystemen / couveusekinderen / fysiologie / autonome zenuwstelsel
Subject headings: blood pressure / newborn infants / spectral analysis / autonomic nervous system.

Druk: Universiteitsdrukkerij TU Eindhoven
Omslag: Nena Mobach

Blood Pressure Variability in Neonates

with a special focus on signal acquisition and signal processing

PROEFSCHRIFT

ter verkrijging van de graad van
doctor aan de Technische
Universiteit Eindhoven, op gezag
van de Rector Magnificus, prof.dr.
M. Rem, voor een commissie
aangewezen door het College voor
Promoties in het openbaar te
verdedigen op woensdag 19 januari
2000 om 16.00 uur

door

Wim de Jong

geboren te Rotterdam

Dit proefschrift is goedgekeurd door de promotoren:

prof.dr.ir. P.F.F. Wijn
en
prof.dr.ir. K. Kopinga

Overige leden kerncommissie:

prof.dr. M.J.A. de Voigt,
prof.dr. G.W.J.M. Tangelder (VU-Amsterdam)

Overige leden promotiecommissie:

prof.dr. C. Blanco (AZ-Maastricht), onder voorbehoud
prof.dr.ir. K.H. Wesseling
prof.dr. M. van de Bor (AZN-St. Radboud)
prof.dr.ir. H.L. Vader
dr.ir. P.J.M. Cluitmans

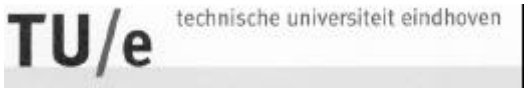

Dit proefschrift is tot stand gekomen binnen het samenwerkingsverband tussen het Sint Joseph Ziekenhuis Veldhoven en de Technische Universiteit Eindhoven. De uit- en afwerking heeft gedeeltelijk plaatsgevonden in het St. Elisabeth Ziekenhuis Tilburg.

Het in dit proefschrift beschreven onderzoek werd mede mogelijk gemaakt door de financiële steun van het Wetenschapsfonds van het Sint Joseph Ziekenhuis Veldhoven.

Contents

1. Introduction

In a neonatal intensive care unit, care is given to very ill neonates, most of whom are prematures. In the prognosis and treatment of such neonates, both lung and brain conditions play an important role. The treatment of immature lungs has been significantly improved by a routine use of surfactant. The assessment of the brain function remains an important issue.
The patients are continuously monitored. Treatment is evaluated using data recordings from the monitors (vital signs) and intermittently obtained values (blood gases, weight, and defecation). The vital signs, however, are often disturbed by movement artefacts and cannot be measured as easily as in adult intensive care conditions. The evaluation of the condition of the patient and his or her treatment needs a reliable vital signs data set and effective use of the small number of signals measured. A physiological-data acquisition system, capable of real-time artefact reduction and analysis, combining data, and archiving of the measurements, is necessary to optimise the information on the condition of the patient.
Such an acquisition system would allow - for example - the assessment of additional information present in the invasive arterial blood pressure signal. In this thesis a strategy to quantify the low frequency blood pressure components, related to lung mechanics, brain and nervous functions, will be described. Two applications, built on this strategy and made for use in neonatal practice, will be presented and evaluated.

In a neonatal intensive care unit (NICU), care is given to very ill neonates. More than 75% of them are hospitalised because they were born too early (prematures); others because of severe illnesses. The prematures often suffer from multi-organ failure, since several functions have not yet developed: respiration, cardiovascular regulation, temperature regulation and metabolism. Immediately after an early birth, the problems due to immaturity present themselves. For example, more than half of the children born after a gestation of less than 30 weeks need artificial ventilation in the first days of their lives, and all of them need the regulated temperature and humidity of an incubator. Long-term longitudinal follow-up studies have been set up to gain insight into the effects of treatment after years [Verlove-Vanhorick, Verwey, 1987; Ens-Dokkum, Schreuder, Veen, 1992]. The percentage of liveborn infants with a birthweight below 1500 g surviving without a major handicap has increased from about 20% in 1953 to 65% in 1983 [Verlove-Vanhorick, Verwey, 1987 and to about 80% in 1999 [Verlove-Vanhorick, in preparation]. Systematic evaluation of the treatment of these children led to the improved outcome in this "young" discipline. A large part of the increase of the survival of prematures can be attributed to the use of surfactant, which strongly enhances the gas exchange performance of the lungs. The development and a possible damage to the brain are other very important issues. In this thesis we focus on these issues, using signal analysis methods on the data available from routine neonatal care.

The treatment of a patient and its effectiveness can be evaluated, together with other information, by measuring several physiological factors:

- values that can be measured continuously or semi-continuously: the ECG-signal, heart rate, arterial blood pressure signal, systolic and diastolic blood pressures, respiratory signal, and arterial oxygen saturation;
- values available only intermittently: body weight, blood gas values, nutrition and defecation data.

In physiological measurements on neonates, noise and other disturbances (movements) often affect the signals and make them unreliable during those episodes [Cunningham et al, 1994]. If a signal is perturbed unintentionally, the effect of the perturbation on the signal is called an artefact. The cause may be an external action, such as washing a neonate, or may be a distortion inherent to the signal, such as the influence of the respiration on the arterial blood pressure. Most of the time, artefacts are undesirable. Furtheron in this thesis, ways will be presented to detect them and to filter them out.

In the case of adults admitted to an intensive care unit, many more parameters can be measured. More invasive lines can be brought in (especially measuring in the arteries and veins close to the heart), and blood samples can be taken more frequently than from neonates. In neonates, cardiovascular instability can occur rapidly due to the small blood volume. In addition, many measurements can be performed more accurately in adults than in neonates, because of the greater samples, the larger dimensions of the sensors, and the lower frequencies of the signals. The measurement of the fast neonatal signals, using equipment originally designed for use in adults, may give rise to problems [Hack et al., 1990; Gardner, 1981]. Also, adults tend to move less than neonates, resulting in fewer movement artefacts.

If more parameters could be measured continuously, and these would be less perturbed by (movement) artefacts, a better diagnosis could be made. Evaluation of the treatment could be based on a larger and more reliable set of data.

1.1 Development of an information system

In the past, much effort has been put into the development of patient monitors. These monitors are used for one patient at a time, and most of them are modular. The adult configurations had to be adapted for use with neonates, with respect to, for example:

- the range of the sensors for blood pressure;
- the bandwidth of the ECG measurements;
- the dimensions of transcutaneous sensors;
- the dimension of the cuff for the Non Invasive Blood Pressure (NIBP) measurement.

Furthermore, the algorithms used by the patient monitors had to be adapted to neonatal signals: varying faster and having a range different from adult signals.

In principle, the monitors treat every signal individually and do not correlate the information in different signals, although these signals often will have mutual dependencies. The movement artefacts, which often occur in neonates, could probably be recognised by correlating different signals. In this way, false alarms could be avoided. For example, an alarm caused by an apnoea could be treated more accurately if the respiratory information was adequately evaluated in combination with the information in the ECG signal. Vendors of monitor systems are considering to improve their systems in this way[Hewlett Packard, 1994 (2x)].

The following types of systems are commercially available:
- stand-alone monitors, if required connected to a network for central monitoring. The network is often vendor specific.
- patient data management systems (PDMS);
  The vendors put much effort in the development of PDMS systems, in which data-acquisition facilities are present, but also a large amount of the other (non-measurement) patient information is put together. Opportunities for further analysis on measured signals, using these systems, are minimal.
- small data-acquisition systems, often PCs with a data-acquisition board, enabling the measurement of all signals from one bed at the same time.

A problem is that the exchange of measurement data requires a lot of effort. Many of the monitors only output their signals to a dedicated network, which does not interface to standard computer systems or systems from another vendor. In some cases, an interface between such a network and an RS232 serial line is available, but it does not allow the transfer of a sufficient amount of data. Only recently have monitors become available of which the output can be connected to a network according to standard protocols. The export of signals is now much easier.

At the Eindhoven University of Technology, a modular measurement system has been developed, which can be connected to many instruments and measurement set-ups. It was built for real-time acquisition, processing and analysis of huge amounts of measurement data; parallel to that the system can be used to run the measurement set-up. Although it was not developed for use in a medical environment, in scientific research involving large amounts of data its flexibility and scalability may offer significant advantages. In our experimental set-up, the system is used to perform the real-time data-acquisition of the analog and digital information from the patient's monitors. Its flexibility and scalability enable us to apply fast digital filters to the incoming signals and to extend the number of channels (if required).

1.2 Focus on blood pressure

The invasive blood pressure signal is an interesting and complex result of a number of physiological variables. Apart from the blood pressure values generally used in the clinical setting, i.e., the systolic and diastolic blood pressures, the blood pressure

signal contains a lot of information. On one hand it is contained in the shape of the blood pressure waveform, when plotted against time: it reflects the contraction of the heart in relation to the elasticity of the vessels and the peripheral resistance [Gevers, 1994; O'Rourke, 1990]. On the other hand it consists of the slow fluctuations in the signal as a whole that result from physiological processes in the body: the so-called low frequency (LF) waves. A description of the physiological background of the blood pressure signal and the variations in it will be given in chapter 2. We will focus in more detail on the low frequency variations, since these offer the opportunity to evaluate the function of a part of the nervous system, without making additional measurements.

The blood pressure signal contains lower frequencies belonging to one of the following classes (see figure 1-1):

1. Originating from pressure fluctuations in the thorax caused by the respiration (>0.2 Hz), the so-called Traube-Hering waves [Mayer, 1876, Kaminski, 1970]; it is also thought, that these may originate from a change in venous reflux due to a change in intrathoracic pressure.
2. Originating from changes in the vascular system, caused by a feedback of the blood pressure at a number of places in the body (baroreceptors), through the autonomic nervous system. One part of this system, the sympathetic, works only slowly (in seconds); the other part, the parasympathetic, is able to feedback within a second (for example, to the heart). After a sudden drop in blood pressure, for instance, the parasympathetic feedback induces the next heartbeat to be earlier (0.05 - 1.5 Hz).
3. Originating from changes in the peripheral resistance (0.05 - 0.2 Hz); these changes are driven by the sympathetic part of the autonomic nervous system.
4. Caused by the temperature regulation of the body (0.01 - 0.05 Hz) [Lossius, 1994].

Basically, these variations can be seen as artefacts which disturb an adequate measurement of the desired systolic and diastolic pressures [Ellis, 1985]. On the other hand, knowledge about the origin of the variations in the blood pressure signal might be of interest.

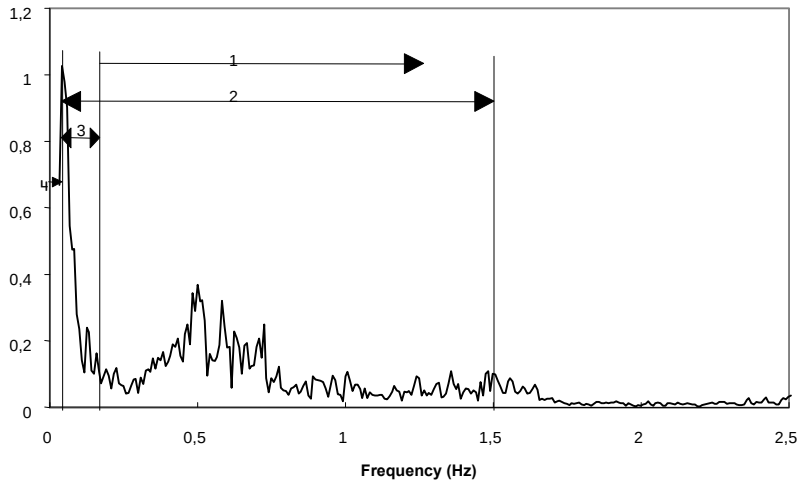

Figure 1-1 The amplitude spectrum of the systolic arterial blood pressure values in a 2 min recording. Around 0.5 Hz the influence of the respiration on the blood pressure can be seen and below 0.2 Hz influences of the nervous system cause an increase of the amplitude. The numbers correspond to the frequency intervals explained in the text. The mean heartrate was 2.16 Hz, so the amplitudes above 1.08 Hz should not be considered as reliable. They were calculated using oversampling of the systolic values (for further explanation see chapter 5).

Low frequency variations of the blood pressure have been extensively investigated in animals [Bertinieri et al., 1988]. For human adults [Parati et al., 1988], the investigations primarily focus on heartrate fluctuations instead of blood pressure fluctuations. Given the invasive character of the blood pressure measurement this is clear. With respect to neonates only a few investigations have been made, most of them being theoretically oriented and focused on the heartrate variability calculation methods [Appel et al., 1993; Baselli et al., 1988]. Investigations using neonatal invasive arterial blood pressure measurements have been performed when a clinical indication existed; they often discuss the relation between intra-ventricular haemorrhage (IVH) and fluctuations in the blood pressure, caused by (artificial) ventilation [Goldstein R, Brazy JE, 1990; Miall-Allen VMM, Vries de LS et al. 1989; Perlman JM, McMenamin JB et al. 1983; Pryts, Greisen, 1989]. Investigations based on large neonatal data sets are not yet available.

Generally, Fourier analysis, parametric methods, or time domain indices are used in the quantification of blood pressure fluctuations. The comparison of results is easiest - in principle - and most straightforward using Fourier transformation. Nevertheless, the analysis can be performed in many different ways [Patel et al., 1965; Kay and Marple, 1981; Malliani et al., 1991; TenVoorde et al., 1994, Part 2]. Due to the limited

capacity of the available computer systems - and also for physiological reasons - one often chooses to use only systolic and/or diastolic pressures. Also, due to the heartrate fluctuations, the systolic or diastolic blood pressure cannot be sampled equidistantly in time [TenVoorde et al., 1994 (2x)]. The implications of this non-equidistant sampling of routine neonatal data have not yet been evaluated. Another problem, which often occurs in neonates, is that the respiratory frequency is higher than half of the heartrate [TenVoorde et al., 1990]. In that case, aliasing of respiratory signal frequency components may occur, since only one blood pressure value per heartbeat is available.

A commonly validated quantification technique of the low-frequency fluctuations is still lacking. Particularly the effects of aliasing, non-linear effects in the interaction between respiration and blood pressure, and the large processing power needed for a real-time analysis are problems that have to be dealt with before an automatic analysis can be implemented [Jaffe, Fung, 1994].

1.3 Objectives

One of the objectives of our project was the development of a physiological-data acquisition and analysis system. It was motivated by the lack of opportunities to perform fast, real-time, additional analysis on signals measured on neonates. For neonates, only a limited number of parameters is available, so it is desirable to use the available signals as optimally as possible. To be able to evaluate a broad group of patients in an accurate way, it is highly desirable to develop and implement a system with which:

- data from the patient monitors and other bedside equipment can be acquired and analysed in real-time;
- the data can be used afterwards (off-line) for the evaluation of treatment and for scientific research;
- the relevant data can be archived properly;
- data exchange with other systems, used for the other patient information (PDMS-systems), is easy.

It is obvious that the system should have a user-friendly interface, since it will be used by physicians, nurses, physicists, and other researchers.

The second objective was, along with the set up of a data-acquisition system as a tool, to evaluate if a combination of the information from the different available signals will result in additional information. The application should be in the field of artefact reduction and improvement of the interpretation of the measurements (e.g., at what moment an apnoea really started).

The third objective was to work out a method of quantification of the blood pressure energy present in frequency bands below the heartrate frequency.

Quantitative information about low frequency variations in the blood pressure could result in a deeper understanding of the mechanics of breathing and of the activity of the sympathetic and parasympathetic nervous system [Malliani et al., 1994; Gupta et al., 1990; Miyakawa et al., 1984; Koepchen et al., 1984].
Although this information is related to the organs that cause most problems in prematures, this information is - unfortunately - normally not available at the bedside of the patient.

1.4 Outline

In chapter 2 some physiological background is given about the neural mechanisms of the cardiovascular system.
In chapter 3, we describe the development of the physiological-data acquisition system used for the data collection at the NICU of the St. Joseph Hospital, Veldhoven. The measurement and the analysis of the signals from the bedside monitors will be addressed in chapter 4.
In chapter 5, strategies will be presented with which the low-frequency activity in the blood pressure can be quantitatively evaluated, together with some representative examples.
Chapter 6 illustrates the application of the system and the strategies of chapter 5 by two examples of applications in clinical practice:

- continuously available spectral estimates
- a first quantification of the relationship between blood pressure variations and heartrate variations.

The general conclusions and discussion are presented in chapter 7.

Literature

Appel ML, Saul JP, Berger RD, Cohen RJ; Closed-loop identification of blood pressure variability mechanisms; Blood pressure and heart rate variability:68-75, 1993

Baselli G, Cerutti S, Civardi S, Malliani A, Pagani M; Cardiovascular variability signals: towards the identification of a closed-loop model of the neural control mechanisms; IEEE Trans Biomed Eng 35:1033-1045, 1988

Bertinieri G, Di Rienzo M, Cavallazzi A, Ferrari AU, Pedotti A, Mancia G; Evaluation of baroreceptor reflex by blood pressure monitoring in unanesthetized cats; Am J Physiol 254:H377-H383, 1988

Cunningham S, McIntosh AGS, N McIntosh; The practical management of artifact in computerized physiological data; Int J Clin Monit Comput 11:211-216, 1994

Ellis DM; Interpretation of beat-to-beat blood pressure values in the presence of ventilatory changes; J Clin Monit 1:65-70, 1985

Ens-Dokkum M, Schreuder A, Veen S; Outcome at five years of age in very preterm and very low birthweight infants in The Netherlands, results from the nationwide collaborative follow-up study: POPS 1983; Proefschrift Rijksuniversiteit Leiden, 1992

Gardner RM; Direct blood pressure measurement - dynamic response requirements; Anesthesiology 54:227-236, 1981

Gevers M; Arterial pressure wave forms in newborn infants, invasive measurements in clinical practice, Proefschrift Vrije Universiteit Amsterdam, 1994

Goldstein R, Brazy JE; Fluctuations of arterial blood pressure decrease with mechanical ventilation in premature infants with respiratory distress syndrome; J Perinatol 10:267-271, 1990

Gupta SK, Wagener JS, Erenberg A; Pulmonary mechanics in healthy term neonates:variability in measurements obtained with a computerized system; J Pediatr 117:603-606, 1990

Hack WWM, Westerhof N, Leenhoven T, Okker A; Accurate measurement of intraarterial pressure through radial artery catheters in neonates; J Clin Monit 6:211-216, 1990

Hewlett Packard; Automatic respiration monitoring algorithm; Palo Alto: Hewlett Packard, 1984

Hewlett Packard; The new respiration algorithm; Palo Alto: Hewlett Packard, 1984

Jaffe RS, Fung DL; Constructing a heart-rate variability analysis system; J Clin Monit 10:45-58, 1994

Kaminski RJ, Meyer GA, Winter DL; Sympathetic unit activity associated with Mayer waves in the spinal dog; Am J Physiol, 219:1768-1771, 1970

Kay SM, Marple SL; Spectrum Analysis - a modern perspective; Proc IEEE, 69:1380-1419, 1981

Koepchen HP; History of studies and concepts of blood pressure waves; In: Miyakawa K, Koepchen HP, Polosa C, (ed.) Mechanisms of blood pressure waves Tokyo/Berlin; Japan Sc Soc Press, 1984; 3-23

Lossius K, Eriksen M, Walloe; Thermoregulatory fluctuations in heart rate and blood pressure in humans:effect of cooling and parasympathetic blockade; J Auton Nerv Syst 37:245-254, 1994

Malliani A, Pagani M, Lombardi F, Cerutti S; Cardiovascular neural regulation explored in the frequency domain; Circulation 84:482-492, 1991

Malliani A, Lombardi F, Pagani M; Power spectrum analysis of heart rate variability: a tool to explore neural regulatory mechanisms; Br Heart J 71:1-2, 1994

Mayer S; Studien zur physiologie des Herzens und der Blutgefässe. Uber spontane Blutdruckschwankungen; Sitzungsberichte der Kaiserlichen Akademie der Wissenschaften. Mathematisch-Naturwissenschaftliche Classe 74:281-307 1876

Miall-Allen VMM, Vries de LS, Dubowitz S, Whitelaw AGL; Blood pressure fluctuation and intraventricular hemorrhage in the preterm infant of less than 31 weeks gestation; Pediatrics 83:657-661, 1989

Miyakawa K, Koepchen HP, Polosa C; Mechanisms of blood pressure waves; Springer-Verlag; Berlin etc.:85-117, 1984

O'Rourke M; Arterial stiffness, systolic blood pressure, and logical treatment of arterial hypertension; Hypertension 15:339-347, 1990

Parati G, Di Rienzo M, Bertinieri G, Pomidossi G, Casadei R, Groppelli A et al.; Evaluation of the baroreceptor-heart rate reflex by 24-hour intra-arterial blood pressure monitoring in humans; Hypertension 12:214-222, 1988

Patel DJ, Mason DT, Ross J, Braunwald E; Harmonic analysis of pressure pulses obtained from the heart and great vessels of man; Am Heart J 69:785-794, 1965

Perlman JM, McMenamin JB, Volpe JJ; Fluctuating cerebral blood flow velocity in respiratory distress syndrome: relation to the development of intraventricular hemorrhage; N Engl J Med 309:204-209, 1983

Pryds O, Greisen G, Lou H, Friis-Hansen B; Heterogeneity of cerebral vasoreactivity in preterm infants supported by mechanical ventilation; J Pediatr 115:638-645, 1989

TenVoorde BJ, Faes ThJC, Rompelman O; Spectra of data sampled at frequency-modulated rates in application to cardiovascular signals: Part 1. Analytical derivation of the spectra; Med Biol Eng Comput 32:63-70, 1994

TenVoorde BJ, Faes ThJC, Rompelman O; Spectra of data sampled at frequency-modulated rates in application to cardiovascular signals: Part 2. Evaluation of Fourier transform algorithms; Med Biol Eng Comput 32:71-76, 1994

TenVoorde BJ, Ree ER, Hack WWM, Bergschneider VM, Hoekstra BPT, Faes TJC et al.; Spectral quantification of respiratory sinus arrhythmia in preterm and fullterm neonates:beyond half the mean haert rate; Automedica 13:15-31, 1990

Verloove-Vanhorick SP, Verwey, RA; Project On Preterm and Small for gestational age infants in The Netherlands 1983 (POPS), a collaborative survey; Proefschrift Rijksuniversiteit Leiden, 1987

2. Physiology

The origin of the blood pressure signal, and the variations on it, can be found in the physiology of the cardiovascular system. The understanding of basic physiological interactions is necessary to be able to develop those derivated parameters with clinical importance. In this chapter we focus on the interactions in which the nervous system is involved; the humoral influence is not a part of the investigations. The nervous system can be divided into the voluntary nervous system and the involuntary nervous system, also called the autonomic nervous system. The latter again consists of 2 parts, generally responsible for an opposite effect: the sympathetic and the parasympathetic system. They are essential in the regulation of the blood pressure: the sympathetic system influences the heart contractility, heart frequency, and peripheral blood vessel constriction, while the parasympathetic system influences the heart frequency almost directly. The neural interaction is driven by baroreceptors at several locations in the cardiovascular system and by the activity of the central respiratory centre. Apart from the neural respiratory influences, a direct interaction exists which results from intrathoracic pressure variations related to the respiration.

2.1 The nervous system

The nervous system can be divided in the central nervous system (CNS) and the peripheral nervous system. The central nervous system consists of the brain, the brainstem and the spinal cord. The peripheral nervous system consists of afferent nerves, which transmit information from the receptors to the CNS, and efferent nerves, which transmit information from the CNS to smooth muscles, the heart muscle, skeletal muscles and glands. A schematic overview of the central nervous system is shown in figure 2-1.

The nervous sytem can also be divided in the voluntary and involuntary nervous sytem. The voluntary system takes care of the interaction of the body with the environment. The involuntary nervous system, also called the autonomic nervous system is involved in the innervation of the heart, the glands and the blood vessels: in short, the visceral system. It is involved in the maintenance of general homeostasis. The autonomic nervous sytem consists of two opposite working parts: the parasympathetic and the sympathetic nervous system. Almost all autonomiccally innervated organs are innervated by both systems. The peripheral blood vessels and the adrenal and sweat glands, however, are only innervated by the sympathetic system.

2.1.1 Parasympathetic and sympathetic nervous system

The parasympathetic nerves are located in the brain stem and in the sacral part of the vertebral column, also called the craniosacral part, see figure 2-2. An important parasympathetic nerve, the nervus vagus, leaves from the brain stem. It innervates, among others, the heart, the lungs, and the stomach. The nerves from the sacral part drive the bladder, the genitals, and lower intestines.

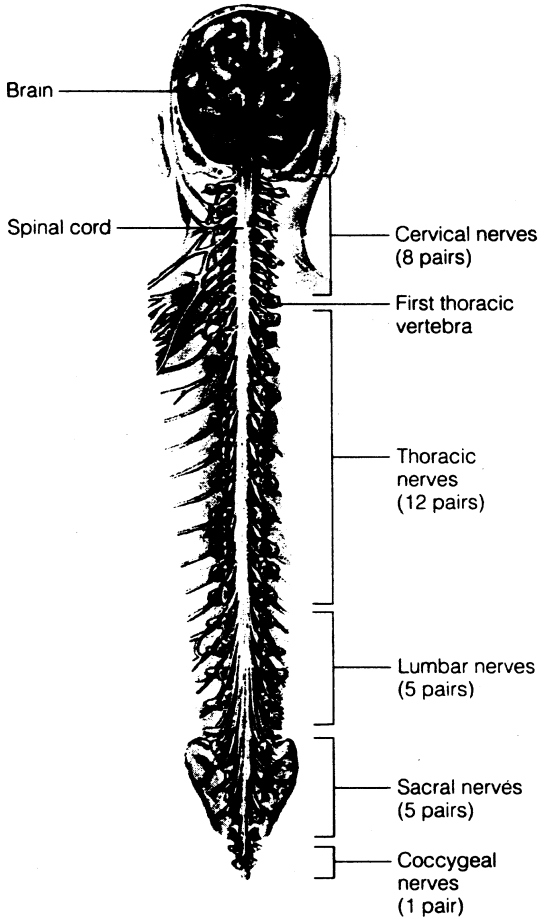

Figure 2-1 Schematic overview of the central nervous system [from Kalat JW, Biological Psychology 104].

The sympathetic nerves are situated in the thoracolumbar part of the autonomic nervous system. The nerves for head and neck start from the upper thoracal segments. The nerves in the thoracal as well as the lumbal part innervate the organs in the breast and abdomen. Table I illustrates the influence of parasympathetic resp. sympathetic system on some organs. An action potential is transferred from one nerve to another nerve through a synapse. Such a transfer takes place in clusters of nervous cells, ganglia. As figure 2-2 shows there is a clear difference between the sympathetic and the parasympathetic nervous system. In contrast to the sympathetic nervous system, in the parasympathetic nervous system the ganglia are located close to the effector organs. In the sympathetic part they lay close to the spinal cord. The sympathetic part forms a network, in contrast to the parasympathetic that goes directly to the organs to be innervated. The parasympathetic system works within several tenth of a second, while the sympathetic system works only after several seconds. [Eckert and Randall, 1983]

organ	***sympathetic effect***	***parasympathetic effect***
heart	acceleration	retardation
arterioles	constriction	generally no effect
bronchi	dilatation	constriction
iris	pupil dilatation	pupil narrowing
bladder	relaxation	contraction

Table 2-1 Some typical effects of sympathetic and parasympathetic nerves on various organs.

2.2 Cardiovascular regulation

The task of the cardiovascular system is proper regulation of the blood flow to all organs and tissues. The necessary blood flow depends on the need for oxygen and nutrition of the specific organs. During physical stress, for example, the blood supply of the active muscles will strongly increase. In that circumstance the heart will have to

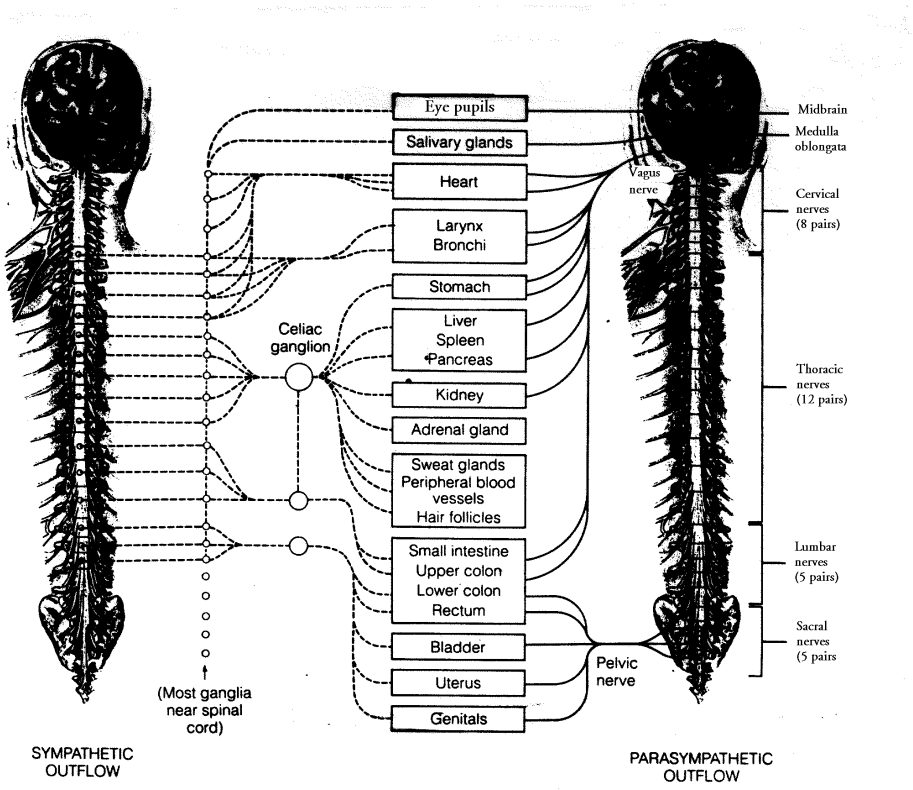

Figure 2-2 Schematic overview of the autonomic nervous system [From: Kalat JW, Biological Psychology].

pump through more blood per minute, and a constriction of the arterioles in the peripheral tissues will occur to increase the peripheral resistance and maintain the level of the arterial blood pressure. In the regulation of the blood flow a large number of neural, chemical and humoral factors is involved. Apart from these, the cardiovascular system is influenced by the respiratory activity. On one hand it consists of a direct influence of the vasomotor centre by the respiratory centre, on the other hand by intrathoracic pressure fluctuations due to the respiration.

2.2.1 Inventory of interactions involving the cardiovascular system

Blood pressure variations are caused by several different effects. These effects can be subdivided in direct pressure components, neural components and circulatory components. A scheme of the cardiovascular interactions known in adults is shown in figure 2-3. First, we will point out the relevant information and assumptions about each of the relations. To what extent the interactions hold in neonates is not yet clear. Qualitatively, they may apply as well, but it is likely that they will quantitatively differ from the adult interactions.

Overview of interactions [West, 1990; Shepherd and Shepherd, 1992; Kandel and Schwartz, 1982; Ravenswaay-Arts, 1993]:

1:
Sympathetic vasomotor action, central origin, modulated by central respiratory activity. It influences peripheral resistance, muscle tone of other vessels
Increase symp. tone => constriction of the vessels t = 6 to 10 s

2:
Sympathetic activity, central origin, modulated by central respiratory effort, efferent to the SA-node.
Increase symp. tone => increase in heartrate t = 6 to 10 s
In adults the respiratory influence on heartrate exists at low respiratory frequencies (approximately < 0.2 Hz)

3:
Parasympathetic activity (vagal), central origin, modulated by central respiratory effort, efferent to the SA-node.
Increase para. tone => decrease in heartrate t = 0.2 to 0.4 s (influence may sustain)

4:
The respiratory centre activates the intercostal muscles and diaphragm muscles to elevate the breast and thus induces intrathoracal pressure changes. In case of spontaneous ventilation a negative intrathoracic pressure causes inflow of air, a positive pressure causes the outflow. In case of artificial ventilation distension of the lungs is normally caused by the positive pressure of the machine instead of negative pressure.
Spontaneous inspiration => pressure decrease
Artificial insufflation => pressure increase t = 0.05 s or less (direct)

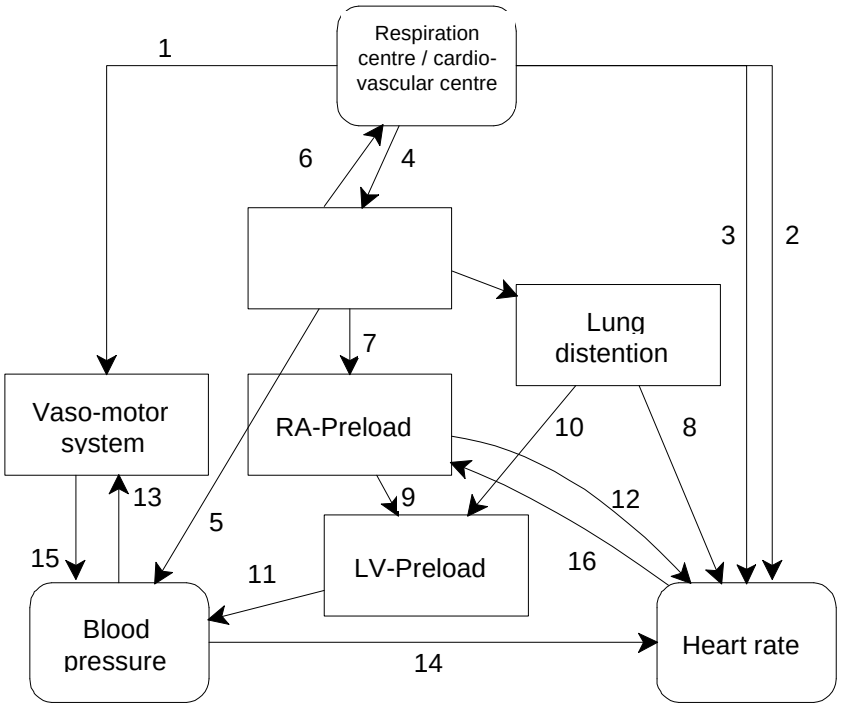

Figure 2-3 An overview of the intractions between blood pressure, respiration and heartrate. RA = right atrium; LV = left ventricle; SA = sinoatrial.

1: Sympathetic activity from central respiratory origin;
2: Sympathetic activity from central respiratory origin efferent to the SA-node;
3: Parasympathetic activity from central respiratory origin efferent to the SA-node;
4: Respiratory effort causes intrathoracic pressure changes;
5: A part of the intrathoracic pressure changes is transmitted directly to the arterial system;
6: Hering-Breuer reflex;
7: The venous return is modulated by the intrathoracic pressure fluctuations;
8: Stretch receptors vagally modulate the heart rate;
9: Preload changes move from right to left;
10: Squeezing out of the lungs at expiration;
11: Higher LV-preload yields a higher blood pressure;
12: Bainbridge reflex;
13: Sympathetic influence on the vaso-motor system;
14: Baroreceptor reflex;
15: Vaso-motor state drives sympathetic influence on blood pressure;
16: The heart rate determines the filling time of the atrium, and thus the preload.
For further explanation see text.

5:
Part of the pressure under 4 is transmitted to the arterial system, especially in the thorax. This influence is still present in the arterial wave form in the periphery. The direct component of intrathoracic pressure change has an almost instantaneous influence on blood pressure (5, see figure 2-3). A part of the intrathoracic pressure is mediated to the arterial system. This influence may depend on the actual part of the heart cycle. A difference in mediation of the pressure depending on the compliance of the artery is likely. Consequently it will differ between systolic phase and diastolic phase.
Increase thoracic pressure => increase BP t = 0.05 s or less

6:
Extension of stretch receptors in the lungs inhibits inspiratory effort. Vagally mediated and called Hering-Breuer reflex [West 1990].
During shallow respiration the frequency is not affected. During inspiration with a large tidal volume, the frequency may be decreased. t = 0.1 s

7:
Pressure fluctuations in the thorax modulate the venous return.
Spontaneous inspiration => decrease in intrathoracic pressure => increase in venous return
t = 0.4 s

8:
Lung and thoracic wall stretch receptors vagally modulate heartrate. It is assumed this only gives a marginal contribution [Ravenswaay-Arts, 1993].
Extension of the stretch receptors => increase heartrate t = 0.1 s

9:
Change in venous preload causes a change in right ventricular (RV) output to the lungs.
Right atrium (RA) preload increase => RV output increase => left ventricular (LV) preload increase
at the heartbeat

10:
Squeezing out the lung circulation on expiration yields an increase in LV preload
t = 0.1 s from expriation

11:
LV preload changes cause a change in cardiac output (given a constant heartbeat).
Increase in LV preload => increase in cardiac output and contractility => increase in BP (if vasomotor state remains unchanged).
from venous return increase: t = 0.4 s
from squeezing out of the lungs: t = 0.1 s

12:
Bainbridge reflex: vagally mediated
Increased filling of the atria => increase in heartrate the coming heartbeat

13:
Sympathetic influence on the vasomotor system (or the sympathico-vagal balance).
Sympathetic increase => constriction of the vessels
t = ≈ 6 s

14:
Baroreceptor reflex: stretch receptors in the aortic arch and carotids
Increase in BP => decrease in heartrate

t = 0.3 s (vagally)

15:
Vasomotor state determines the resistance and compliance of the vascular system (sympathetic); strong influence on BP.
Increased symp. irradiation => increase of BP (constriction of the vessels)

t > 6 s

t > ≈ 6 s (sympathetically)

16:
The heartrate determines the filling time of the atria.
Heartrate increase => shorter filling time => decrease in RA preload.

coming heartbeat

2.2.2 Influences on the blood pressure

Figure 2-3 shows that three items act directly on arterial blood pressure:
a) the intrathoracic pressure variations (5) (the numbers between parentheses refer to figure 2-3)
b) the LV-preload (11)
c) the vasomotor system (15 in figure 2-3)

All three are indirectly affected by the respiratory activity, either spontaneous or artificial. The influence of a) and b) takes place at the respiratory frequency. The influence of c) acts slower because of the time constant of the neural pathway involved (sympathetic nervous system). The heartrate influences the LV-preload indirectly, regulating the ventricle filling time (16). In more detail the relations can be explained as follows:

– Part of the intrathoracic pressure variations is transduced to the adjacent tissues and organs. The pressure variations decrease when the point of measurement is further from the lungs. Due to the compliant nature of many parts of the body, the pressure has been reduced gradually due to an increase of the surrounding volume. In the thoracic region, however, many of the pressure variations still exist and are superimposed on all organs, including the cardiovascular system. This leads directly to a variation in the blood pressure signal level. In the central venous pressure this pressure variation can also be recognised. The pressure transduction is almost instantaneous, so in relation to the extension of the lungs no significant delay will be present. If the inspiration is spontaneous, a pressure decrease will take place; in case of artificial ventilation with positive pressure ventilation, a pressure increase will take place.

- The second influence on the blood pressure is due to the change in venous return when the intrathoracic pressure changes (7,9). During inspiration the intrathoracic pressure decreases, increasing the venous return. This higher RA-preload leads to a higher blood flow through the lungs, a higher LV-preload and thus a higher cardiac output. Due to the increased cardiac output the blood pressure will increase. The whole process will take about 2 heartbeats. Normally there are two stabilising counter-influences on the increase of venous return during inspiration. The first one consists of the increase of the heartrate, causing the higher RV volume to be pumped out earlier (12). The second one consists of the squeezing out of blood from the lungs during expiration (10). If expiration follows one heartbeat after inspiration, the LV-preload is being increased extra, by delay due to the increased venous return, and due to the squeezing out of blood from the lungs. So, depending on the respiratory frequency different increasing and decreasing effects on blood pressure might be observed. Changes in heartrate will affect the LV-preload because of variations in the ventricle filling time. Apart from the mechanism described above the heartrate will variate due to the so-called Respiratory Sinus Arrythmia (RSA): parallel to phrenic nerve activity (respiration) the parasympathetic irradiation of the SA-node is being inhibited, leading to an increase in heart rate (3, respiratory sinus arrhythmia, RSA, t = 0.1 s after start of inspiration). It still is a matter of debate whether this mechanism exists, and, if so, whether it primarily causes RSA. Another contributor to the RSA is the baroreceptor reflex: the aortic arch and stretch receptors in the carotid sini reflect pressure changes through vagal as well as sympathetic pathways (14); an increase in pressure results in a higher vagal activity to the sinus node, prolonging the current heart interval. The sympathetic influence is opposite and slower (scale of seconds) and only plays a role below the respiratory frequency.
- Thirdly, the blood pressure is influenced by the vasomotor system. This system regulates the peripheral resistance and muscle tone of the vessels. The respiration modulates the vasomotor system sympathetically. The low-pass character of the sympathetic activity only leads to an averaged respiratory influence on the vasomotor system. The averaged variations that result on blood pressure are called Breath Amplitude Sinus Arrhythmia (BASA). This influence becomes important at the respiratory frequency itself when it drops to approximately 0.2 Hz or less (within the bandwidth of the sympathetic nervous system), which is very unlikely in neonates. A back-regulation also exists from the blood pressure to the vasomotor system (13). It is also sympathetically mediated. We conclude that due to the integrative effect only the average respiration frequency influences blood pressure by variation of the vasomotor characteristics. An influence on blood pressure in neonates can thus be expected due to breath amplitude variations at the lower frequencies. The closed circuit 13,15 may result in oscillatory changes, the so-called Mayer waves [Mayer, 1876].

Literature

Eckert R, Randall DJ; Animal Physiology; New York: WH Freeman and Company, 1983

Kalat JW; Biological Psychology, 1990

Kandel ER, Schwartz JH; Principles of neural science, New York ; Amsterdam :Elsevier, 1982

Mayer S; Studien zur physiologie des Herzens und der Blutgefässe. Über spontane Blutdruckschwankungen; Sitzungsberichte der Kaiserlichen Akademie der Wissenschaften. Mathematisch-Naturwissenschaftliche Classe 74:281-307 1876

Ravenswaay-Arts van CMA; Heart rate variability: Physiology and clinical applicability in very preterm infants; Proefschrift Nijmegen, 1993

Shepherd RFJ, Shepherd JT; Control of blood pressure and the circulation in man; In: Autonomic Failure, Bannister R and Mathias CJ(ed.), Oxford University Press, 1992

West JB; Best and Taylor's physiological basis of medical practice, 12th ed.; Baltimore: Williams & Wilkins; 1990

3. Data acquisition system

A physiological information system is required, capable of acquisition of all data from the patient s monitors, processing and analysis of that data, and providing a user friendly output of the results. The set up and the development of the system are described.

3.1 data acquisition system requirements

A system is required that is capable of acquisition and processing of all data from the patient's monitors and other relevant devices, to yield a defined result which is accessible in a user friendly way. The system has to be suitable for scientific research, medical research, evaluation of treatments, and eventually better monitoring.

The system should be able to acquire the following types of data:
- automatically obtained data:
    - parameter values from the patient monitor: heart rate, blood pressure values, respiratory rate, peripheral arterial saturation, etc.;
    - signals from the patient monitor: sampled signals;
    - RS232 or otherwise interfaced: connection with other medical devices.
- manually obtained data: logging of treatment times, blood gas values, scores;

The system should be able to process the acquired data:
- data correction: correct for artefacts and distortions of the data, use also information from other types of data;
- processing: statistics, correlations;
- reduction: only keep the relevant information, delete raw signals after the extraction of parameters.

The results should be presented in a user friendly way:

- graphic display of the data as a function of time;
- conversion to other software packages (word processing, advanced statistics, spreadsheets);
- printing facilities;
- access to the results from several locations (local area network).

3.2 set up of the measurement system

The set up of the system is described by consecutively considering the acquisition, processing, analysis, display, and administration part. Generally, the acquisition is performed without interfering with the treatment of the patient, using the monitor information available for routine care. Processing and analysis are performed on a dedicated system and on PCs connected to a local area network (LAN). The display and administration are provided by PCs connected to the LAN.

3.2.1 acquisition

The information to be acquired belongs to one of the following classes:

- automatically obtained data:
  - parameter values from the patient monitor: heart rate, blood pressure values, respiratory rate, peripheral arterial saturation, etc.; these consist of values updated every one or two seconds;
  - signals from the patient monitor: sampled signals; the required sample frequency lies between 100 and 500 Hz, depending on the frequency content of the signal;
  - RS232 or otherwise interfaced: connection with other medical devices; the data flow is limited to about 3000 values (8-bit) per second (in addition, about 35 % of the transmission capacity is needed for overhead);
- manually obtained data: logging of treatment times, blood gas values, scores; the update is limited to several times an hour for practical reasons.

patient's monitor

Because of the choice for a system that has to perform 24 hours a day and interferes as less as possible with clinical practice, it was decided to take the signals of the patient's monitors as input signals. At our NICU Hewlett Packard Merlin monitors (HP, Böblingen, Germany), HP M1166A, model 56s are used. The monitor system consists of a module rack, click-in modules, a computer module, a monitor screen, an analog output interface, and a connection with an HP Serial Distribution Network (SDN). A signal needed for monitoring can be obtained by plugging in one of the available signal modules in the module rack (see figure 3-1).

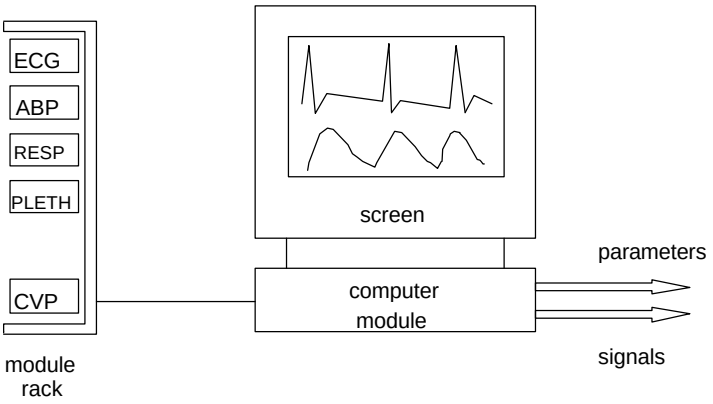

Figure 3-1 Modular patient monitoring system.

Commonly used modules are: ECG/RESP (ECG and thoracic impedance respiration signal, see below), PLETH (photo plethysmogram), IBP (invasive blood pressure), NIBP (non invasive blood pressure), CVP (central venous pressure), and FiO_2 (fraction of inspired oxygen). The modules perform the acquisition of the signals (125 Hz, ECG 500 Hz) and realise galvanic separation to ensure the patient's safety. The sampled information from the modules is aggregated in the computer module, where further analysis for the patient monitoring is performed. At first, the signals are filtered, analysed, and individually screened on errors, i.e., without use of the information from the other signals. Parameters are derived from the signals, e.g., the respiratory rate (RR) from the RESP signal, the systolic, diastolic, and mean blood pressure from the IBP signal, the oxygen saturation from the photo plethysmography signal, etc. The parameters are shown on the monitor screen and are updated every 2 seconds. A moving average of several seconds is taken to avoid excessive fluctuations. All communication in the computer module occurs via the internal Message Passing Bus. The analog output module and SDN also obtain their information from the Message Passing Bus. The analog output module supplies a maximum of eight user-defined signals or parameters. Their precision is 12 bit. D/A-conversion in this module occurs at 500 Hz, followed by a 150 Hz third order low-pass filter.

connections

Two main connections transport the signals and/or parameters to our measurement system: an analog connection and a digital connection. The analog connection takes care of all signals measured by the patient's monitor and occasionally some additional signals. Most of these signals are issued by the analog output card and are transported by a 40 m shielded twisted pair cable to the data acquisition system. The digital connection is only used to acquire the parameters calculated by the monitors. All

monitors write their parameters to the SDN. A Careport interface (HP) enables us to pick them from the SDN by an RS232 communication protocol. The maximum baudrate of 38k4 bit/s (4k8 bytes/s) is sufficient for the parameter information, which is refreshed on the network every second. A PC is used because the Careport interface cannot be easily read out by the data acquisition system "PhyDAS". This is due to a lack of handshake facilities, which would result in an unacceptably large software overhead on the PhyDAS system. On the other hand, the use of the SDN for the acquisition of signals is strongly hampered by the Careport transfer speed. (figure 3-2).

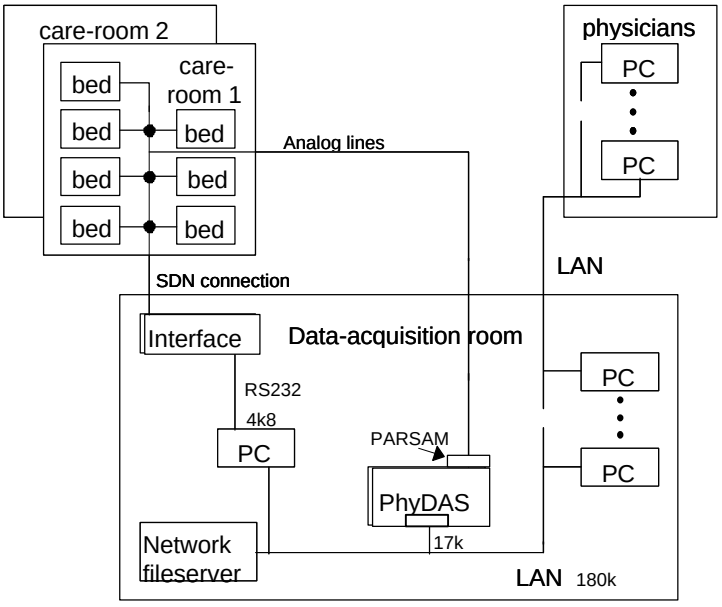

Figure 3-2 The configuration of the data acquisition system. Parameter values of all beds are sampled continuously through the SDN and careport interface by a PC and are put on the LAN. Signals of selected beds are transported to the PARSAMs in the data acquisition system, sampled by the PhyDAS system, and put on the LAN. Further analysis and visualisation is performed on PCs connected to the LAN. The maximum throughputs are given in bytes per second (the electronics notation 4k8 means 4800).

PhyDAS

All analog signals are linked to the Physics Data Acquisition System (PhyDAS). PhyDAS has been developed at the faculty of Physics of the Eindhoven University of Technology as a basic system that can be used in a wide variety of experiments. It contains everything necessary to control an experiment. The basic idea underlying this system is the separation of the computer bus and the measurement bus containing the interfaces, and the possibility for the individual interfaces to communicate without computer intervention. The system is optimised for real-time applications and allows the use of multiple processors. We use one processor (Motorola 68030) with 4 MB RAM (extendable up to 64 MB) and an interface to the LAN. Several dedicated parallel samplers (PARSAMs) are used for the sampling of the signals. Each PARSAM autonomously samples 16 signals, and every 3 seconds the acquired signals are transferred to the LAN. The parallel samplers are set to a sample frequency of 400 Hz for the ECG signal and 100 Hz for the other signals. The throughput capacity of the computer memory is 2 Mbyte/s, from the memory to the LAN it is 17 kbyte/s.

A chosen subset of the available signals can be connected to the PARSAMs. In the near future digital signal processors will become available, that can be coupled directly to the PARSAMs. In that case direct processing of the signals offers the possibility to perform real-time statistics or filtering of the results (moving average, moving cross correlations, ARMA-filter implementations, waveform detection by templates) and a possibility for real-time reduction of the signals (e.g., by calculating the amplitude of the principal components). The processing will be performed at the front end, thereby freeing the computer bus from the data flow of the raw signals.

PC network

As shown in figure 3-2 the interface to the user is provided by a LAN. It is a Novell Ethernet LAN with PCs connected to it at convenient locations in the neonatal department. The capacity of the LAN, although 2 Mbyte/s (including overhead), in our case is limited by the speed of the fileserver to about 180 kbyte/s. A throughput of 48 signals at 500 Hz, however, only requires a capacity of 48 kbyte/s.

parameter values on the PC network

The parameter values computed by the monitors are continuously read from the SDN network by an additional programmable interface (Careport). The communication with this interface occurs according to an RS232 protocol at a maximum throughput of 38.4 kbit/s, enough for the transmission of all parameter values of all beds (16) at 1 Hz, but insufficient for an additional transmission of signals.

throughput requirements

For a given number of parameters and signals (both are 2 byte values) to be simultaneously measured, analysed, and stored, we can calculate the required average data throughput of the whole system:

- The parameter values:

  The average throughput *t* depends on:

  b the number of beds attached to the system,
  n the available number of parameters/bed (average),
  c a correction factor due to the overhead (approx. 35%) of the RS232 protocol,

  and can be expressed by:

$$t = 2 \cdot b \cdot n \cdot c \quad byte / s$$

- The signals:

  The throughput *t* depends on:

  e the number of ECGs being measured
  n the number of other signals (blood pressure, respiration) being measured

$$t = 100 \cdot 2 \cdot (4e + n) \quad byte / s$$

Table 3-1 lists the results of the above equations, applied to several representative numbers of parameters and signals:

Required throughput (kbyte/s)	no parameters	5 parameters per bed	10 parameters per bed
4 ECG and 4 other signals	4.0	4.2	4.4
4 ECG and 8 other signals	4.8	5.0	5.2
8 ECG and 8 other signals	8.0	8.2	8.4
8 ECG and 16 other signals	9.6	9.8	10.0
16 ECG and 32 other signals	19.2	19.4	19.6

Table 3-1 The required throughput for several representative numbers of parameters and signals.

From the table it is clear that only a very small number of signals can be acquired using the RS232 connection of 4.8 kbyte/s (overhead inclusive). The situation with 1 ECG and 2 other signals of *all* beds (16) simultaneously needs a faster PhyDAS - LAN connection than the one available yet (17 kbyte/s). However, if adequate signal reduction can be performed *before* the transfer to the LAN (front-end processing), the throughput requirements can be adjusted downwards. If not, this connection limits

the number of signals that can be measured simultaneously. We will return to this point in section 3.3.

3.2.2 processing, analysis, and reduction

With processing we mean the additional operations continuously performed on the raw signals. These operations are meant to screen the signals on artefacts and determine statistics and intermediate results, ready to use for further off-line analysis. They also direct the information to the proper directory and file on the file server.

signals

The processing of the signals is performed on-line at PCs using the raw data that has been written to the file server. The capacity of a single PC is not sufficient to handle all the data. Therefore we developed a continuous processing cycle that can be performed at several network PCs and allows for distribution of the tasks (see figure 3-3). The signals are stored on the network drives without compression to avoid (time consuming) decompression during processing or display.

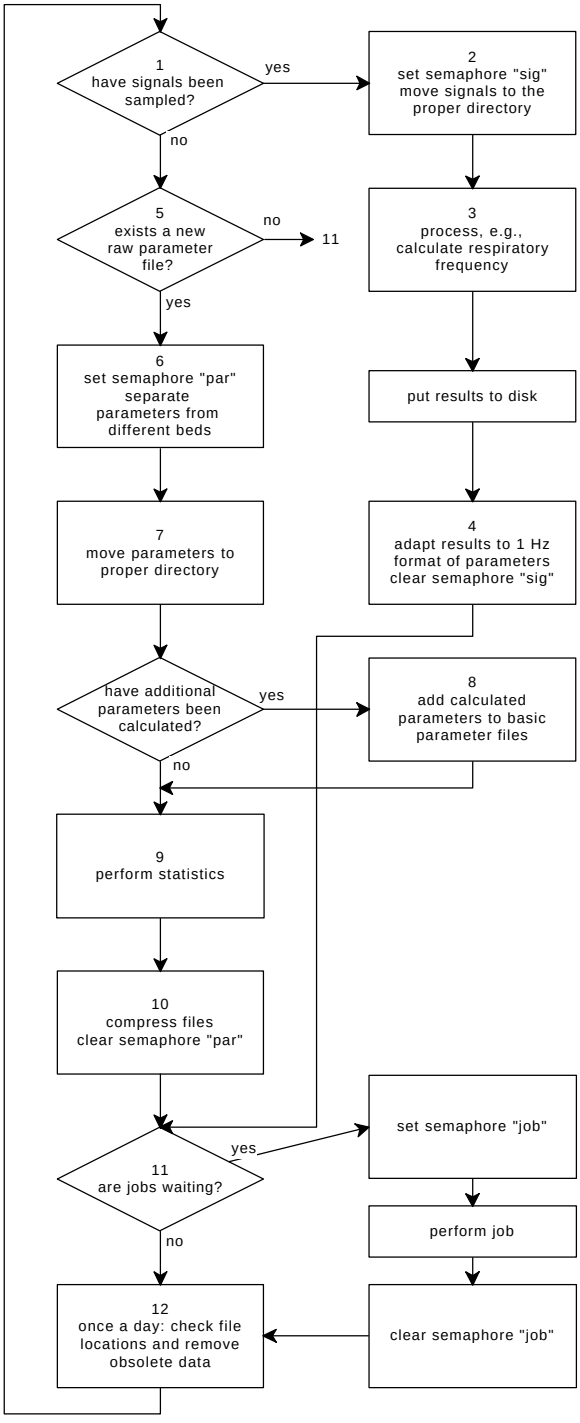
1
have signals been sampled?
yes
no
2
set semaphore "sig"
move signals to the proper directory
3
process, e.g., calculate respiratory frequency
put results to disk
4
adapt results to 1 Hz
format of parameters
clear semaphore "sig"
5
exists a new raw parameter file?
no
11
yes
6
set semaphore "par"
separate parameters from different beds
7
move parameters to proper directory
have additional parameters been calculated?
yes
no
8
add calculated parameters to basic parameter files
9
perform statistics
10
compress files
clear semaphore "par"
11
are jobs waiting?
yes
no
set semaphore "job"
perform job
clear semaphore "job"
12
once a day: check file locations and remove obsolete data

Figure 3-3 The continuous processing cycle. This cycle can be executed identically on an arbitrary number of PCs, allowing distribution of tasks and a more efficient use of available arithmetic capacity. The PC s are not synchronised; semaphores are used to prevent different PC s from starting the same jobs at the same time. 1: Determine whether signals have been sampled during the last 3 seconds: signals should be processed within several seconds at the most, so if the answer is yes, the acquired signals are immediately moved to a proper directory from which they can be accessed from everywhere at the network (2). Next, additional processing can be performed (3), which may result in additional parameters (raw parameter file , normally processed at 1Hz) (4). A semaphore sig in the central job directory is used to prevent other PC s from starting the same job at the same time. If no raw signal data are available (1), the processing cycle determines whether raw parameter value files have to be processed (5) (If so, a semaphore par is set to prevent other PC s from taking up the same job at the same time). They have to be split in files per patient (6); subsequently, they are moved to a proper directory from which they can be accessed from everywhere at the network (7). Next, if additional parameters have been calculated from the signals, they are integrated in the files containing the basic parameters (8). From every parameter series general descriptive statistics are calculated (9), after which the parameter files are compressed (10) (the semaphore par is cleared). A check on pending off-line jobs takes place (11); if they exist, a semaphore job is set, the job is performed, and the semaphore job is cleared. Finally, once a day, file locations are checked and obsolete data are removed from the network drive (12). Now the cycle starts again at 1.

Algorithms to detect certain events, e.g., a heartbeat or a respiration, are evaluated off-line, and are foreseen to run in real-time at the PhyDAS system in the near future. Artefact reduction methods, on the other hand, strongly depend on the information sought for and will therefore not yet be implemented as standard routines at the PhyDAS system. In the thoracic impedance signal, for example, the heartbeat can be seen as an artefact. However, the presence of the heartbeat in this signal can be used to detect an apnoea period. In the latter case the influence of the heartbeat no longer is an artefact but carries significant information.

An example of the processing defined above is the evaluation of the respiratory frequency. Of course, the bedside monitors deliver a respiratory frequency, but that values often are spoiled by artefacts, escpecially during periods of apnoea. A breath-by-breath respiratory frequency is calculated by comparing the heart rate derived from ECG with the instantaneous respiration rate derived from the thoracic impedance signal. The resulting breath-by-breath values can be converted to one value per second, ready to add to the other parameter values. Furtheron, in figure 3-5 and figure 3-6 (they will be discussed later), the resulting parameter values as a function of time are shown, compared with the original values acquired from the monitor.

parameter values

Every second a PC reads all actual parameter values (not being beat-to-beat values) from all monitors connected to the Serial Distribution Network. Every hour these

values are separated and written to different files, one for every patient. The information is compressed and moved to the patient's directory. From this information a PC running the continuous processing cycle automatically computes statistics over a period of 30 min (user defined interval length): # seconds with valid parameter values, mean, median, p16%, p84%, minimum and maximum value, # seconds above and below a user defined level. If the processing of the signals yielded breath-by-breath respiratory frequencies, these are added to the proper parameter files. The parameter values of one day (16 beds) take about 3 Mbytes disk space after reduction, using standard file compression software.

3.2.3 Display

signals

A visualisation of several signals simultaneously is possible on any PC connected to the network. The date and time of the start of the episode have to be given, after which a fast scrolling through the signals is possible. This visualisation is particularly useful for a manual check on artefacts. Besides, every job performs an additional check on artefacts by itself. In figure 3-4 a screen dump of the visualised signals is shown.

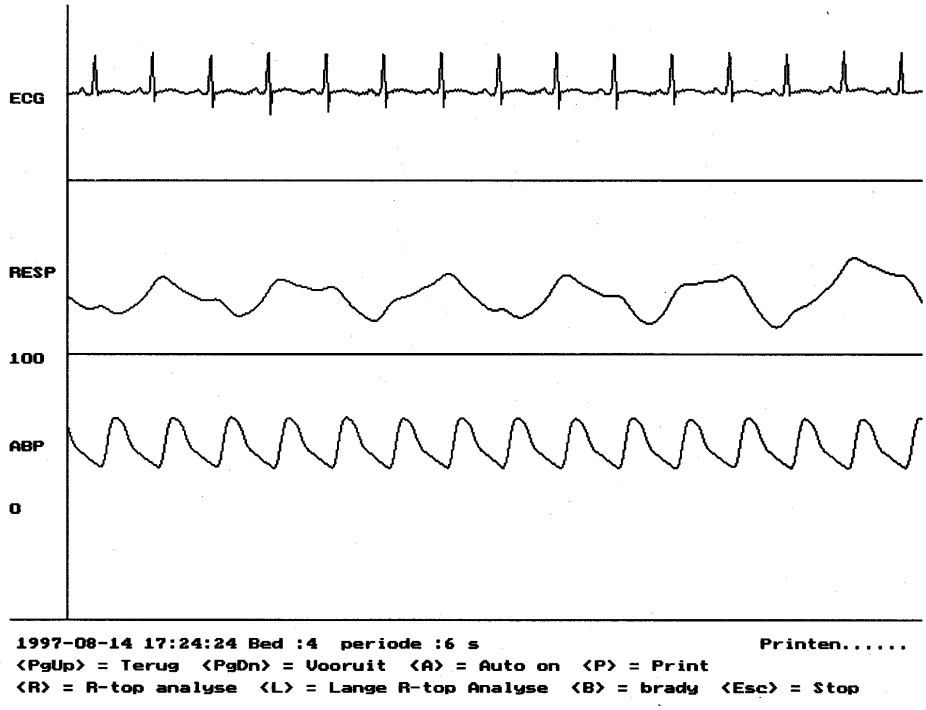

Figure 3-4 Visualisation of the waveforms of the ECG, respiratory signal, and the arterial blood pressure signal. The horizontal axis is 6 s (time scale can be chosen between 3 and 120 s). The fast horizontal scrolling capability allows a manual/visual check on artefacts.

parameter values

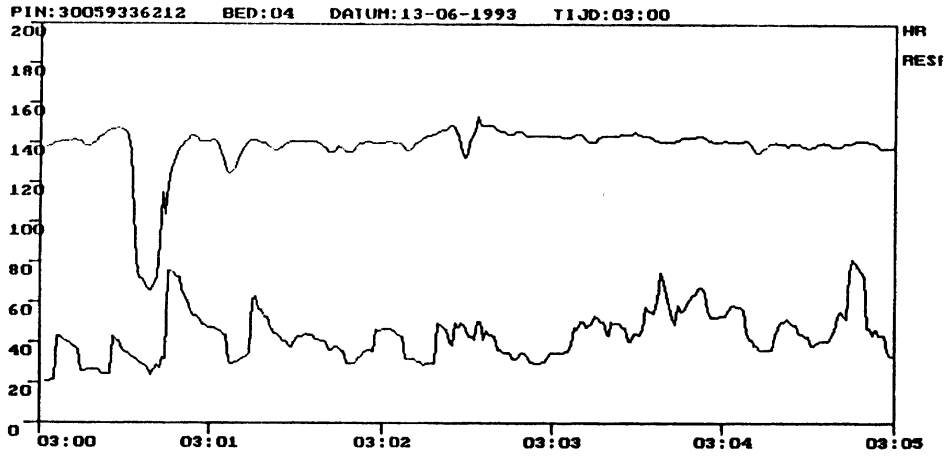

Figure 3-5 Display of 2 parameters (heartrate and respiratory frequency), as given by the monitor.

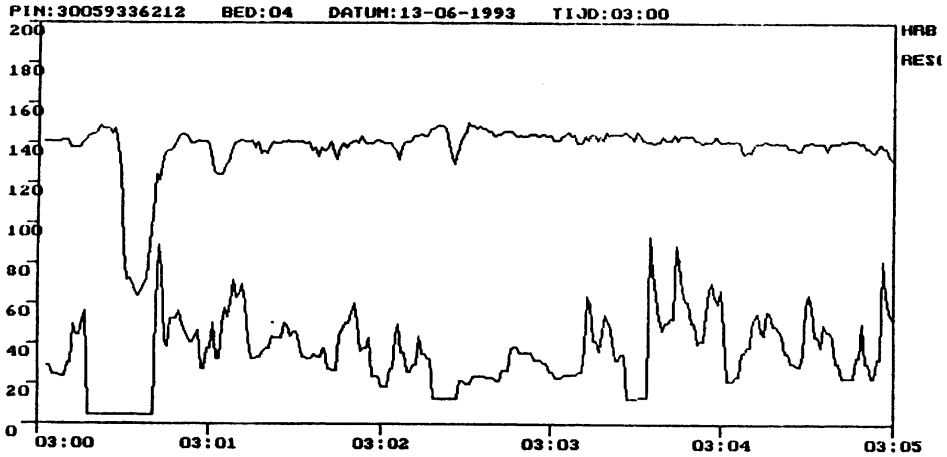

Figure 3-6 Display of the same episode as in figure 3-5, but now the heartrate and respiratory frequency were beat-to-beat (breath-by-breath) calculated and added to the available parameter data set.

A Turbo Pascal® program was developed to display and print parameter data of any patient admitted to the intensive care unit. In an example of the display facility (see figure 3-5 and figure 3-6) the effect of beat-to-beat analysis of two of the signals on the corresponding parameter values is shown. The user can select a patient and give

the episode of which the chosen parameters should be displayed as a function of time. The time axis range may be varied from 3 min up to 9 hour. All values can be converted to an ASCII or a spreadsheet file format.

The automatically generated files mentioned under parameter values in section 3.2.2 can be used to produce a summary of the parameters of a patient. They may be displayed interactively in a spreadsheet application. Macros lead the user to the desired graphs. The numerical values in the spreadsheet are available for dedicated (non-standard) analysis.

3.2.4 archiving and administration

The administration of the data is kept in a database, consisting of 2 sub-databases. One part contains the general patient data and the location of the monitor the patient was connected to, the other part contains project information. The data belonging to projects will be kept for future reference or additional analysis. All members of the research group can add projects to the database. Thereby, the corresponding data are given a special status: the project data are stored on magneto optical disks; data of recent projects are available on-line from the file server harddisk.

The parameter values of every patient admitted to the intensive care are available on the network up to 50 days after discharge. Only the values corresponding to days at which signals have been registered for projects, including one day before and after, are kept after expiration of the 50 day limit. For signal values roughly the same procedure holds: only those data registered as project data are kept. All other signals are deleted when they are 3 days old. The period for deletion of signal data is shorter than for parameter data because of the 300 times more disk space needed for (temporary) storage.

3.3 development

The system has been set up according to the following strategy:

- at first, only the parameter values from the monitors were acquired and stored. Software has been developed to show plots of the parameters of every patient;
- secondly, a few physiological signals, from one patient, were acquired and stored. Processing and analysis took place (off-line) on a stand-alone PC;
- the presentation of the data and the results was evaluated;
- the number of patients whose signals were acquired simultaneously was gradually increased;
- a LAN was implemented, allowing for easy access of the data and distribution of tasks;
- trends and variations in trends of the parameter data were logged and kept in a database;

- artefact detection and other analysis algorithms were developed and tested off-line and implemented on-line afterwards;
- the M68030 processor and the VME-bus/PhyBUS converter of the PhyDAS system will be replaced by a Pentium processor (or one comparable to that) in combination with a PCI bus - PhyBUS converter. The acquisition will be controlled by a graphical user interface developed using Labwindows/CVI software. The throughput of the system will thereby increase significantly;
- as a next step in the development of the measurement system, part of the processing will be performed between the acquisition in the parallel samplers and the transfer to the computer bus of the PhyDAS. This pre-processing, performed by one or more Digital Signal Processors (DSP's), will be especially useful for (adaptive) filtering, correlation, and perhaps autoregressive modelling. It is expected to lead to a significant reduction of the load of the CPU in the PhyDAS system and also of the amount of data that has to be transported via the LAN;
- information from different signals will be linked together, e.g., using real-time correlation. The correlation can be used in the detection of artefacts and gives insight in certain physiological relations;
- at a later stage a reduction of artefacts and a selection of reliable data will be performed in real-time, leading to a significant reduction of the amount of data to be stored;
- at a later stage the acquired information may be added into an expert system, facilitating the assessment of the condition of a patient or the evaluation of his or her treatment.

3.4 conclusion

A measurement system was developed capable of acquisistion, processing, display, and archiving of all relevant information continuously measured by the patient's monitor. Additionally, some extra signals from other devices can be handled. The acquisition is performed via analog lines, except for the parameter values generated by the monitors. The PhyDAS system used for this acquisition offers flexible and scalable real-time processing capabilities. Raw values and results are written via a LAN to a file server, where general access is possible by PCs. A number of predefined jobs can be specified from any PC connected to the LAN, and can be executed on an arbitrary number of PCs running a continuous processing cycle. In the future pre-processing at the front end will be implemented, resulting in a significant reduction of processing time. A proper administration of the information has been set up, and deletion of obsolete files is performed automatically.

The fact that the development strategy, used from about 6 years ago till now, is still actual, illustrates its value.

Literature

Jong W de; Een informatiesysteem voor fysiologische signalen op een intensive care voor pasgeborenen; Instituut Vervolgopleidingen, Technische Universiteit Eindhoven, 1993

Voskamp JH, Nijmweegen FC, Van der Wal AJ; Data-acquisistie met PhyDAS; Electronica 23:18-35, 1988

Voskamp JH, Nijmweegen FC, Van der Wal AJ; Besturing van experimenten; Electronica 24:21-31, 1988

4. Measurement of the signals

In this chapter the main signals needed for the monitoring of the neonatal patient are discussed: the blood pressure, the electrocardiogram (ECG), and the respirogram. Most of them are continuously measured and registered by the patient's monitor. The possibilities for (real-time) calculation of additional information, using the blood pressure signal, the ECG, and the respirogram, individually as well as in relation to each other, are evaluated.

4.1 blood pressure measurements

Since 1628, when W. Harvey described for the first time the circular motion of blood through the body, the interactions between heartbeat and vascular state have been a topic of interest [Harvey, 1628]. Probably the most important signal for these studies is the blood pressure signal. This signal not only contains systolic (maximum) and diastolic (minimum) blood pressure values at every heartbeat, but also incorporates information about the volumetric state, peripheral resistance, heart function (contractility), influence of respiration on blood pressure and autonomic nervous system influences. The blood pressure level is an important tool in the evaluation of the condition of a critically ill patient. In the critically ill newborn infant not only the early determination of hypo- or hypertension, but also the determination of fluctuations in blood flow and blood pressure were found to be important. Among others, Perlman has shown in 1983 that these fluctuations are involved in the pathogenesis of intracranial lesions [Perlman et al., 1983, Miall-Allen 1989, Goldstein and Brazy 1990, 1991]. To monitor fluctuations in the blood pressure a continuous registration is needed. Non-invasive methods for continuous blood pressure registration in neonates are not available. The research group therefore remains restricted to the neonates having a clinical indication for an arterial catheter. This is about half of our NICU population.

4.1.1 physiology

Blood is pumped around in the body by a rhythmic contraction of the heart. In the system circulation it goes from the heart through arterial vessels to the peripheral tissues and organs, and circulates back to the heart via venous vessels. In the lung blood circulates through the pulmonary artery to small capillary vessels where oxygen/carbon dioxide exchange takes place, and back to the heart in the lung veins. Because of the rhythmic contraction of the heart the pressure in the arteries also fluctuates. The volume and the contour of the arterial pulses not only depend on the left ventricular stroke volume and the ejection velocity, but also on the relative compliance and capacity of the arterial system. Furthermore, they are composed of forward and backward waves, reflected from the peripheral system. The waveform thus contains a lot of implicit information about the contractility of the heart

(septum) and peripheral resistance. Therefore the arterial pressure waveform depends on the measurement position and the quantities mentioned above.
In infants, the blood pressure values are influenced by the presence of asphyxia, sepsis, infant respiratory distress syndrome (IRDS) and patent ductus arteriosus (PDA). The influence of these pathologies on the contour of the blood pressure signal has not been investigated yet. In adults, altered waveforms have been reported in case of shock, hypo- and hypertension, atherosclerosis, vasodilatation, atrial fibrillation, valvular disease, hypertrophic cardiomyopathy, aortic coarctation and chronic uremia [O'Rourke, 1982, Gevers, 1994]. Apart from the waveforms, the fluctuations in blood pressure (beat-to-beat and slower) are known to contain information about the function of the autonomic nervous system. The assessment of these fluctuations by spectral analysis will be worked out in chapter 5.

4.1.2 non-invasive blood pressure measurement techniques

Although in this thesis we focus on invasive arterial blood pressure measurements, in some situations we may use the non-invasive alternatives. These all have in common that the assessment of the blood pressure is not very accurate, but, on the other hand, an arterial cannulation is not required. The oscillometric method is the oldest one used in man. In 1866 this method was described by Marey [Marey, 1866]. He used a small cuff, snugged around a limb, which was inflated with water above systolic pressure. During deflation he registrated the oscillations of a mercury column on a carbon drum. Pressure was read from a mercury manometer. The point of maximal oscillations was decided to be the mean arterial pressure. In 1896 Riva-Rocci introduced the palpatory method, only suitable to determine the systolic pressure. He used a cuff with air connected to a mercury manometer to measure the pressure applied to the brachial artery. The pulse was determined by palpation of the a. radialis at the wrist and the pressure was increased until the pulse disappeared (systolic pressure). The oscillation of the cuff pressure with the heartrate, when the cuff was smoothly being deflated, was noted. It results from pressure transmission from the artery to the cuff, which is the basis of all oscillometric measurements.
The problem where to locate the point of diastolic pressure in the sequence of oscillations could not be solved. In 1905 a solution was proposed by Korotkoff, who introduced the auscultatory blood pressure measurement [Korotkoff 1905]. He described the characteristic sounds (named after him) heard with a stethoscope in the "elbow" when the pressure in the inflated cuff was lowered through systolic and diastolic pressure. He used the same cuff as Riva-Rocci. This method still is the basis of the auscultatory method used today. The method slightly improved after 1940, when intra-arterial measurements had become available that could be used as a "gold standard". In particular attention was given to the small size of the cuff, which especially in the obese turned out to overestimate the blood pressure level. The American Heart Association recommends for the cuff-bladder dimension a width of 40% of the circumference of the limb, long enough to encircle 80% of the circumference, to be placed such that it is centered over the artery to be compressed

[Kirkendall et al., 1980]. For premature neonates this leads to the use of a smaller cuff.

The automated oscillometric devices currently used still follow the oscillometric principle described by Marey, using a cuff snugged around a limb. A detailed description, characteristic for many of these devices, is given by Ramsey [Ramsey 1991]. The cuff is inflated to approximately 160 mmHg for the first determination, or to 30 mmHg above the previous systolic pressure found. Oscillations in the cuff pressure are sampled (by a microprocessor) at a constant cuff pressure to improve artefact reduction. If no oscillations occur the pressure is lowered a few mmHg, and sufficient sample time is allowed. If oscillations occur the amplitude of two consecutive pulses should only differ a small amount, and the time interval between them has to match closely the previous time intervals. When two consecutive pulses meet this criterion their amplitude is averaged and stored for later determination of systolic, diastolic or mean pressure. This criterion avoids many of the artefacts arising from strong respiratory variation, premature ventricular contraction, and external motion. If artefacts occur, the measurement time will be increased by the time waiting for two acceptable pulses. If the delay is too long the actual cuff pressure level is skipped. The cuff pressure is lowered again a few mmHg and sampling for the oscillations starts again. In general no oscillations are found any more after going several deflation steps through the diastolic pressure. An algorithm is applied to the average values, stored at each deflation step, to determine the systolic and diastolic arterial pressures. The mean is also calculated from the averaged values. The systolic (diastolic) pressure normally is associated with the cuff pressure at which the increase (decrease) of the oscillation amplitude has a maximum. The algorithm is an important part of the measuring device, because it has to reduce artefacts from the set oscillation amplitudes of many different patients and patient groups.

Problems in blood pressure measurements may occur due to:
- physiologic variation (shock, large blood pressure variation during the measurement, variation in pulse rate (>15%));
- anatomic variation (conically shaped arm, calcified arteries, subclavian compression);
- cuff compression variation (movement (of cuff or arm), shivering, bumping the cuff, vehicular or helicopter vibration).

In neonates additional care has to be taken in the interpretation of blood pressure values. Studies in which oscillometric and invasive arterial measurements are compared report a significant disagreement between them. Many report an overestimation of low pressures [Gevers 1994, Diprose 1986] and unacceptably large errors for the individual infant [Briassoulis 1986, Wareham 1987].
Furthermore, attention is required to the cuff size used: too small sizes yields too high pressure values, too large sizes only have a small effect. The cuff has to be applied snugly enough and all air has to be squeezed out before applying the cuff. The cuff hoses may not be kinked and the air system may not leak. The patient must

be still and quiet, the cuff should be at heart level (if no hydrostatic compensation is applied) and subclavian compression by the arm or retraction of the chest should be avoided.

Some automated devices use microphones or a Doppler signal to determine the systolic, diastolic and mean pressure points during deflation of a cuff. The microphone instruments use the abrupt change of frequency content of the Korotkoff sound. A filter circuit is able to detect the muffled end point of the sound at diastolic pressure, which is more reliable than the detection of disappearance of sound [McCutcheon and Rushmer, 1967]. Nevertheless, errors may occur due to ambient sounds or sounds generated by patient movement. These errors can be reduced either by ECG triggering or by use of a second microphone that only registrates the ambient sounds. Subtraction of this signal from the original with the Korotkoff sound gives a purer Korotkoff registration. Doppler blood flow detection under the cuff can be used to determine the systolic pressure in specific small arteries. It is useful in the evaluation of peripheral vascular disease [Sumner 1984].

Only recently a continuous *non-invasive* measurement of finger arterial blood pressure in adults and children older than one year has become available [Smith et al., 1985, Peñáz 1973]. Up till now this method is considered to be inappropriate for use with neonates.

Summarizing we can state that automatic non-invasive blood pressure measurements currently are performed by the oscillometric method. In manual blood pressure measurements the auscultatory method is used. In both cases a significant deviation from the intra-arterial pressure cannot be excluded, especially not in case of a patient with several affected organs and systems.

4.1.3 invasive blood pressure measurements

The invasive techniques, being more accurate, were not readily available for human patients until about 1900 [Frank 1905, Hansen 1949]. In the 18th century, however, Hales described the first measurement of blood pressure with a glass manometer connected to an artery of a living horse [Hales 1733] and in 1876 Mayer already used invasive measurements in rabbits for determination of low-frequency blood pressure fluctuations [Traube 1865, Mayer 1876].
Invasive blood pressure measurements are always performed by indwelling of a measurement device in the artery or vein in which the pressure has to be known. The measurement device may either consist of a pressure transducer on the tip of a catheter or of a cannula through which the pressure waves are conducted to a pressure transducer outside the patient. Measurement by a tip-catheter is preferable when high frequency components are investigated, because of its excellent frequency response. However, for use in neonates the catheter has to be very thin (less than 4 French). Although such catheters exist they still are very expensive. When the device

is used for continuous measurements, problems occur due to blood clotting around the tip [Webster 1988].

Clinically, often the possibility of blood sampling is more important than the the measurement of accurate blood pressure values. A catheter manometer system (CMS), applied primarily for blood sampling, contains a cannula that is coupled to a pressure transducer. It can be used for at least a week, preventing the baby from being cannulated again and again, and allows a continuous monitoring of the arterial blood pressure. A CMS only is applied at clinical indication, taking into account the possible risks: thrombus forming, infection and transient ischaemia. The risks of umbilical artery cannulation are higher than the risks of peripheral artery cannulation [Schober 1990, Aldridge and Gupta 1992]. Accurate measurements of blood pressure require a transmission of pressure wave frequencies to at least the 10th harmonic of the base frequency [Weindling 1989, Hack et al., 1990^{a}]. In premature neonates this corresponds to a bandwidth of approximately 30 Hz. The transmission of high frequency components is often corrupted by air bubbles or blood clots in the system. In this section we describe a method to check in situ the transmission capability of the CMS.

a catheter manometer system

If a clinical indication for an indwelling catheter exists, routinely blood pressure is measured with a fluid-filled catheter manometer system. The system consists of a cannula, an extension tube, two stopcocks, and a pressure transducer chamber, that is connected to an infusion pump for flushing (see figure 4-1). The cannula is brought into the radial artery of the neonate. In the period following delivery normally a longer cannula is used, which is brought into the aorta via the umbilical artery. The total length of the system is about 50 cm and it is flushed with heparinised 0.65% saline solution at approximately 1 ml/h. This continuous flushing prevents the blood from clotting around the catheter tip. The risks for complications, i.e., partial obstruction of the artery, are acceptable [Hack et al., 1990^{b}]. In the pressure transducer chamber a strain gauge is used to convert the pressure variations to electric signals.

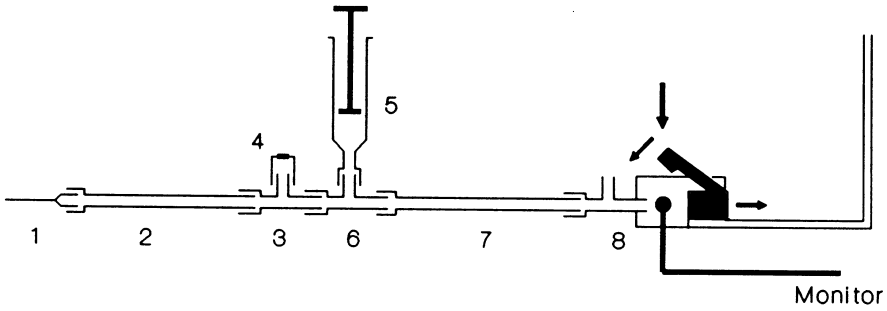

Figure 4-1 A Catheter Manometer System consisting of a cannula, an extension tube, two three-way stopcocks with an accessory blood sampling unit, a second tube, and a pressure transducer with a fast-flush valve. One of the two three-way stopcocks is closed with a rubber membrane and a screw cap, whereas a syringe pump is mounted on the other stopcock. The fast-flush valve (solid black component) has an open microchannel to provide continuous flushing. Fluid from the infusion pump flows through this channel into the transducer chamber, tubes, and cannula at a preset rate. The electrical signal of the pressure transducer is fed into the monitor. [Van Langen et al., 1993]

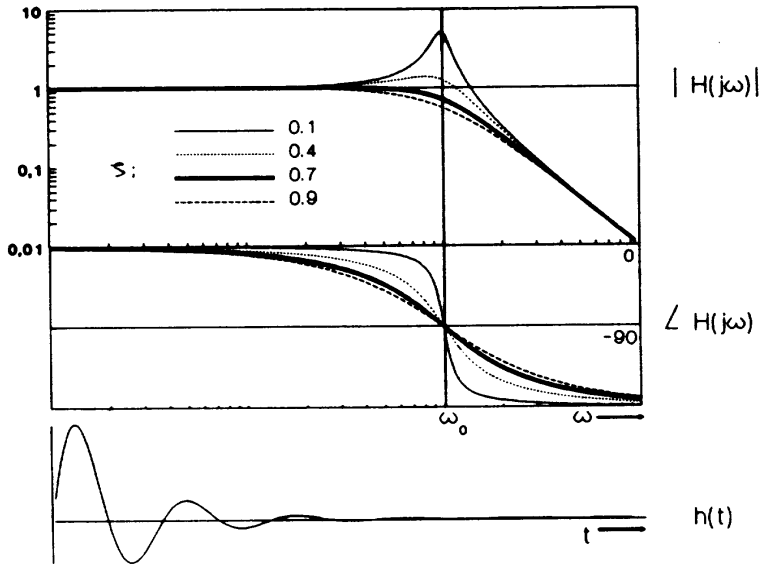

Figure 4-2 The amplitude response of a CMS. ω_0 *is the undamped natural angle frequency,* ζ *the damping coefficient.*

The transmission of a pressure pulse by a CMS can be approximated by a 2nd order differential equation. The so-called dynamic response is characterised by the resonance frequency and the damping. The description of the system normally is done in the frequency domain, where the transmission and phase as a function of frequency are plotted. The optimal response corresponds to a frequency-independent and a phase that varies linear with frequency, representing a fixed delay. Unfortunately, this is only roughly achievable for frequencies below a certain maximum frequency. The actual amplitude transmission of a signal is plotted in figure 4-2. It has been related to the undamped natural frequency, i.e., the resonant frequency in case no damping is present. In case the damping ζ=0, the fluid column will oscillate indefinetely. If there is little damping, e.g., ζ=0.1, the column will oscillate but eventually come to rest. If the damping increases, there is a point where the oscillations just have been faded out (ζ =1). This point is called critical damping. When the damping further increases (ζ>1, overdamping) a pulse dies out in a nonoscillatory exponential decay. The damping at which the amplitude response is constant over the widest range of frequencies is defined as the optimal damping (ζ=0.64) [Fry, 1960]. The output signal still shows an overshoot, because ζ < 1. The undamped natural frequency and the damping can be expressed in the properties of the fluid and the system. The differential equation of the linearised problem reads

$$Pa = a\rho L\frac{d^2x}{dt^2} + b\frac{dx}{dt} + kx \qquad \textbf{(4-1)}$$

with
P the pressure applied at the catheter tip
a the cross-sectional area of the catheter
b the friction coefficient
ρ the density of the fluid
L the length of the catheter
k Hooke's constant (spring stiffness)

The assumption was made that the forces of acceleration and the viscous forces are confined to the catheter, and that the elastic forces are confined to the transducer. The elasticity modulus, E, can be defined by a and k

$$E = \frac{k}{a^2} \qquad \textbf{(4-2)}$$

and the viscosity of the fluid, μ, can be expressed in a and b:

$$\mu = \frac{b\pi r^4}{8La^2} \qquad \textbf{(4-3)}$$

with r the catheter radius.

Solving this equation one can show that the undamped natural frequency equals

$$f_n = \frac{1}{2\pi}\sqrt{\frac{E\pi^2 r^4}{a\rho L}} \qquad \textbf{(4-4)}$$

and the damping can be expressed by

$$\zeta = \frac{8\mu L\rho}{2\sqrt{\rho LE\pi r^2}} \qquad \textbf{(4-5)}$$

with E the elasticity modulus, the reciprocal of the compliance of the system
r the catheter radius
μ the viscosity of the infusion fluid.

The background of the model and the solution the differential equation are extensively outlined by Kleinman [Kleinman 1989].

It is important to test the system if accurate blood pressure measurements (frequencies up to 30 Hz) are desired. Many investigations have been done on the assessment of the CMS in vitro, but reliable methods for testing the system in situ still are under discussion. Van Langen et al. successfully validated the flush-pulse method in situ with the step response method in vitro [Van Langen et al., 1993]. Hipkins et al. compared (systolic) blood pressure values obtained from a CMS tested with the flush-pulse method with those obtained from a tip-catheter in the carotid artery in sheep. These findings did not agree [Hipkins 1989]. Schwid reported a significant difference between damping values found in situ with the flush pulse method and directly afterwards in vitro. This inconsistency may be attributed to the presence of the cannula in the patient in the in situ situation, whereas in the in vitro situation the CMS was directly coupled to the pressure simulator (Biotek 601) [Schwid 1988]. The characterisation of a CMS by a natural frequency and damping is not simply a property of the system itself, but strongly depends on the configuration in which the system is used, and the impedance matching at the cannula side.

the flush-pulse method

In our NICU an automated procedure was developed and validated to test the CMS in situ [Van Langen et al., 1993]. The existing step response method, validated in adult monitoring systems, is not appropriate for use in preterm neonates due to restrictions with respect to the fluid balance in the neonate. In the clinical situation we used a CMS as shown in figure 4-1. This CMS, without cannula, is carefully filled with infusion fluid. Next, the cannula is inserted into the artery of the neonate, and screwed to the extension tube of the CMS. The residual blood is removed by complete flushing of the CMS. The infusion fluid consists of heparinized 0.65% NaCl solution. The flush rate normally is 0.5 to 1.0 ml/h. The dynamic response is analysed assuming a second order linear system. After a pulse has been applied to the system the exponential decaying pressure oscillations P(t) are characterized by the damped natural frequency (f_n) and damping coefficient (ζ):

$$P(t) = Ae^{-2\pi f_n \zeta t}\sin(2\pi f_n\sqrt{1-\zeta^2}\,t) + B \qquad \textbf{(4-6)}$$

A and B are constants,

t is the time after the pulse.

The oscillating pulse response is superimposed on the patients blood pressure waveform. To avoid complications due to the influence of the original blood pressure waveform only pulses in the diastolic part of the wave were analysed. Prior to evaluation of the pulses the first derivative was taken to eliminate the almost linear decrease of the background. Using the derivative the interval between the extremes (giving ω) as well as the decrease in amplitude due to the damping (giving ζ) can be measured. We suggest to evaluate the system before every measurement to check the accuracy of the sampled waveform. When measuring continuously we suggest to apply several pulses after every blood sampling with the CMS, or at least several times a day. Depending on the purpose of measurement the criteria for the accuracy of f_n and ζ have to be specified. We will go into that in more detail in the section *error determination*.

radial, tibial or umbilical artery measurement

With the development of little catheter tubes in the 80's peripheral instead of umbilical cannulation had become applicable. Peripheral cannulation offers the possibility for blood sampling and blood pressure measurements a longer time after birth. With the requirements that signals up to at least 30 Hz should be measurable with a distortion less than 10%, umbilical artery measurements are inadequate. This is mainly due to the long and elastic tubing, necessary to lead the cannula through the umbilical artery to the lower or higher aorta. From equation 4-4 and 4-5 it follows that with a longer and more compliant system (lower elasticity), f_n will decrease and ζ will increase. In practice, the umbilical CMS is almost always overdamped.

infusion fluid

The influence of the infusion fluid on the accuracy of measurement used proved not to be significant. We investigated the difference with respect to f_n and ζ between two commonly used fluids. These are a heparinised weak saline solution (0.65%) and a heparinized 5% glucose solution. We expext that significant differences may occur in the density (ρ) and viscosity (μ) of the fluid. For the density we have $\rho_{gluc}/\rho_{sal} \approx 1.05$, and for the viscosity we measured at a temperature of 29 °C $\mu_{gluc}/\mu_{sal} \approx 1.1$. The change in f_n and ζ is inversely proportional to the square root of ρ, which would result in a reduction by 2.5% going from a saline to a glucose solution. Only ζ is proportional to μ (Equation 4-5), so it increases by 10%. We conclude that this in total only leads to changes in f_n and ζ, that are negligible compared to the large range of these values resulting from the adequacy of filling or blood sampling.

error determination

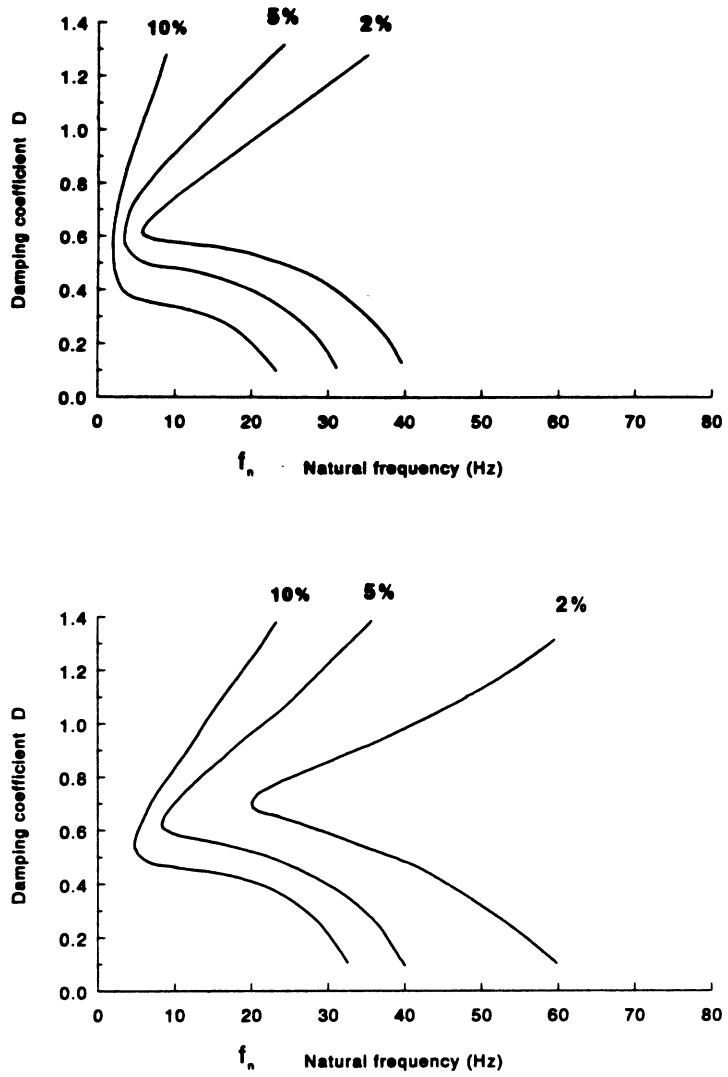

Figure 4-3 Relative error in systolic (upper graph) and pulse (lower graph) pressure evaluation from a neonatal radial artery waveform using a CMS with given f_n and damping coefficient (from:Gevers, M; Arterial pressure wave forms in newborn infants; Free University of Amsterdam, 1994).

The most important parameters directly derived from the blood pressure waveform are the systolic and diastolic pressure values. The question arises what systematic error is made in these parameters given a CMS with a certain f_n and ζ. Given the characteristics likely to be present in clinically used systems [Van Langen et al., 1993], we conclude that the highest relevant frequencies in neonates are likely to be too high for proper transmission by the CMS. These relatively high frequency components lead to a distortion of the CMS waveform. The errors in the parameters can be calculated by a simulation assuming the second order characteristics of the system. Given a

certain real waveform, the error can be plotted using a grey scale or by iso-error lines in a graph with damping coefficient and natural frequency plotted along the two axis. From such a graph, for a given f_n and ζ, the expected error can be found. Simulations reveal that the error in the systolic value is larger than in the diastolic, due to the higher frequency components in the signal just before the systolic value is reached. The sign of the error in the diastolic value differs from the error in the systolic value. If the system is overdamped, the actual values will not be reached; if the system is underdamped, the actual values will be over- and underestimated respectively. The error in the pulse pressure is even larger than in the systolic pressure, because the former is defined as the difference between systolic and diastolic pressure. Van Genderingen calculated the error in the systolic and diastolic blood pressure values starting from neonatal radial artery waveforms, acquired with a high fidelity CMS [Van Genderingen, 1994, Hack et al., 1990[a]]. The results, summarised in iso-error plots, are given in figure 4-3. If the blood pressure is measured in the aorta through an umbilical artery catheter, we may expect approximately the same frequency components in the real waveform. The larger and more compliant canule will yield a lower f_n and larger ζ. The results are due to be poor compared to peripheral artery measurements. In case the damping $\zeta \geq 1$, it is not possible to determine f_n with the flush pulse method. Because of the inverse linear relationship between f_n and ζ (μ and ρ unchanged) it is not likely that f_n is large enough for an accurate measurement (see equations (4-4) and (4-5)). If the system is not overdamped and the flush pulse is assumed to originate from a really short pulse, the blood pressure signal can be deconvoluted by the flush pulse response to correct for the dynamic behaviour of the CMS. If the flush pulse response changes with time due to changes in the CMS, the pulse response used in the deconvolution procedure should obviously be changed as well.

optimisation of filling

From the above it is clear that a better performance is required in most of the CMS's in clinical situation. Although the flush pulse method recently became available, it only allows a check of the CMS' characteristic f_n and ζ. The problems caused by air in CMSes in adults have previously been reported. Even minimal air bubbles have been shown to drastically decrease f_n and increase ζ. From experiments in a laboratory situation it is clear that the CMS potentially has adequate response characteristics. Clinically, these characteristics are spoiled by the sampling of blood and by the entrapment of air. Several methods are proposed to minimise the entrapment of air while filling the system:

- Flushing with alcohol, prior to flushing with the infusion fluid and filling of the system;
- Flushing with CO_2, prior to flushing with the infusion fluid and filling of the system;

– Filling the system with degassed infusion fluid.

Experiments have shown that the use of any of these methods in laboratory situations leads to a significantly better frequency response. Tests were performed *in vitro* using the sinusoidal method [Gardner 1981]. An increase of f_{max}, defined as the maximum frequency below which the amplitude ratio is uniform within 10%, was found [Van Genderingen, 1994]. In normal filled CMS's the median f_{max} was 27 Hz. One of the methods 1, 2 or 3 increased f_{max} to median values of 34 to 39 Hz. After applying all methods an increase of f_{max} to a median of 51 Hz was found. The damping coefficient did not change significantly. When the system has been used for blood sampling, a deterioration of its performance is likely to occur. The system will be less affected when a larger flush rate can be used (several ml/h) or fast flushing is permitted. Because of the fluid balance in the neonate this is often not desirable. Flushing at a higher rate with glucose instead of saline has been suggested, in which case the Na^+ concentration in the body is not disturbed. This procedure applies if glucose is already being infused separately.

When an accurate waveform registration is required we conclude that filling of the CMS according to 1, 2 or 3 increases *the possibility* that the system will meet the requirements. Use of the flush pulse method in situ still remains necessary to check the filling and monitor the characteristics of the system in time. If the performance of the CMS appears to be acceptable, a deconvolution with the flush-pulse response might be performed to approximate even better the original blood pressure wave.

artefact reduction

Our system is set up in a way that a large part of the analysis can be performed automatically. Therefore, a permanent check on the validity of the signals involved is preferred, because otherwise the results will be based on inadequate information. It strongly depends on the way the signal is used what kind of artefacts have to be detected or corrected. The blood pressure signal usually is sampled at a frequency of 128 Hz. When the waveform is used we usually inspect the signal manually. Errors in the signal may consist of:

1. Interruption of the pressure information because of blood sampling through the CMS;
2. Movement artefacts;
3. Bad CMS condition;
4. A manually given pulse, required for the flush pulse method.

Artefacts from categories 1 or 2 yield very high time derivatives and thus spectral components at high frequencies. If the flush pulse method is used, a given pulse can be recognized automatically. From the flush pulse response the in-situ condition of the CMS is derived.

Many analyses use the systolic and diastolic blood pressure levels only.

From the signal primarily the occurrence time and value of the systolic blood pressures and the diastolic blood pressures are determined. These values will be used

in the remaining part of the thesis in the analysis of respiratory and autonomic nervous system components.
In the blood pressure signal is sought for artefacts of the categories 1 and 4. If they occur the signal cannot be used for further analysis. From the flush pulses it can be determined (preferably at least several times a day) if the condition of the CMS is sufficient for further analysis. Then, the following algorithm is performed. It has been developed by trial and error on many neonatal data sets and copes with most of the remaining (movement) artefacts.
In a relevant block of signal values local maxima and minima (extremes) are searched for. They are marked as possible systole resp. diastole values.
A systole is found as follows:

- The extreme requires a rising slope followed by a falling slope.
- In the period of 0.25 s prior to the extreme there has to be a period of at least 0.04 s in which the signal raises with a least 40 mmHg/s.
- If these conditions are fulfilled, the difference in time between the current maximum and the previous maximum is compared to a time treshold. If the interval is smaller than the treshold the systoles lie too close together (a twin peak) and the extreme with the maximum value is taken as the systole. The initial value of the treshold is set to 1/3 of the heart interval, which has to be entered by the user in advance. If the criteria are met the extremum is considered to be a systole. When a systole is found the treshold is adapted as follows:

$$treshold_{new} := \tfrac{1}{3}(interval\_found) + \tfrac{2}{3}(treshold_{old}) \qquad \textbf{(4-7)}$$

A diastole is found analogously:

- The extreme requires a falling slope followed by a rising slope.
- In the period of 0.25 s after the extreme there has to be a period of at least 0.04 s in which the signal raises with a least 40 mmHg/s.
- If these conditions are fulfilled the difference in time between the current minimum and the previous minimum is compared to a time treshold. If the interval is smaller than the treshold the minima lie too close together (a twin valley) and the extreme with the minimum value is taken as the diastole. The value of the time treshold equals that of the maximum (equation 4-7). If the criteria are met the extremum is considered to be a diastole.

The occurrence times and values of systole and diastole are calculated for episodes of 30 seconds. To avoid boundary problems the episode is extended with 3 second periods preceding and following the 30 second interval.

4.2 heartrate measurements

The heart activity interacts with other processes in the body in order to provide the body enough oxygen and nutrition and take away the waste products. The heart activity is controlled by the autonomic nervous system and the humoral system. Both

systems are driven by chemo- and baroreceptors located at several places in the body. The control mechanisms act on both the contractility of the heart and the heartrate. In neonates the changes of the contractility are assumed to be of little importance. As a consequence, the heartrate reflects an important part of the interaction of the body with the cardiovascular system, and therefore monitoring of the heartrate is very useful. The strong decrease of the heartrate in case of an apnoea is an important example of this interaction.

The heartrate can be assessed by different measurement techniques: the ECG, the blood pressure signal, the photo plethysmogram or during noninvasive measurement of the blood pressure. The ECG can be acquired simply and generally is the most reliable source from which the heartrate can be determined. The values calculated from the other measurements may eventually be used to assess the validity of the heartrate value found from the ECG. In this paragraph we will focus on the determination of the heartrate using the ECG signal.

Diagnostic use of the ECG requires a standard configuration of the electrodes from which the ECG is acquired. In figure 4-4 we show the standard waveform of the ECG. The phases P, Q, R, S, and T can be classified:

- P the depolarisation of the atria,
- QRS the depolarisation of the ventricles,
- T the repolarisation of the ventricles.

The continuous use of the ECG for monitoring of the heartrate (and variations in it) - in principle - does not require a registration made in standard conditions (see for example figure 4-5). The resulting non-standard waveforms, however, complicate the automatic analysis of the signal, because all kinds of ECG waveforms have to be dealt with.

4.2.1 acquisition

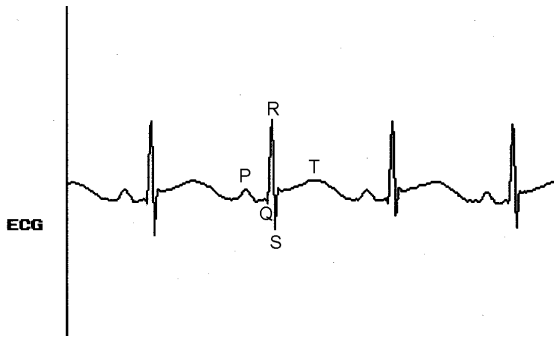

Figure 4-4 Sample ECG waveform.

In our heartrate analysis we use the ECG signal measured for monitoring of the neonate. The ECG signal for routinely monitoring is not a standard ECG, but is only intended to allow the detection of every heartbeat. In the evaluation of this signal the

actual waveform is not known. The nurses take care to position the electrodes in such a way that the QRS-complex is being recognized by the patient's monitor, but this does not guarantee a well-defined waveform. Two different forms that occur in normal clinical setting are presented in figure 4-4 and figure 4-5. They may have either positive or negative R-waves. From these signals the occurrence time of a heartbeat is evaluated, and from the differences of these occurrence times the heartbeat interval or the heartrate. A proper assessment of these occurrence times (OT) is outlined in the next section.

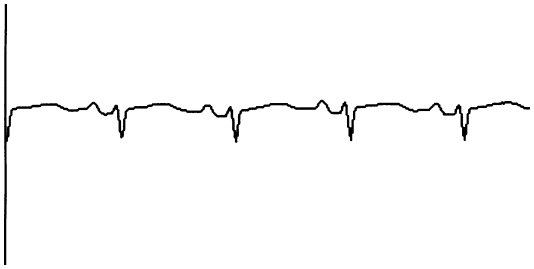

Figure 4-5 Example of an ECG waveform as registrated in clinical practice

4.2.2 determination of the moment of heartbeat

From the ECG-signal a set of heartbeat times is determined at which the heartbeats are assumed to have occurred. The problem can be described as a two stage problem [Rompelman 1986]:

1. the presence of a waveform has to be detected;
2. the occurrence time of a certain feature of the waveform has to be estimated.

Ad 1): The first problem, in our situation, is not the most difficult. It is mainly difficult when a patient suffers from heart diseases that strongly affect the shape of the waveform. Furthermore, we have to analyze the ECG signal starting from the knowledge that it is not a standard ECG waveform. We have to take a definition of the OT of a certain feature of the waveform, which physiologically may differ from the time found in another non-standard ECG. Due to the fact that no standard ECG is available, we are unable to automatically identify, for example, the time at which the firing of the SA-node starts or the time at which the ventricular contraction starts. If the waveform itself is assumed to be more or less time invariant we can reliably use the OTs to evaluate the (variations in) inter-beat interval time. If we use the occurrence time in relation to other signals, e.g. blood pressure fluctuations or respiration, we have to take into account that fluctuations may occur when the ECG waveform changes with time. The information that reliably can be achieved is the presence of a heartbeat (a certain feature of the waveform), and an OT that is defined in such a way that its jitter resulting from the detection algorithm is minimized.

At our clinical site the ECG signal is digitized at 400 Hz and is processed in consecutive blocks of 30 s. The presence of a heartbeat is detected, looking for the most R-wave comparable part of the waveform. The maximum and minimum values during the first 5 seconds of the signal are determined to prepare for the heartbeat detection. A signal threshold is set to 60 % of their difference. A slope threshold is defined as a percentage of the difference between maximum and minimum of the slopes in that episode. We seek for an R-wave at the first slope that exceeds the slope threshold. Next, within 0.05 s an opposite crossing of the slope threshold has to occur. If this opposite slope is found, in the time interval of 0.1 s symetrically around both slopes, a minimum and maximum of the signal are determined. The difference between these signal extrema has to exceed the signal threshold. If so, the maximum is assumed to be a positive R-wave if the first slope was positive. If the first slope was negative, the minimum is assumed to be a negative R-wave. The tresholds are not adapted on every R-wave, but are determined again for every 30 s data block.

Ad 2)
If we have found a waveform, it is not obvious what is the most appropriate definition of the OT. It seems the most ideal to take the start of the depolarisation at the SA-node, in a standard ECG expressed by the start of the P-wave. However, due to the fact that we do not have a standard ECG, it is not always possible to recognise the P-wave. If the waveforms are more or less time invariant, we may take any other point of the depolarisation complex, e.g. the R-wave, which is less difficult to determine. In case the waveform is not time-invariant, we have to accept that P-R-wave variability will corrupt the data if it is large. The best we can do is define an OT with minimal jitter due to sampling and due to waveform variations.

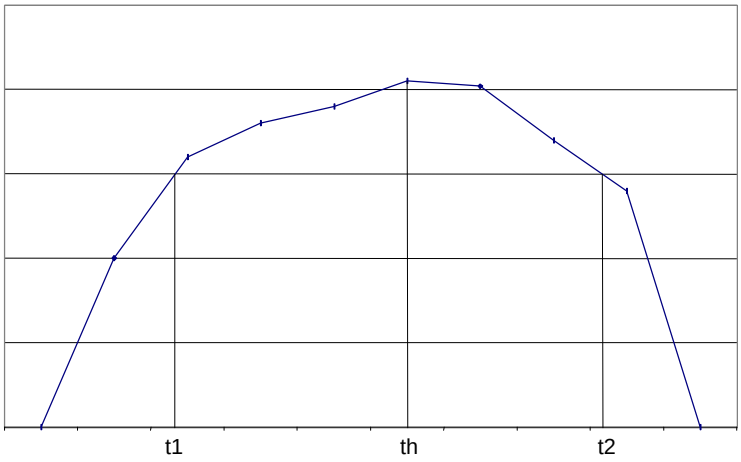

Figure 4-6 Definitions of the OT of an R-wave

Some researchers suggest to use an R-wave interpolation [Merri et al., 1990], but in many studies more effort is put in the recognition of the QRS complexes than in reducing the sampling error. They simply use the time at which the waveform reaches

its maximum ($T_{R\text{-}wave}$=th, see figure 4-6), or the midpoint between the positive and first negative passing through a certain level around the R-wave [Rompelman 1986]: $T_{R\text{-}wave}$= 1/2·(t2-t1). A better method uses the output level of a matched filter, which, however, requires a relatively large computational power. Most often this strategy is used to solve problem 1), the actual determination whether a QRS complex occurs, and not the time at which it occurs. We worked out a method with which we could reduce jitter due to sampling without claiming too much knowledge about the waveform of the ECG-complex, and without need for a large computational power. This method will be discussed below.

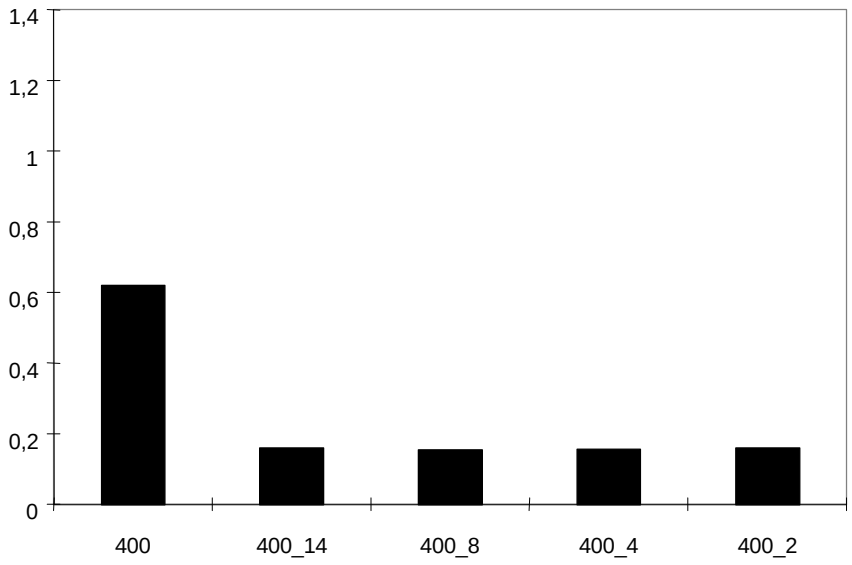

Figure 4-7 Mean absolute sampling errors using 400 Hz sampling frequency without and with polynomial fits of different order.

The error due to sampling in the determination of the OTs in a dataset can be expressed by the mean absolute sampling error:

$$\overline{E} = \frac{1}{N} \sum_{\substack{all\,QRS- \\ complexes}} \left| t_s - t_r \right| \qquad \textbf{(4-8)}$$

with N the number of QRS-complexes in the dataset
t_s the time the sample was taken
t_r the real OT of the heartbeat.

An error of 1.25 ms is the maximum that can be made, being exactly between two time samples. With a sampling frequency of 400 Hz the mean absolute sampling error would be 1.25 * ½= 0.63 ms. This jitter restricts the accuracy with which the variability can be calculated.

We evaluated whether the reduction in mean absolute error of the OT could be reduced with respect to the mean absolute sampling error by using a polynomial fit of the ECG. An ECG signal of a neonate was sampled with 800 Hz during 15 min. A 14th order polynomial fit with 15 points, 7 preceding and 7 following every R-wave maximum found according to the criteria just described, was considered as the gold standard. The same ECG signal was also sampled at 400 Hz and at 200 Hz. We compared the mean absolute (sampling) errors to the gold standard using a 2nd, 4th, 8th and 14th order polynomial fit. The number of sample points fitted equals the order plus 1. The R-wave maximum originally found was chosen to be the middle point. The results of this simulation are shown in figure 4-7 and figure 4-8. The label 400 means sampled at 400 Hz and not fitted; 400_8 means sampled with 400 Hz and fitted with an 8th order polynomial (9 data points). The results show that the amount of error reduction mainly depends on whether interpolation is used or not, and on the sample frequency. The use of interpolation reduces the mean error to about 1/6th of the original. The error is still roughly proportional to the sampling frequency. The use of a higher order polynomial in principle gives more freedom to fit exceptional waveforms. The 2nd order (parabolic) fit, however, is an acceptable choice in the determination of the OTs.

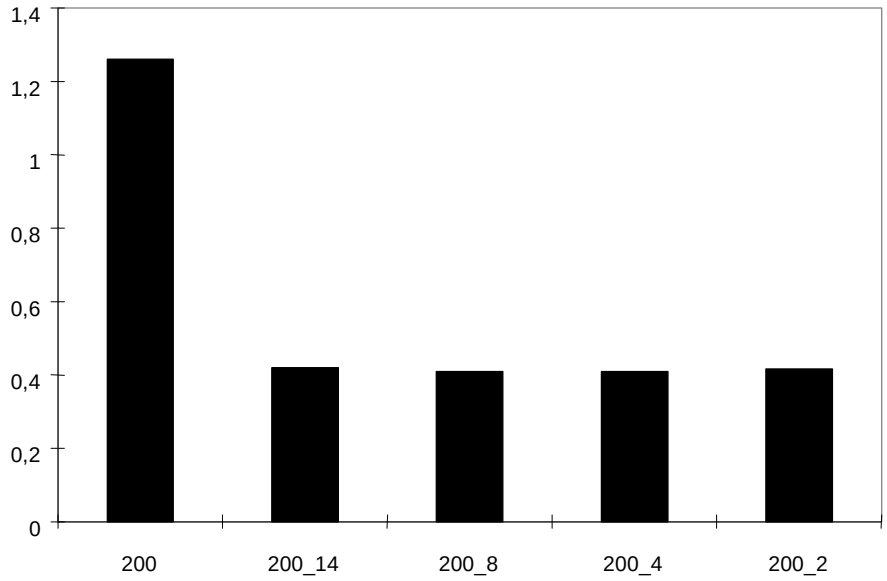

Figure 4-8 Mean absolute sampling errors using a 200 Hz sampling frequency without and with polynomial fits of different orders

4.2.3 conclusion

A significant increase in accuracy in the OT can be obtained using a polynomial fit (parabolic fit) of the R-wave. The use of the R-wave simplifies the detection of a beat of the heart, although theoretically the start of the P-wave should be preferred as definition of the start of the heartbeat. As a result, additional jitter may occur due to a variation in P-R interval time. Generally, this jitter is neglected in neonatal data sets.

4.3 respiration measurements

The monitoring of respiration is important if an indication exists that the oxygenation of (important parts of) the body might become inadequate. If hypoxemia in the blood occurs suddenly, it might well be caused by cessation of respiration (apnoea). If it is possible to detect the apnoea without delay, one can anticipate on the resulting overall hypoxemia and intervene in the body's respiratory function.
There are several methods available to measure the respiration, many of them have only been evaluated in adults and children. Furthermore, most of them only measure the expansion and contraction of the lungs indirectly. The widest known method, except for visual observation, is the thoracic impedance measurement. It can be simply implemented, using the ECG-electrodes already present on the patient's skin. Other methods are breathing-air temperature measurement, capnography, auscultation [Toubas et al., 1990], a fibre optic sensor measurement [Vegfors et al., 1992, 1993], inductive plethysmography [Cohen et al., 1994], and pneumotachography [Adams et al., 1993]. We restrict ourselves to the routinely measured impedance signal, and a nasal airflow measurement by the temperature of in- and exhalated air. The latter enabled us to evaluate the behaviour of the signals during (obstructive) apnoea periods.

4.3.1 thoracic impedance measurements

Thoracic impedance measurement is the usual method for the monitoring of the respiration. Although it has some serious disadvantages it is commonly being used because of its easy availability.

methods and application

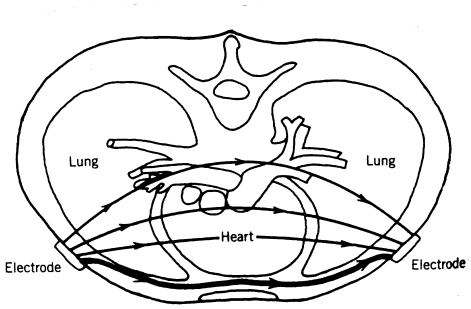

Figure 4-9 Components contributing to the thoracic impedance [Webster 1988].

The method is based on the measurement of impedance between two electrodes, placed at the chest. The impedance is determined using two of the electrodes already in use for the measurement of the ECG signal. In order to avoid interference of both measurements the impedance is determined using a frequency far outside the physiologic range of the ECG signal, but suitable for the detection of changes in the chest (39 kHz). Measurement in a narrow frequency band around this center frequency reduces the influence of electric muscle activity. Several effects contribute to the impedance measured in this way [Webster 1988, figure 4-9]:

- basic impedance (static)
  This is the part of the impedance that does not change on a timescale of seconds or less. It consists of the mean impedance of all substances in the thorax (muscles, tissue, blood) and the impedance of the electrode-skin transitions and involved wires. This impedance is of the order of several hundred **Ω**.
- changes due to respiration
  Due to breathing or artificial ventilation the amount of air in the lungs will change. This modifies the current flow between the electrodes, and thus will cause a change in impedance. This change allows the use of this signal for monitoring the respiration. It typically is of the order of 2 **Ω**.
- changes due to heart activity
  Every heartbeat blood is pumped out of the thorax into the aorta and next the atria are being filled with blood returning from the body into the thorax. These changes in blood distribution in the thorax cause changes in the thoracic impedance of the order of 0.5 **Ω**.

The resolution of the impedance measurement is about 10^{-3} **Ω**. The time resolution is 0.01 s. In special circumstances, e.g., periodic breathing (the respiration of the patient changes back and forth between normal breathing and very superficial breathing) or cessation of breathing, the changes due to heart activity become larger than the changes due to respiration. In those cases misinterpretation is likely to occur.

The AC-part of the demodulated impedance signal is filtered by a 3th order low-pass Butterworth filter with a -3dB point at 2.5 Hz, resulting in the thoracic impedance signal that is used in this thesis in the interpretation of the respiration.

interpretation

The HP merlin monitor has two modes for evaluation of the resulting impedance signal: the manual mode and the automatic mode. In the manual mode a treshold is set at a fixed point. This treshold is used to discriminate between non-breathing fluctuations and breathing fluctuations. The manual mode is advised in the following cases:

- the breathing frequency nearly equals the heart frequency;
- the breathing is superficial or the patient is being ventilated with intermittent mandatory ventilation (IMV);
- the heart activity is influencing the impedance signal considerably (> 30%).

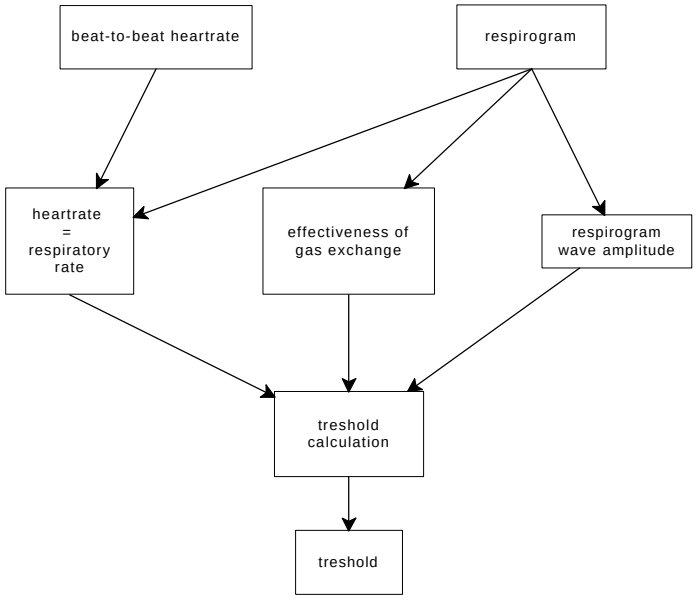

Figure 4-10 Adaptation of the treshold for detection of a valid breath in the automatic mode

In other cases, normally, the automatic mode is used. In that mode the signal is analysed by the monitor using the scheme illustrated in figure 4-10. The difficulty lies in the interpretation whether an impedance fluctuation is a significant breath or not: in such a case the breathing activity leads to an adequate oxygenation of the body.

The rule of thumb used by the monitor states that the longer the respiratory intervals are, the larger the amplitudes of the breaths should be. At very short respiratory intervals, however, the dead space of the respiratory system precludes a proper oxygen-carbondioxide exchange.
If the heart frequency and respiratory frequency are (nearly) equal, they cannot be properly separated, with the risk of counting heartbeats as respiration. This situation is very likely in case of an apnoea, followed by a bradycardia. During a bradycardia the filling of the heart has a greater influence on the impedance signal because of the increased filling. Its contribution will also increase due to the lower frequency which is less filtered out. We will go further into these problems in section 4.3.3.

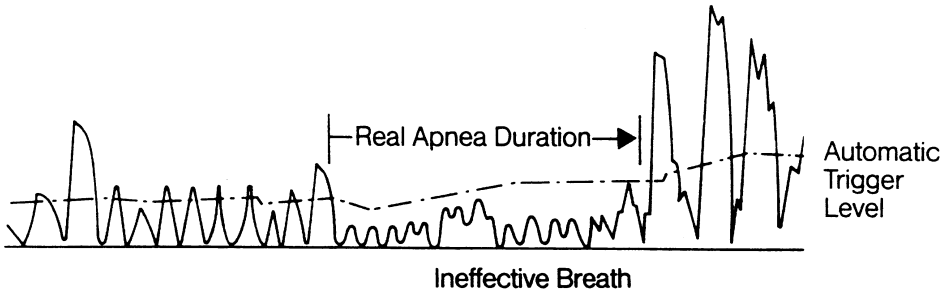

Figure 4-11 Treshold behaviour in the HP Merlin monitor in case of an apnoea in case the algorithm performs properly.

Adequate gas exchange at low respiratory frequencies requires that the depth of respiration is greater than at a higher frequency. Therefore the treshold will only be lowered if the actual frequency is high enough. This algorithm should prevent the monitor from interpreting heartbeats in the impedance signal as respirations (see figure 4-11). However, most of the time it turns out not to be working properly.

parameter extraction

In a standard situation, monitoring of the respiration takes place by evaluation of the respiratory rate, i.e., the number of breaths in a minute. This parameter is normally derived from the thoracic impedance signal, using the treshold defined in the previous section. The algorithm used by HP calculates a breath-by-breath respiratory rate (the reciprocal of the interval time) and displays a moving average of the last 8 breath-by-breath values.

In our own analysis we would rather like to know the breath-by-breath values instead of the average presented by the monitoring equipment. We therefore evaluate the interval time from the impedance signal in the following way:
A moving average of ¼second is carried out on the signal. In this way, many artefacts due to motion (relatively high frequencies) are removed. In the resulting signal complexes of subsequent minimum-maximum-minimum (min_1, max, min_2 in

equation 4-9) values are examined. They are assumed to be a breath if they comply with the following constraints:

1) the time between the minimum and maximum has to be limited

2) the difference between every minimum and the maximum has to exceed a threshold. This treshold is adapted after every detection:

$$treshold_{new} := \frac{1}{2} treshold_{old} + \frac{1}{5}\left[\max - \frac{1}{2}(\min_1 + \min_2)\right] \qquad \textbf{(4-9)}$$

This adaptation stabilises at 40% of the top-top level and has shown good test results for large patient data records from different patients.

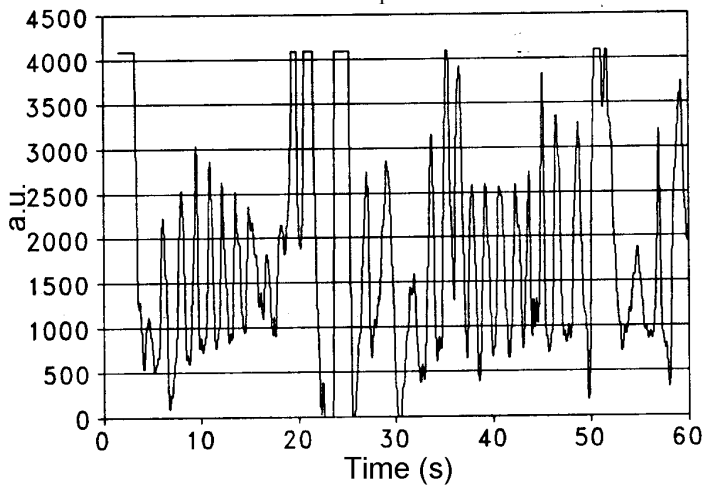

Figure 4-12 A thoracic impedance signal.

In this way the respiratory activity is detected, and during periods of apnoea the heart activity. A simultaneous check on the beat-to-beat heartrate derived from the ECG signal reveals when heart activity is detected.

conclusion

The advantages of the thoracic impedance method:

- No extra apparatus is required. The patient-load is not increased by the measurement;
- It is a non-invasive measurement.

Disadvantages are:

- it is an indirect measurement, that does not assess the actual flow of air (obstructive apnoea may not be detected);
- with an inadequate algorithm heartbeats might be counted as resprirations, especially during apnoea periods;

- the amplitude of the signal is not linearly related to the amount of air being exchanged; moreover, the gain of the signal can be manually adapted by the user/nurse;
- artefacts due to motion have the same order of amplitude and may easily disturb the signal.

The continuous evaluation of the thoracic impedance signal is nearly always routinely done, because of the low patient load. However, the signal has to be interpreted carefully because of the large number of artefacts introduced by the standard algorithm, especially in life threatening circumstances as apnoea periods.

4.3.2 measurements by a thermistor

introduction

The monitoring of the respiration by the thoracic impedance signal alone turns out to be often inadequate. In particular during periods of apnoea the interpretation of the impedance signal is complicated by the heartbeat artefacts in it. figure 4-13 shows an example of the heartrate and respiratory frequency calculated by the monitor in the presence of an apnoea (in this figure at 06:26 h). In these circumstances a better estimate of the actual state of the respiration is strongly desired. Furthermore, information about the actual in- and outflow of air would be more reliable than an indirect measure like the thoracic impedance. Anyhow, the detection of obstructive apnoeas cannot be done properly without information about the airflow. For this reason, we developed a device that enables us to evaluate the respiration of the neonate, also during episodes in which the thoracic impedance signal is contaminated by large artefacts.

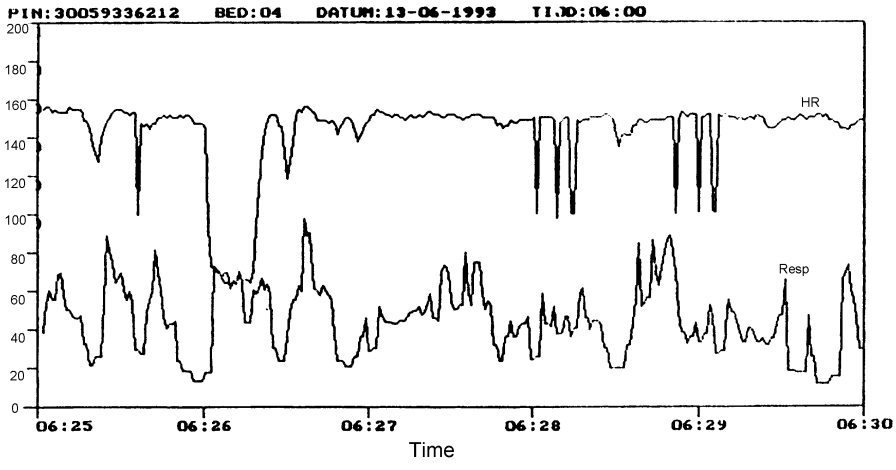

Figure 4-13 Example of heartrate (HR) and respiratory frequency (RES) calculated by the monitor during an apnoea. At time 06:26 an apnoea occurs. However, the monitor holds the heartrate for the respiratory rate and does not notify the apnoea event.

specifications

The thermistor to be realised has to fulfil the following requirements:
Electrical:
The device has to comply with the S3 security rules in the neonatal intensive care unit. An absolute must is the use of a floating potential. The use of a battery is preferred, to ensure independence of the mains voltage and its inherent risks. In that case the power consumption has to be low enough to guarantee an uninterrupted use of 12 hours.

Physical:
The sensor has to be able to register the respiration of the neonate properly. The time constant has to be small enough.

Mechanical:
The manipulation of the sensor has to be easy, and because of the size of the neonate it has to be very small.

Hygienical:
The material of the sensor has to be inert, and may not lead to reactions with the skin or the interior of the nose. Cleaning with alcohol, disinfectants and other means must be possible.

methods

Detection of the respiration may take place either by passive or by active measurement of the temperature of the in- and outgoing air. An example of measurement by an active device is a heated thermistor that is kept at a constant temperature (usually > 100 °C to avoid problems with humidity). The current needed to keep the temperature constant is a measure of the airflow along the thermistor. For reasons of safety and battery consumption we rejected this method. Passive temperature measurement offers the best perspectives, primarily because of its safety.

The temperature of the air in or right before the nose is measured continuously. Usually it is higher during the expiration phase and lower during the inspiration phase. If the incubator has a temperature higher than the temperature of the neonate, the reverse holds.
The sensor should have a very high sensitivity, especially when the temperature in the incubator is close to the body temperature of the neonate. Another complication may be the very low airflow generated by a preterm neonate, being only several millilitres per respiratory cycle. Nevertheless, we expect that a sensor can be developed which is

sensitive enough to measure the minimal differences in temperature between in- and expiration.

realisation

A small NTC resistor was chosen because of its physical size and the small mass, inducing a small time constant. The sensor has a high resistance, R_{25} = 5 kΩ at 25 °C, that limits the load of the battery.

The resistance of the NTC is (inversely) exponentially related to the temperature. The relation can be linearised by integration of the NTC in a resistance network. The following parameters are necessary for the design of the resistance network:

- the value of R_{25}
- the source voltage and the desired voltage at the working point
- the upper and lower boundaries of the temperature range.

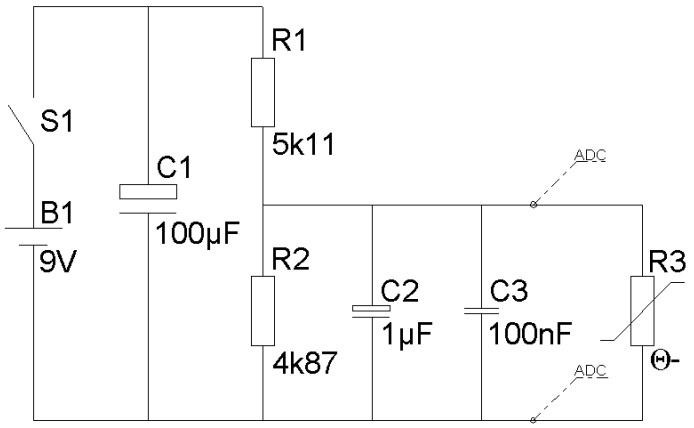

Figure 4-14 The thermistor network.

With these parameters the best linear relation between temperature and resistance is calculated. The relation is described by linear regression. A schematic drawing of the network is given in figure 4-14. C_1 stabilises the power supply, the capacities C_2 and C_3 suppress the noise possibly induced by the cable between the sensor and the network. The resistances R_1 and R_2 are metal film resistors which have a low tolerance and temperature coefficient.

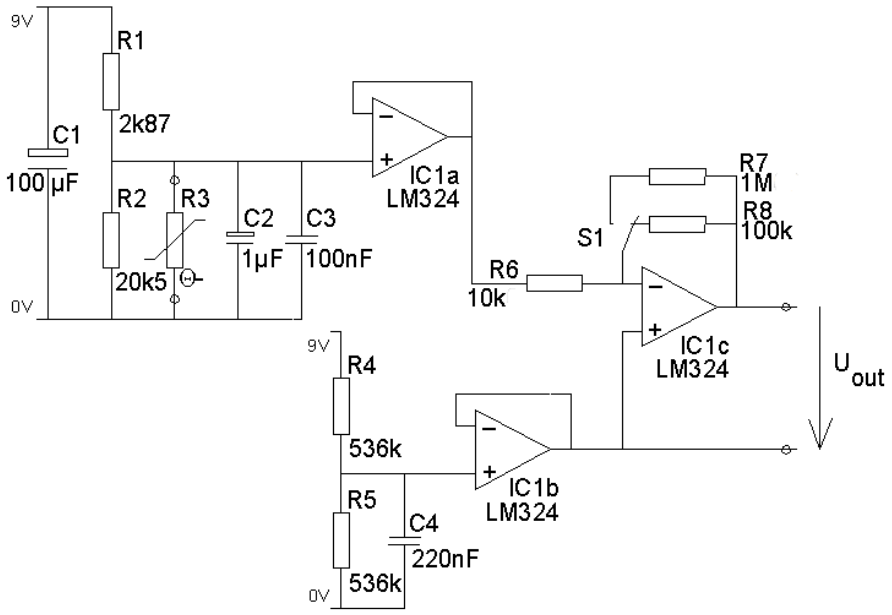

Figure 4-15 The modified scheme of the thermistor.

Although the first test measurements were very promising, a modification has been made to optimally use the input range of the PhyDAS data acquisition system. The desired temperature range of 30 °C to 40 °C has to map on the range -5 V to 5 V. If we use a 9 V battery, a reference voltage of 4.5 V has to be taken to realise the bipolar output. Also the thermistor circuit is equipped with an amplifier of 10 or 100 times, depending on the incoming signal. If the temperature difference between the inspirated and expirated air is low, an amplification of 100 can be used (see figure 4-15). One LM324 is used for the bipolar output, the other LM324's are used as buffer amplifiers.

test measurements

Before operation for measurement of respiration a calibration was performed. The thermistor is calibrated by measurement of the voltage at two different temperatures. The measurement is continued for at least 1 minute to assess the stability. The two temperatures (23.1°C and 36.1°C) have been measured by the temperature module of the HP monitoring system. During the calibration the amplification was 10 times, the battery voltage was 9.28±0.01 V, and the reference voltage was 4.53±0.01 V. A straight line was fitted to the data in the region of interest. It is expressed by:

$$U = -28.213 + 0.822 \times T \qquad \textbf{(4-10)}$$

The accuracy of the temperature measurement is limited by the resolution of the ADC: $2.44 \times 10^{-3} V \div 0.822 V/°C \approx 0.003° C$. The absolute accuracy depends on the accuracy of the temperature calibration. The fluctuations during 1 minute were 4 ADC steps (39 mV), the standard deviation 0.7 steps (1.7 mV).

Before modification the thermistor was tested upon an adult, breathing in a room with an ambient temperature of about 24 °C. In figure 4-16 the result is presented. During the first 40 s normal breathing took place, next the breath was hold after a partial inspiration. The temperature tends to drift to the skin temperature. The last 10 s breathing at a higher frequency took place (50 /min) and the tidal volume was decreased. At 10 s the experimenter swallowed. The insensitivity to movements, often the origin of artefacts, is shown in figure 4-17. From second 0 to 10 normal breathing took place, from 10 to 20 sec shallow breathing took place at a constant frequency. This was repeated in the next interval of 20 s. From 50 to 60 s shallow breathing took place. In the mean time a possible artefact was deliberately introduced by shaking the head. The last 10 seconds the motion of the head was combined with normal breathing. There appears to be only little influence of the movements on the signal.

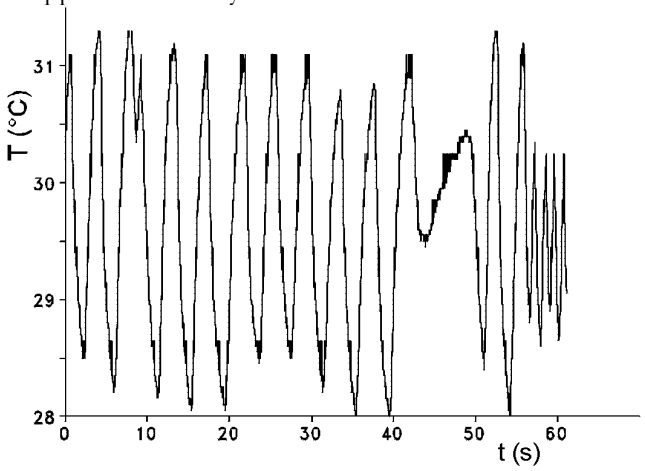

Figure 4-16 Thermistor respiration test

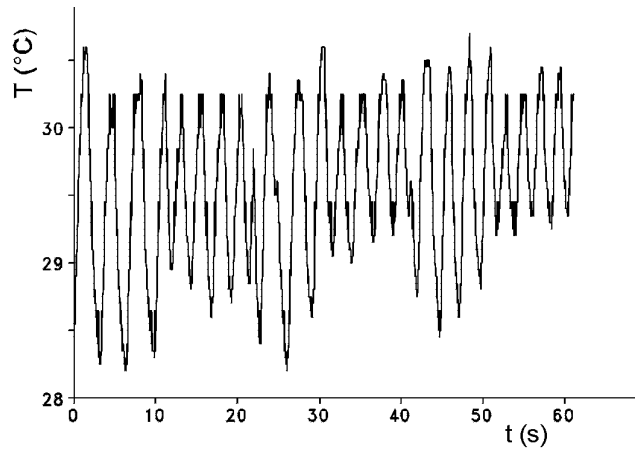

Figure 4-17 Thermistor artefact test

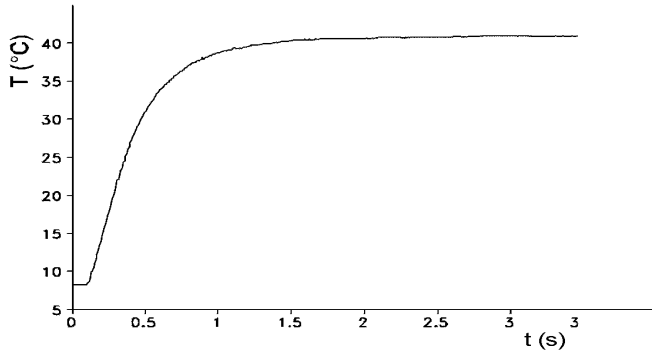

Figure 4-18 Thermistor step response. Note that the range is larger than the range of interest for neonatal breathing.

The characteristic response time τ of the sensor was measured using a step response. The sensor was put from a cold water reservoir (T ≈ 7°C) into a warm water reservoir (T ≈ 42°C) (see figure 4-18). If a first order process is assumed, the characteristic value τ is reached at 63% of the step: T_{begin} = 8.25±0.05 °C; T_{end} = 41.00±0.05 °C. The 63 % value is reached at τ = 0.349±0.004 s. Although, formally the value of τ is a combination of the physical (heat capacity and transport) and electrical (RC-time of 0.01 s) time constants, the data plotted in figure 4-18 suggest that the step response is

dominated by the thermal time constant. In air the heat exchange will be much lower than in water. The resulting increase of τ will also depend on the airflow velocity.

measurements in clinical situation

The device was tested at premature neonates to see whether application in clinical practice is easy and accurate. The following issues were considered:
- position of the thermistor
- registration of normal breathing
- registration during periods of apnoea
- movement artefacts.

Position of the thermistor
A requirement was that the thermistor could be easily attached and fixed, and impairs the neonate as little as possible. We investigated two possibilities: before the nose and in the nose. The advantage of measurement before the nose is that no skin contact is made by the thermistor. The airflow, however, is less than in the nose due to the divergence beyond the end of the nose hole. Measuring in the nose leads to heating of the thermistor by the skin. We compared the amplitudes of both positions in 16 breathing episodes and only found a slight preference for measurement in the nose.

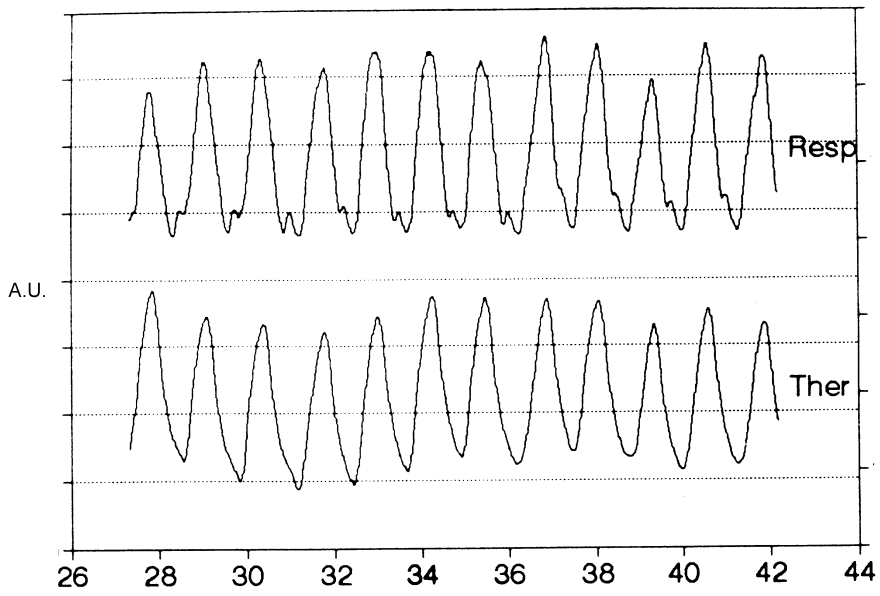

Figure 4-19 Registration of normal breathing using thoracic impedance (upper trace) and thermistor signal (lower trace) (both arbitrary units). In the thoracic impedance a slight distortion caused by heart activity is seen.

Registration of normal breathing

The registration of normal breathing is good, as is shown in figure 4-19. The thermistor values are arbitrary units. A time delay between the signals cannot be observed and is therefore less than 8 ms, the sampling interval time. Note the disturbance by the heart activity in the lower part of the thoracic impedance curve.

Registration during periods of apnoea

The thermistor signal should be able to show periods in which the patient does not breath. When breathing is interrupted we expect the thermistor resistance to drift to an asymptotic value, determined by the temperature of the skin or the environment. In figure 4-20 a short period of non-breathing is shown. In figure 4-21 a one minute registration of an apnoea is shown. The ECG is shown as well, to allow an optimal comparison of the artefacts in the ***Resp*** signal with the heartbeat. In particular, when the heartbeat drops, the influence on the respiratory signal becomes significant. A detailed view of the seconds 20 to 38 is given in figure 4-22. During the apnoea the thermistor signal only shows small fluctuations; the respiratory signal fluctuates with the heartbeat.

Movement artefacts

The thoracic impedance signal is very sensitive to movement artefacts. If the neonate moves or flounders with an arm or leg, the signal is disturbed in such a way that analysis becomes very complicated. The behaviour of the thermistor signal in these circumstances is shown in figure 4-23. In contrast to the impedance signal, the thermistor signal still produces small undulations. The robustness against movement appears to be much better than that of the impedance signal.

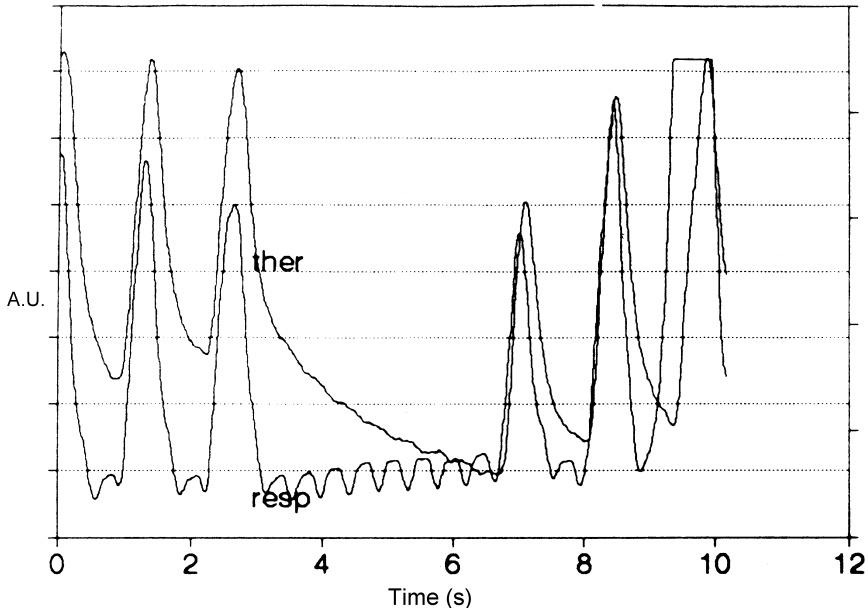

Figure 4-20 A short period of apnoea registrated by the thermistor (ther) and by the thoracic impedance signal (resp) (both arbitrary units). The heartbeat artefact in the thoracic impedance signal is fully absent in the thermistor signal.

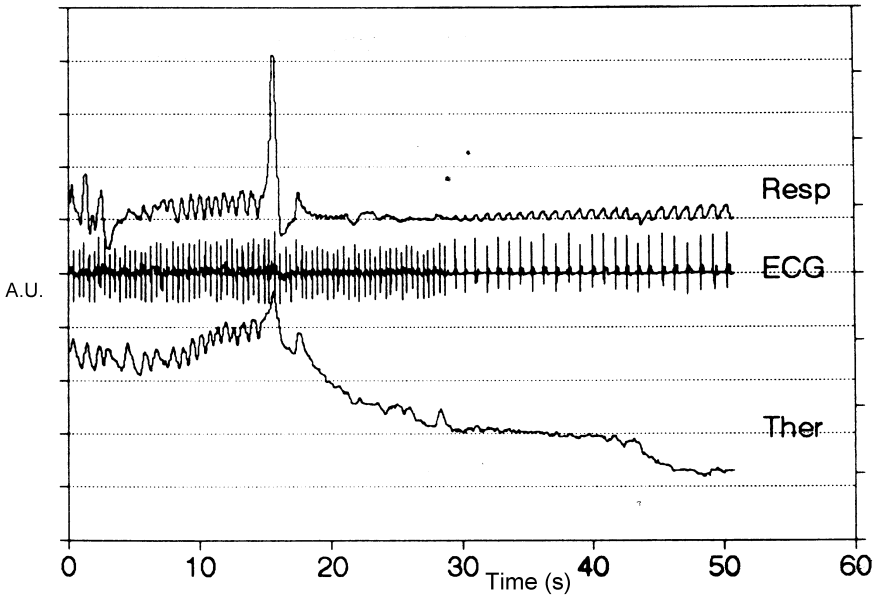

Figure 4-21 Registration of an apnoea. Shown are the thoracic impedance signal (resp), the ECG signal (ECG), and the thermistor signal (Ther) (both arbitrary units). Mind the deep breath at second 16, preceding the apnoea. This phenomenon is observed frequently. A bradycardia starts at second 29.

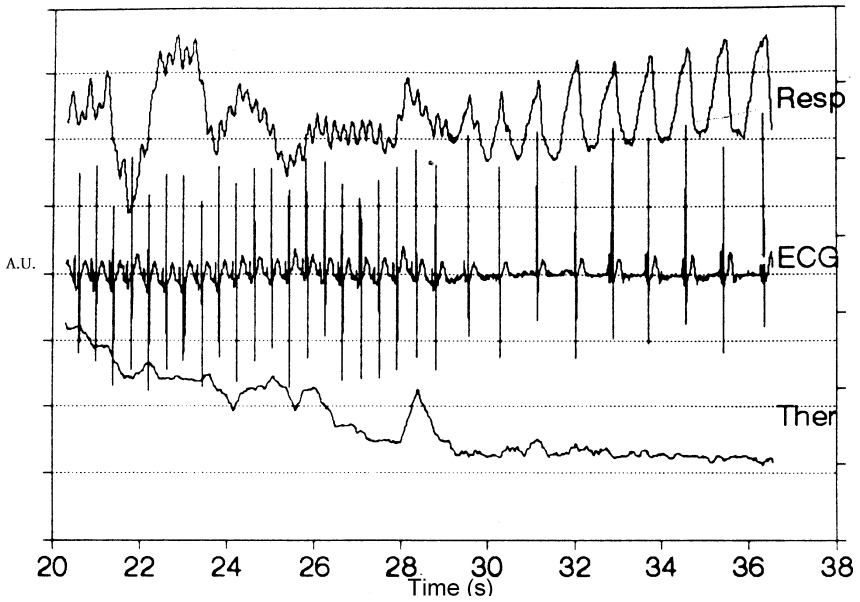

Figure 4-22 A detailed view of the start of the apnoea period.

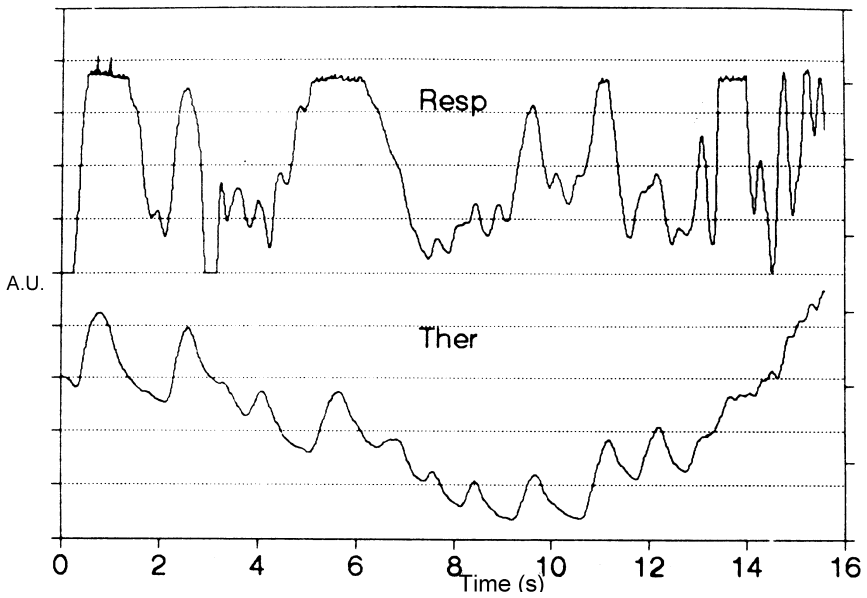

Figure 4-23 Thoracic impedance signal (resp) and thermistor signal (ther) during movement of the neonate.

conclusions

The thermistor device we developed was intended to verify respiratory effort in neonatal circumstances. We conclude that the device is capable to registrate small differences in temperature very accurately in a qualitative way. The dynamic characteristics and amplification meet the difficult conditions at which respiration information is wanted. Because of its little size the device is fast enough to trace the respiration and it is hardly sensitive to limb movements. Particularly in situations where the thorax moves in an effort to breathe, but an obstruction in the upper airways exists, the thermistor signal shows an apnoea (obstructive apnoea).

The thermistor signal is not sensitive to heart activity. This is a strong advantage with respect to the impedance signal.

A disadvantage is that, although the thermistor is very small (∅ = 1 mm), it causes a certain load for the neonate. A thermistor device cannot be used when the neonate breathes by mouth instead of by nose. A thermistor in or in the neighbourhood of the mouth would present a very high load for the neonate and would be too ineffective. Fortunately, almost every child under the age of ½has obligatory nose breathing. In this section, we only scarcely observe behaviour that expresses awareness of the thermistor.

Before every use of the thermistor is has to be cleaned. It is sterilised without problems by immersion in alcohol for 5 minutes, and just before it is brought in the incubator it is again wiped clean by a cloth with alcohol.

4.3.3 detection of apnoea periods

The proper detection of periods in which the neonate does not respirate is very important. If the non-respiratory period (apnoea) lasts too long, nurses intervene and reactivate the neonate, for instance, by touching it with the hand. If the apnoea is caused by a lack of neural input to the respiratory muscles, it is called a central apnoea. If the cause lies in an obstruction present between the mouth and the upper airways of the child, it is called an obstructive apnoea. In neonates the prevalence of a central apnoea is much higher than of an obstructive apnoea.

As we described in section 4.3.1, the interpretation of the thoracic impedance signal might fail during periods of apnoea. This problem mainly arises because the thoracic impedance signal contains heartbeat fluctuations that become dominant when the respiratory fluctuations have vanished. We developed an algorithm that takes into account the interference of the heartbeat and offers real-time respiratory frequency information. This algorithm will be discussed below. A second case where the interpretation of the respiration fails is when an obstructive apnoea occurs. In that case the child strongly attempts to breath. The respiratory attempts make the breast move and the thoracic impedance signal exhibits fluctuations that are interpreted as proper respirations.

signal characteristics

We investigated how the detection of apnoea periods could be improved. For this purpose, we used information from many episodes like figure 4-21 and figure 4-22, registrated from several neonates, in which the signal characteristics are clear: The thoracic impedance shows a small fluctuation induced by the heartbeat; this fluctuation becomes more pronounced when the heartrate decreases due to the bradycardia following the start of the apnoea; the thermistor temperature tends to an equilibrium with only minor noisy fluctuations. The thermistor signal corroborates the fact that no or hardly any air is going in and out.

a preliminary algorithm

It is clear that the beat-to-beat evaluation of the ECG and the thoracic impedance signal can straightforwardly detect identical intervals in ECG and impedance signal. When identical intervals are found, one might conclude that an apnoea occurs. This approach obviously fails when the true respiratory frequency and heartrate are (nearly)

the same. This fortunately is very rare. Detection of an apnoea might also be masked when movement artefacts strongly affect the impedance signal.

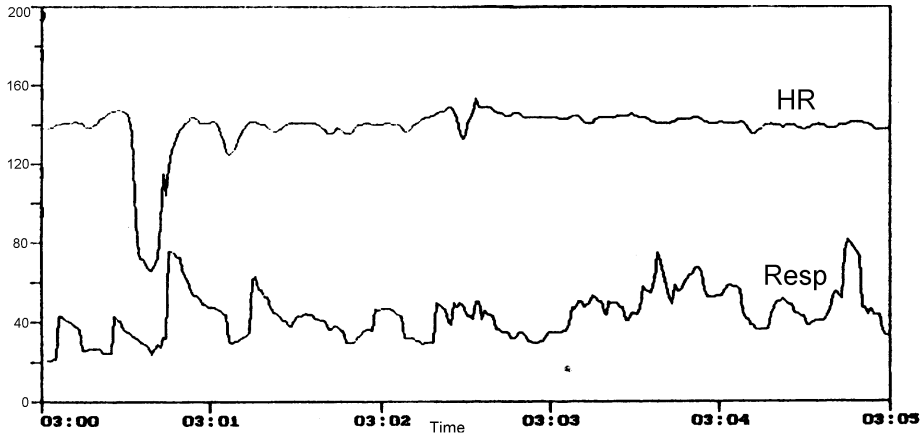

Figure 4-24 *The heartrate and respiratory frequency calculated by the monitor.*

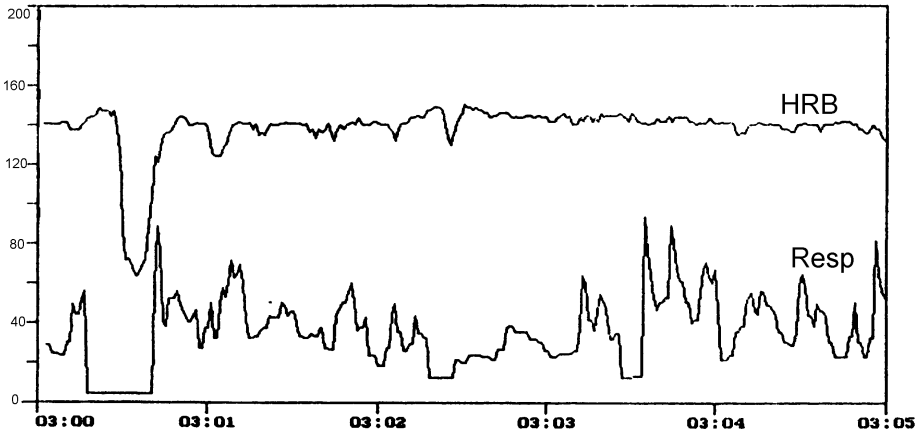

Figure 4-25 The beat-to-beat heartrate and breath-by-breath respiratory frequency calculated by our real-time algorithm.

The algorithm we developed works as follows:
The beat-to-beat heartrate is derived from the ECG; the breath-by-breath respiratory rate is determined from the impedance signal. These two are compared and if they are identical within 5 % an apnoea is supposed to occur. The improved respiratory rate, identifying apnoea periods by a very low respiratory frequency, is added to the standard files in which we keep all parameter values and is updated every second. During detected breathing activity we add the actual value for that second; when the frequency is more than 1/s an average is being taken over a 1 second period. In case of an apnoea, the reciprocal of the apnoea duration is taken to be the respiratory frequency.

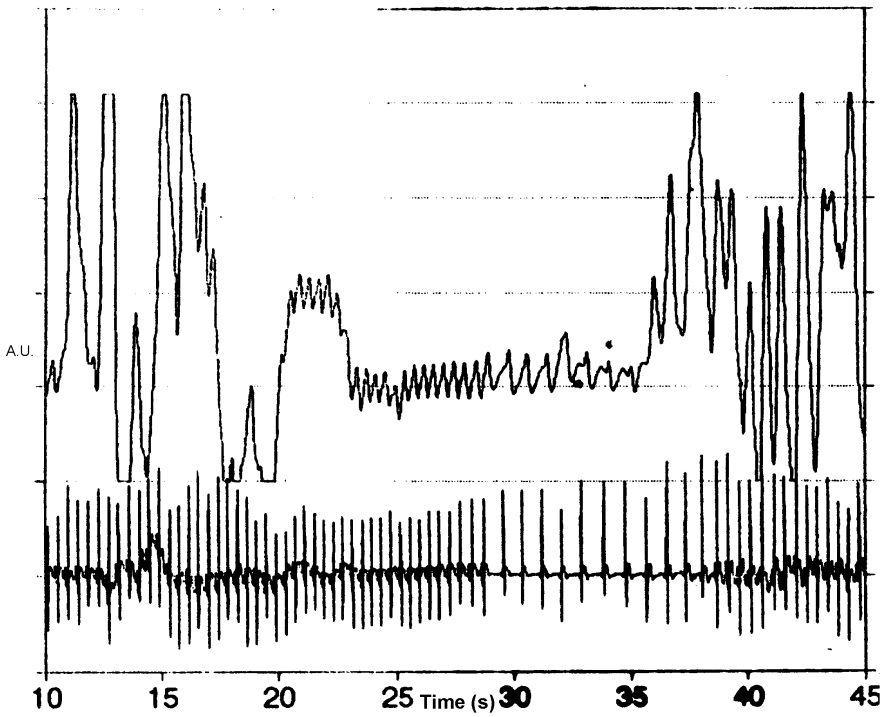

Figure 4-26 ECG and impedance signals during the apnoea and bradycardia plotted in the figure 4-24 and figure 4-25 (time in sec after 03:00).

Results of our real-time algorithm are illustrated by figure 4-24 and figure 4-25. Figure 4-24 shows the heartrate and respiratory frequency as calculated by the monitor and registrated every second, figure 4-25 shows the newly calculated respiratory frequency using the above scheme. As figure 4-26 shows, at second 18 an apnoea truly started.

conclusions

The automatic detection of apnoea periods by the patient's monitors is far from ideal, due to heartrate artefacts in the impedance signal. We showed that the apnoea periods can be detected by an algorithm that compares the beat-to-beat heartrate and respiratory frequency. We checked this approach using many apnoea periods in which also a thermistor measurement was performed, offering the possibility to check that an apnoea really took place. It appeared that even the obstructive apnoeas, during which the heart activity dominates the chest movements in the impedance signal, could be determined with only thoracic impedance and ECG signals. The measurement of an additional thermistor signal is not necessary in those cases.
The automatic (real-time) calculation of the respiratory frequency (or the cessation of respiratory efforts) offers a better respiratory estimate than the respiratory frequency delivered by the patient's monitors.

Literature

Aldridge SA, Gupta JM; Peripheralartery cannulation in newborns; J Singapore Paediatr Soc 34:11-14, 1992

Berne RM, Levy MN; Cardiovascular physiology, Mosby, St. Louis, 1986

Briassoulis G; Arterial pressure measurement in preterm infants; Crit Care Med 14:735-737, 1986

Cohen KP, Panescu D, Booske JH, Webster JG, Tompkins WJ; Design of an inductive plethysmograph for ventilation measurement; Physiol Meas 15:217-229, 1994

Diprose GK, Evans DH, Archer LNJ, Levene MI; Dinamap fails to detect hypotension in very low birthweight infants; Arch Dis Child 61:771-773, 1986

Evans DH, Lark GM, Archer LNJ, Levene MI; The continuous measurement of intra-arterial pressure in the neonate: method and accuracy; Clin Phys Physiol Meas 7:179-184, 1986

Frank, O; Der Puls in den Arterien; Z Biol 46:441-553, 1905

Gardner RM; Direct blood pressure measurement - dynamic response requirements; Anesthesiology 54:227-236, 1981

Genderingen van HR, Gevers M, Hack WWM; Prevention of air introduction in catheter-manometer systems for accurate neonatal blood pressure measurement: an in vitro study; J Clin Monit 10:35-38, 1994

Gevers M, Hack WWM, Ree EF, Lafeber HN, Westerhof N; Arterial blood pressure wave forms in radial and posterior tibial arteries in critically ill newborn infants; J Dev Physiol 19:179-185, 1993

Gevers, M; Arterial pressure wave forms in newborn infants; Proefschrift Vrije Universiteit Amsterdam, 1994

Goldstein RF, Brazy JE; Narcotic sedation stabilizes arterial blood pressure fluctuations in sick premature infants; J Perinatol 11:365-371, 1991

Goldstein R, Brazy JE; Fluctuations of arterial blood pressure decrease with mechanical ventilation in premature infants with respiratory distress syndrome; J Perinatol 10:267-271, 1990

Hack WWM, Westerhof N, Leenhoven T, Okker A; Accurate measurement of intraarterial pressure through radial artery catheters in neonates; J Clin Monit 6:211-216, 1990[a]

Hack WWM, Vos A, Okken A; Incidence of forearm and hand ischemia related to radial artery cannulation in newborn infants; Intensive Care Med 16:50-53, 1990[b]

Hales S; Hemastatiks 1733; New York: Acad Med, Hist Med Ser, Hafner, 1964

Hansen AT; Pressure measurement in the human organism. Acta Physiol Scand (Suppl) 19[68]:1-227, 1949

Hewlett Packard; Automatic respiration monitoring algorithm; Palo Alto: Hewlett Packard, 1984

Hewlett Packard; Component Monitoring System, Service Manual, Palo Alto: Hewlett Packard, M1046-90000, 1988

Hipkins SF, Rutter AJ, Runciman WB; Experimental analysis of catheter-manometer systems. In vitro and in vivo; Anesthesiology 71:893-906, 1989

Kirkendall WM, Feinleib M, Freis ED, Mark AL; Recommandations for human blood pressure determinations by sphygmomanometers; Circulation 62:1146A-1155A, 1980

Kleinman B; Understanding natural frequency and damping and how they relate to the measurement of blood pressure; J Clin Monit 5:137-147, 1989

Langen van H, Brienesse P, Kopinga K, Wijn P: Dynamic response of a neonatal catheter-manometer system in situ; J Clin Monit 9:335-340, 1993

Marey EJ; Physiologie expérimentale. Traveau du laboratoire de M. Marey. Paris, France; in: G. Masson, 388, 1866

McCutcheon EP, Rushmer RF; Korotkoff sounds:an experimental technique; Circ Res 20:149-161, 1967

Miall-Allen VMM, Vries de LS, Dubowitz S, Whitelaw AGL; Blood pressure fluctuation and intraventricular hemorrhage in the preterm infant of less than 31 weeks gestation; Pediatrics 83:657-661, 1989

O'Rourke MF; Arterial function in health and disease; Churchill Livingstone, Edinburgh, 1982

Peñáz J; Photoelectric measurement of blood pressure. In: Digest of the 10th international conference on medical and biological engineering. Dresden, 104, 1973

Perlman J, Thach B; Respiratory origin of fluctuations in arterial blood pressure in premature infants with respiratory distress syndrome; Pediatrics 81:399-403, 1988

Perlman JM, McMenamin JB, Volpe JJ; Fluctuating cerebral blood flow velocity in respiratory distress syndrome: relation to the development of intraventricular hemorrhage; N Engl J Med 309:204-209, 1983

Ramsey M III; Blood pressure monitoring: automated oscillometric devices; J Clin Monit 7:56-67, 1991

Rompelman O, Janssen RJ ; Practical limitations for the estimation of P-wave and QRS-complex occurrence times; Automedica 6:269-284, 1986

Schober PH; Perkutane Kanülierung der Arteria radialis bei schwerkranken Früh- und Neugeborenen; Wien Klin Wochenschr 16:476-479, 1990

Schwid HA; Frequency response evaluation of radial artery catheter-manometer systems: sinusoidal frequency analysis versus flush method; J Clin Monit 4:181-185, 1988

Smith NT, Wesseling KH, Wit de B; Evaluation of two prototype devices producing noninvasive, pulsatile, calibrated blood pressure measurement from a finger; J Clin Monit 1:17-29, 1985

Stocks J, Sly PD, Tepper RS, Morgan WJ, (ed.); Infant respiratory function testing; New York: Wiley & Sons, 1996

Sumner DS; Measurement of segmental arterial pressure. In: Rutherford RB (ed.), Vascular surgery, 2nd ed., Philadelphia (etc.): Saunders, 109-135, 1984

Toubas PL, Duke JC, Sekar KC, McCaffree MA; Microphonic versus end-tidal carbon dioxide nasal airflow detection in neonates with apneu; Pediatrics 86:950-954, 1990

Traube L; Über periodische Tätigkeitsäußerungen des vasomotorischen und Hemmungs-nervenszentrums; Zentralbl Med Wiss, 3:881-885, 1865

Vegfors M; A comparison of new sensors for respiratory rate monitoring; J Clin Monit 8:177-178, 1992

Vegfors M, Ugnell H, Hökss, Oberg PA, Lennmarken C; Experimental evaluation of two new sensors for respiratory rate monitoring; Physiol Meas 14:171-181, 1993

Wareham JA, Haugh LD, Yeager SB, Horbar JD; Prediction of arterial blood pressure in the premature neonate using the oscillometric method; Am J Dis Child 141:1108-1110, 1987

Webster JG; Encyclopedia of medical devices and instumentation; New York, etc.: John Wiley, 1988

Wilks PAD, English MJ; Accurate segmentation of respiration waveforms from infants enabling identification and classification of irregular breathing patterns; Med Eng Phys 16:19-23, 1994

5. Frequency domain analysis of the invasive blood pressure signal

The analysis of the invasive blood pressure signal is useful because of the high amount of information it contains: not only the beat-to-beat blood pressure values, but also natural lower frequency fluctuations that occur in these values. These fluctuations are related to the respiratory mechanics and to interactions mediated by the autonomic nervous system.
The quantification of these fluctuations in a series of systolic or diastolic blood pressure values by spectral analysis is more complicated than in case of standard sampled signals, because the sampling intervals of these values are modulated by the heart rate. A model exists in which this non-equidistant sampling has been taken into account, but conclusions drawn from this model so far only apply to adults. The impact of this model on neonatal data will be outlined and highlighted by several typical examples. Finally, the frequency analysis of the systolic or diastolic blood pressure values will be compared with a direct analysis of the full blood pressure signal. After low-pass filtering of the signal Fourier analysis is performed on a truly equidistantly sampled signal.

5.1 Introduction

The analysis methods of blood pressure variability can be split in two different categories: time domain analysis methods and frequency domain analysis methods. Time domain methods do not transform the whole signal into an alternative representation, but directly act on the signal as a function of time. Going through the signal, in real-time or off-line, several indices are calculated to estimate the characteristics one is interested in. Many different indices have been described, mainly for heart rate variability estimation [Parer et al, 1985; VanGeijn, 1980] Most of them:

- use variations of the mean heartrate between consecutive time intervals
- use a variant of the standard deviation
- use percentile ranges of values derived from the heartrate
- are based on time derivatives of values derived from the heartrate.

Also, most of these indices depend on the length of the time interval chosen to analyse the signal. The large variety of definitions makes comparison of data between different laboratories difficult. The calculation of most of the indices does not require a large computer capacity.

In many cases where spectral information of a measurement series has to be determined, frequency domain methods are used. The frequency methods quantify the power content of the signal as a function of frequency. The well known Fourier transform is often used. The main advantages with respect to other spectral analysis methods are its robustness and generality. These advantages become more

pronounced if little a priori knowledge of the signal is available. A disadvantage is that the signal is often assumed to be equidistantly sampled, periodic, and stationary. Furthermore, frequency components are expressed as multiples of a base frequency, determined by the length of the data set. As a result, Fourier analysis of short data sets of very slowly varying signals (e.g., the beat-to-beat systolic blood pressure signal) may sometimes be inadequate.

Other methods have been developed to estimate the spectra of short data sets of slowly varying signals, like physiological signals. Examples of these methods are: Autoregressive model, Moving-Average model, ARMA model (a combination of the previous two models), Pisarenco spectrum, Prony models, and the Maximum Likelihood model. All these models form a compromise between stability, efficiency, and accuracy. We will not go into them in further detail; a thorough discussion of the pro's and contra's of these methods is presented by Kay and Marple [Kay and Marple, 1981].

In literature on the blood pressure variability, the Fourier Transform and the Autoregressive models are most frequently used. The autoregressive models show the following characteristics [Press, 1988; Kay and Marple, 1981]:

- spectral resolution better than the Fourier Transform;
- suitable for shorter measurement series;
- no side lobes;
- adaptive filtering applications possible;
- peaks in spectra can be better determined than valleys;
- spectral line splitting can occur;
- output is not proportional to the power in a certain frequency range;
- the order has to be determined. The choice of the order puts constraints on the spectrum to be determined.

The last two characteristics are a strong disadvantage. They imply that every analysis has to be done according to a strict protocol if comparisons with other measurements are required. The obtained quantities strongly depend on the estimated order of the calculated model.

Another point forms the patient group on which the measurements are performed. Many reports have been written on the spectral analysis of the blood pressure signal in adults [Parati et al, 1988; Triedman and Saul, 1994; Inoue et al, 1991]. In case of neonatal measurements, however, little methodological background is available. The main differences between adults and neonates with respect to spectral analysis of the blood pressure signal are:

- the frequencies of several processes, appearing in the signal, are higher in neonates than in adults;
- the heartrate variability in neonates is often weaker, probably due to the immaturity of the autonomic nervous system.

The fact that the frequencies in neonates are higher is not so important on itself. Because the heart rate determines the sample frequency of the systolic and diastolic blood pressure values, however, the ratio between the heart rate and the frequencies of the processes we are interested in is an important experimental parameter.

We choose the *Fourier transform* to be able to compare results from spectral analysis with results from other laboratories more directly and straightforwardly than with the other methods mentioned above. It offers a reproducible spectrum, not depending on additional choices or settings.

5.2 Discrete Fourier transforms

For those who are not familiar with the basics of Fourier transformation, we will point out the general characteristics and properties in the next intermezzo.

INTERMEZZO

General characteristics of the discrete Fourier transform

The Fourier transform performs the conversion of a function from the time domain to the frequency domain and vice versa. h(t) is being converted to H(f) or just the reverse. In the continuous form the transforms are given by:

$$H(f) = \int_{-\infty}^{\infty} h(t)\, e^{2\pi i f t}\, dt \qquad \textbf{(5-1)}$$

$$h(t) = \int_{-\infty}^{\infty} H(f) e^{2\pi i f t}\, df \qquad \textbf{(5-2)}$$

The Fourier transform is a linear time invariant transformation. In the continuous form the functions have to be known from -∞ to ∞. In case of sampled signals we will have to use the discrete form.
The function h(t) will be sampled every T seconds to give the discrete function

$$h_k = h(t_k), \qquad t_k = kT, \qquad k = 0,1,\ldots,N-1 \qquad \textbf{(5-3)}$$

If N (even) data points have been sampled, there will be N points in the frequency domain at the values:

$$f_n \equiv \frac{n}{NT}, \quad n = -\frac{N}{2}+1,\ldots,\frac{N}{2} \qquad \textbf{(5-4)}$$

Using equations 3 and 4, the continuous transform (1) can be approximated by:

$$H(f) = \int_{-\infty}^{\infty} h(t)\, e^{2\pi i f_n t}\, dt \approx \sum_{k=0}^{N-1} h_k\, e^{2\pi i f_n t_k} T = T \sum_{k=0}^{N-1} h_k\, e^{2\pi i k n/N} \qquad \textbf{(5-5)}$$

The Discrete Fourier transform (DFT) is defined by

$$H_n \equiv \sum_{k=0}^{N-1} h_k\, e^{-2\pi i k n/N}, \quad H(f) \approx T H_n \qquad \textbf{(5-6)}$$

and the Inverse Discrete Fourier transform (IDFT) is defined by

$$h_k \equiv \frac{1}{N} \sum_{n=0}^{N-1} H_n\, e^{2\pi i k n/N} \qquad \textbf{(5-7)}$$

H_n can be written as $|H_n| \cdot e^{i\varphi(n)}$, with $|H_n|$ the amplitude of component n and $\varphi(n)$ the phase of component n.
Use of the power of spectral components instead of the amplitude is also quite common. The following definitions apply in case of a real signal h(t) or h_k in the time domain:

$$\begin{cases} P_0 = \dfrac{|H_0|^2}{N^2} = \dfrac{H_0^* H_0}{N^2} \\ P_n = 2\dfrac{|H_n|^2}{N^2} = 2\dfrac{H_n^* H_n}{N^2} \end{cases} \qquad \textbf{(5-8)}$$

where H_n^* is the complex conjugate of H_n. In this thesis we chose to use the amplitude instead of the power.
In the explanation of the Fourier transform and its characteristics we will use the convolution of two functions, defined by

$$x[kT] * h[kT] = \sum_{i=0}^{N-1} x[iT]\, h[(k-i)T] \qquad \textbf{(5-9)}$$

with x and h both periodic functions with period N,

$$\forall_{r \in Z} \quad x[kT] = x[(k \pm rN)T] \qquad \textbf{(5-10)}$$

$$\forall_{r \in Z} \quad h[kT] = h[(k \pm rN)T] \qquad \textbf{(5-11)}$$

We will also use the frequency convolution theorem, which states that a multiplication in the time domain is equivalent to a convolution in the frequency domain, and vice versa.

$$x(t).h(t) \Leftrightarrow \frac{1}{N} X(f) * H(f) \qquad \textbf{(5-12)}$$

$$x(k) * h(k) \quad \Leftrightarrow \quad X(f).H(f) \qquad \textbf{(5-13)}$$

The symbol ⇔ denotes (inverse) Fourier transform. The functions on both sides are called a Fourier transform pair. The basic steps of a discrete Fourier transform of a certain function are described in many books [Brigham, 1988, Elliott, 1982, Childers, 1978]. In figure 5-1 we will show the main characteristics of a discrete Fourier transform, illustrated by the corresponding Fourier pairs.

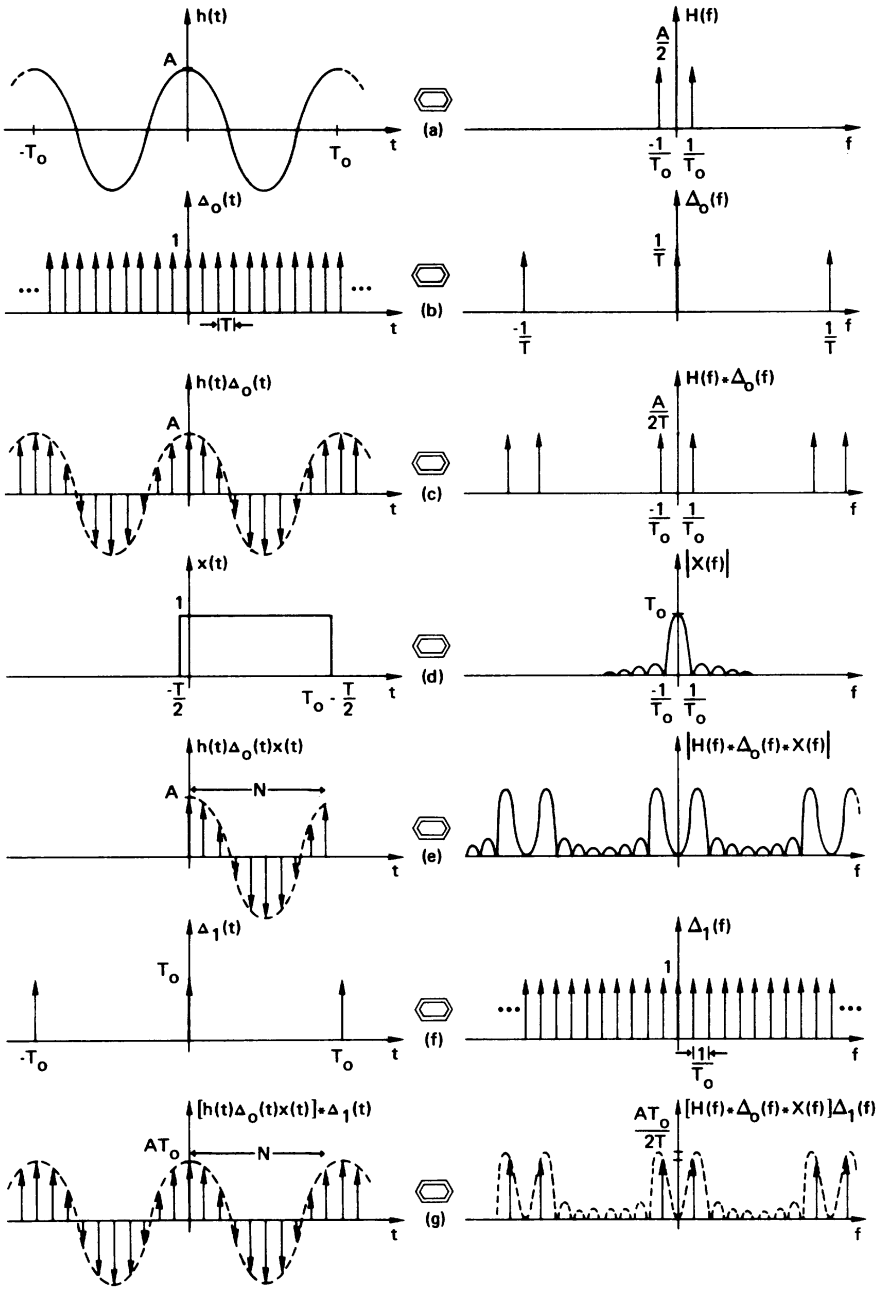

Figure 5-1 Discrete Fourier transform of a band-limited periodic waveform: the truncation interval is equal to one period [Brigham, 1988]. For further explanation see text.

In figure 5-1a we start with a continuous Fourier pair, a time domain function h(t) and its frequency domain representation $|H(f)|$. Sampling of the function h(t) in the time domain can be seen as a multiplication with the sampling function $\Delta(t)$, a series of δ peaks with spacing T, the sample interval time. The frequency domain representation of Δ is shown at the right side of (b). It is also a series of δ peaks, now with spacing 1/T. The result of the multiplication in the time domain is given in (c, left). In the frequency domain a convolution has to be performed of H(f) with Δ. Due to the properties of the Fourier transform of a sum of delta functions, periodicity results in the frequency domain. Next, we truncate the signal in the time domain by multiplication with the rectangular function x(t) (d, left). In the frequency domain the convolution with the corresponding sin(x)/x function (d, right) gives rise to the result given in (e, right). The final step is the discretisation of the frequency domain function: we sample the frequency domain with the sampling function Δ_f (f, right) with sampling interval $1/T_0$. This sampling leads to a periodicity in the time domain (f, left). The sampling of the frequency domain in the time domain corresponds exactly with the cosine components (c), because the truncation interval corresponds exactly to one period of that cosine. Apart from the cosine amplitude components, the sample points in the frequency domain correspond exactly to the zero-crossings of the sin x/x function. The resulting function in the time domain is the "sampled" cosine function given in (g). We see that the discrete Fourier pair consists of a periodic time domain function and a periodic frequency domain function, both consisting of N points. Finally, the amplitude of the spectral components $\sqrt{|H_n H_n^*|}$ can be calculated.

Fast Fourier Transform

A fast algorithm exists to perform the DFT, using a subsequent splitting of the measurement series in 2 equal parts. It requires a number of calculation steps of the order of $N.^2\log N$ instead of the order N^2. The algorithm is called the Fast Fourier Transform (FFT). As a result of the splitting it requires a number of samples equal to a power of two. If the series does not contain the appropriate number of samples one has to either reduce or expand it to a power of two. Expansion to the next power of two can be performed by (linear) interpolation of the values or by zero-padding: adding zeroes to the dataset of the measurement series until a power of two is reached. Ideal interpolation in the time domain would result in zero-padding in the frequency domain; linear interpolation in the time-domain will cause an increase of the number of bins in the frequency domain, although the actual frequency resolution does not increase.

END OF INTERMEZZO

5.2.1 Common distortions of the discrete Fourier transform

Following this general introduction we will discuss four common distortions of the digital Fourier transform, and the consequences they have for our invasive blood pressure signal analysis:

- aliasing,
- spectral leakage,
- errors due to non-equidistant sampling,
- errors due to a lack of stationarity.

Aliasing

The phenomenon called aliasing is illustrated in figure 5-2. The original signal in the frequency domain spreads over a broader band than from -1/(2T) to 1/(2T). The convolution of H(f) with $\Delta_0(f)$ in the frequency domain, resulting from the sampling with interval T, is plotted in figure (c). The frequency components beyond 1/(2T) add to the components below 1/(2T), mirrored with respect to 1/(2T). This effect is called aliasing and is a result of the time domain sampling. To avoid aliasing, the sampling frequency should be at least twice as large as the highest frequency components in the signal (the Nyquist criterion). If a frequency analysis is performed on cardiovascular beat-to-beat values, the Nyquist criterion is violated when frequences above half the heartrate are present (for example, caused by the respiration). The practical consequences of this violation are considered in section 5.4.2. The steps (d) to (g) correspond to those in figure 5-1.

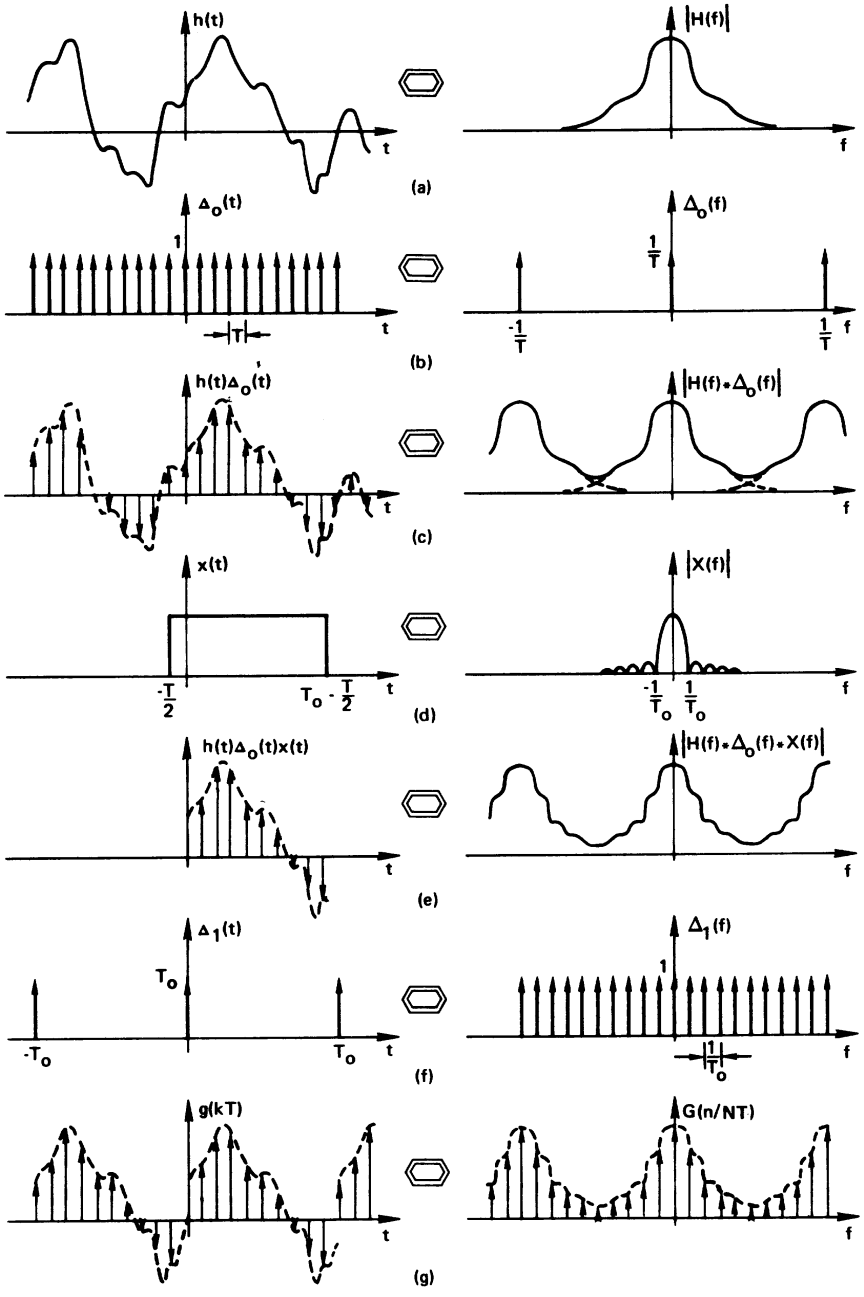

Figure 5-2 Discrete Fourier transform of a general (not band-limited) waveform [Brigham, 1988].

Spectral leakage

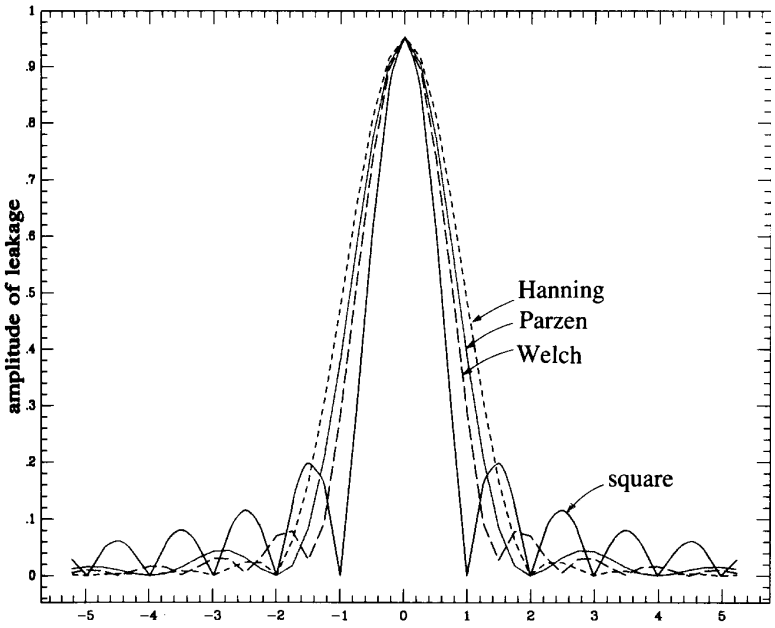

Figure 5-3 The effect of leakage to neighbouring frequency bins for various window functions [Press, 1988]

Due to the discretisation of the frequency domain, the time domain is treated as if it was periodic (see figure 5-1 and figure 5-2). The available signal is supposed to repeat in time infinitely.
If a periodic function is not truncated at the same phase as it starts, the convolution with the sinc function leads to a considerable spread of the spectral components, called spectral leakage. If there is only little a priori knowledge of the frequencies in the signal, spectral leakage cannot be avoided by a proper choice of the truncation interval. In that case leakage can be reduced by the use of a data-weighting function. Instead of a rectangular truncation function in the time domain, with the sin(x)/x function as its transform, another truncation function is used. Well known weighting functions are the Hanning, Hamming, Parzen, or Bartlett window functions. These functions, called lag windows, have spectral transforms that have lower side lobes, but a broader main lobe, than the sin(x)/x function. The leakage in neighbouring frequency bins is presented in figure 5-3. The particular choice for one of the windows is often of minor importance; it is important to use one of them anyhow.

Non-equidistant sampling

In order to apply the Fourier transform, the values have to be equidistantly sampled. However, the evaluation of the beat-to-beat blood pressure or the instantaneous

heartrate is only possible once per heartbeat. As a consequence of the fluctuations of the heart interval, an equidistant sampling is impossible. There are several ways to cope with this problem. In section 5.3 we will outline the consequences of non-equidistant sampling and a way to estimate the spectral changes due to non-equidistant sampling.

Lack of stationarity

A measurement series to be Fourier transformed is assumed to be stationary. A check on stationarity can be performed by splitting the series in N parts and determining the mean and variance of every part. The data can be expected to be stationary if:

- the mean and variance measured during the time intervals do not change with time different from what can be expected for a series of random data, and,
- if periodic variations in the series exist, their periodicity does not change with time.

In mathematical terms a measurement series is called weakly stationary if the mean and autocovariance funtions of a realisation k of it do not depend on t:

$$\mu(t) = \lim_{N\to\infty} \frac{1}{N} \sum_{k=1}^{N} x_k(t) = \mu \qquad \textbf{(5-14)}$$

$$R_{xx}(t, t+\tau) = \lim_{N\to\infty} \frac{1}{N} \sum_{k=1}^{N} x_k(t) x_k(t+\tau) = R_{xx}(\tau) \qquad \textbf{(5-15)}$$

The blood pressure data we use is often not stationary, e.g., due to very slow changes of the mean blood pressure value. Also, if underlying periodic processes change as a function of time, e.g., as a result of the change of a respiratory pattern or as a result of temperature changes, the blood pressure variations will also change.

5.2.2 Accuracy of estimated spectral components

The estimated spectral components of the realisation of a Gaussian white noise process have a standard deviation of 100% [Press, 1988], which is independent of the number of samples. If the number of samples increases, the number of estimated components increases proportionally. As for many physiological data series, the blood pressure signals we analyse can be assumed to be the sum of definite physiological-signal components and the realisation of a Gaussian white noise process. The noise level in our measurements, estimated from the spectra at frequencies where apparently no physiological influence is present, has a value of about 0.04 mmHg. As has been worked out by Jenkins and Watts (1968, p251) for the realisation of a white noise process, the variance of the spectral components is proportional to:

$$\frac{1}{2M} \int_{-M}^{M} w^2(u)\, du \qquad \textbf{(5-16)}$$

with *2M* the width of the window and *w* the time domain window function, the so-called *lag window*.
Using the Parzen (triangular) window, for example, this equation shows that the variance will reduce to 2/3 of the variance using the standard rectangular window. If further smoothing is required one can take the average of *n* neighbouring frequency bins. In that case the $1/\sqrt{n}$ law applies for the reduction of the variance of the components. The same holds for averaging the corresponding frequency components in the estimated spectra of consecutive independent time segments. Optimal reduction of the variance can be achieved using half-overlapping, thus dependent, time segments. Using a Parzen window and *n* segments the reduction becomes (Childers, 1978):

$$\sqrt{\frac{9n-1}{8n^2}} \qquad \textbf{(5-17)}$$

The result of the smoothing is illustrated in figure 5-4.

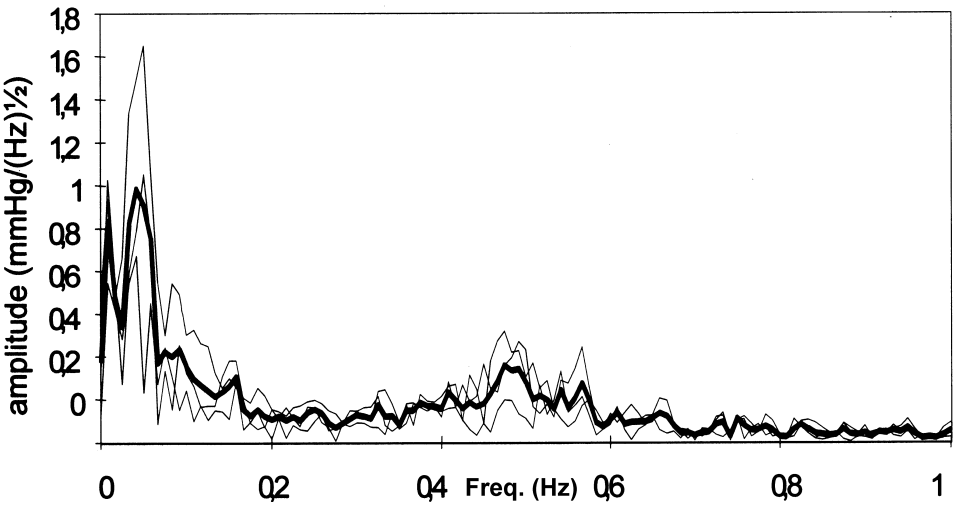

Figure 5-4 Amplitude spectra of three successive data segments and the mean amplitude spectrum (bold).

5.2.3 Linearity

The system is supposed to be linear. Due to the fact that the Fourier transform is a linear operation, it is not suitable to analyse non-linear systems. Generally a nonlinear system will to some extent rectify its input signal (produce a constant term at the output) and will produce several harmonics of the frequencies at its input. With the frequencies f_1 and f_2 at the input, the output will consist of $nf_1 + mf_2$, with *n*,*m* integers. In the interpretation of the spectra this should be realised.

5.3 Non-equidistant sampling

5.3.1 Short introduction to the IPFM model

The systolic and diastolic blood pressure series are both amplitude and frequency modulated. The *amplitude* modulation of the blood pressure values results from respiration and other physiological influences (see section 2.2). The *frequency* modulation is a result of heartrate variability, caused by the influence of the respiration on the heartrate, the so-called respiratory sinus arrhythmia (RSA). Because of the beat-to-beat structure of the data the spectral analysis is not straightforward. In studies on heartrate variability the frequency modulation process has often been described by the Integral Pulse Frequency Model (IPFM) [Rompelman, 1986; Rompelman et al., 1987; Berger et al., 1986; DeBoer, 1985; Hyndman and Mohn, 1975]. That model was proposed to describe the neural modulation of the firing moments of the cardiac pacemaker cells in the SA-node. The model is accepted as a first order description of the frequency modulation induced by the heartrate fluctuations. A theoretical description of an amplitude modulation process combined with a frequency modulation, described by the IPFM model, has been given by TenVoorde et al. in 1994. They did not focus specifically on neonatal data. In section 5.4.2 we will present the results from different calculation methods used on routine neonatal blood pressure measurement series.

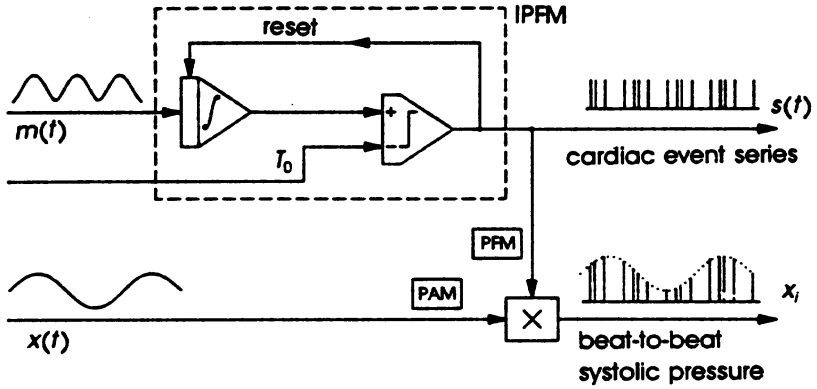

Figure 5-5 IPFM as a model for the cardiac pacemaker. Details can be found in the text. [TenVoorde et al., 1994, Part 1]

The IPFM model is schematically given in figure 5-5. The IPFM generates a pulse series s(t) modulated in repetition frequency by a neural input signal m(t); subsequently, s(t) serves as the sampling function for the continuous signal x(t), that is modulated in amplitude (PAM, in this example the sum of a constant and a sine wave). The samples x_i are the result of a PAM as well as a Pulse Frequency Modulation (PFM) process, and in our application represent beat-to-beat systolic or diastolic pressure values. If we consider the input of the IPFM to be a single harmonic:

$$m(t) = 1 + m_p \cos(2\pi f_p t + \varphi) \quad 0 \le m_p < 1 \qquad \textbf{(5-18)}$$

where m_p is the PFM modulation index (modulation depth expressed as a factor between 0 and 1), f_p the PFM frequency, and φ an arbitrary phase factor, the sample function s(t) and its frequency domain transform can be calculated [TenVoorde et al., 1994, Part 1]. If f_p is smaller than the mean sampling rate $f_0 = 1/T_0$, which is a reasonable assumption for the heartrate variability, the spectrum S(f) consists of three clusters (see figure 5-6):

a) a DC component with an amplitude $1/T_0$;
a) a PFM component at $\pm f_p$ with an amplitude proportional to the modulation index m_p;
a) components at harmonics $k.f_0$ of the mean sampling rate, each surrounded by a cluster of side components at frequencies $k.f_0 \pm n.f_p$. The upper and lower side components have different amplitudes.

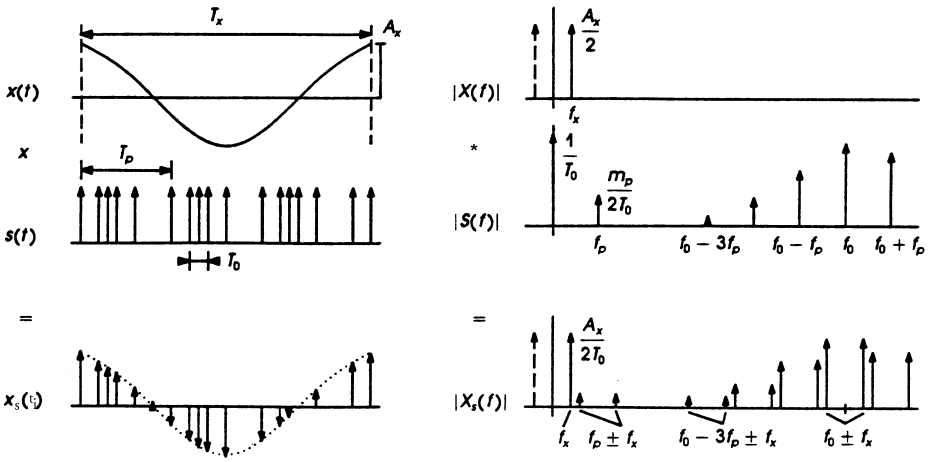

Figure 5-6 Various signals in the IPFM. At the left and right the Fourier pairs of the measurement series, x(t), the sample function s(t), and the sampled data, respectively. In this example the DC offset of x(t), A_0=0. [TenVoorde et al., 1994 Part 1]

If, e.g., *x(t)* is a cosine function with a DC offset A_0, the resulting sampled spectrum consists of a convolution of the PFM sampling spectrum s(t) and the original consine spectral components at $\pm f_x$. The resulting spectral components can be grouped in 4 series:

1. The convolution of the DC component A_0 and the IPFM spectral components implies that the entire spectrum of the sampling function (shown in figure 5-6 in the right-middle) will appear in the spectrum of the sampled signal;
2. The Dirac pulse at $\pm f_x$ represents the main PAM component, equal to the PAM component in the uniformly sampled case (figure 5-6; $X_s(f)$);
3. At the sum and difference of the PFM and PAM frequencies $f_p \pm f_x$, components appear with an amplitude proportional to the PFM modulation index;

4. Side bands appear at the IPFM spectral cluster components $\pm f_x$, around the harmonics $kf_0 \pm nf_p$ $(k,n \neq 0)$.These components may leak into the signal band (the frequencies up to half the mean heartrate), even when the mean heartrate is at least twice the modulating frequency. Several components are shown in figure 5-6; $X_s(f)$.

Table 5-1 and table 5-2 show the calculated amplitudes at circumstances comparable to the PAM and PFM variability in the blood pressure signal. An important constraint is that the PAM and PFM frequencies are taken equal ($f_x = f_p$ = "respiratory rate"), because of the dominant influence of the respiration on both the blood pressure and heart rate fluctuations. In the resulting spectrum a relatively strong DC-component ($f_x - f_p$) is present, and a relatively strong first harmonic ($f_x + f_p$). Also, several side bands around the mean heartrate (f_0) are present down to frequencies below half the mean heartrate. In the methods that we use for the spectral analysis we may expect these frequency components to show up and we have to take care of a proper interpretation of them. As was indicated under a), large spectral components of the sampling function will appear when the signal contains a DC component. To avoid the unnecessary manifestation of these components, and spectral leakage of a DC component in the bins near zero frequency, the signal will always be averaged to zero. If $f_p \neq f_x$, PAM components at frequencies *below* the respiratory frequency f_p are present in the blood pressure signal. In that case, strong components will be present at the frequencies $f_p + f_x$ and $f_p - f_x$. The spectral components around the mean heartrate ($f_0 \pm nf_p \pm f_x$) are less strong (see figure 5-6b).

spectral	component, Hz	spectral	amplitude, V
f_x	0·24	$\frac{1}{2}A_x$	100·000
$f_p - f_x$ $-f_p + f_x$	0·00	$\frac{1}{2}A_x\frac{1}{2}m_p$ $\frac{1}{2}A_x\frac{1}{2}m_p$	20·000
$f_p + f_x$	0·48	$\frac{1}{2}A_x\frac{1}{2}m_p$	10·000
$f_0 - 6f_p + f_x$ $f_0 - 4f_p - f_x$	0·08	$\frac{1}{2}A_xB_{1,-6}$ $\frac{1}{2}A_xB_{1,-4}$	0·079
$f_0 - 5f_p + f_x$ $f_0 - 3f_p - f_x$	0·32	$\frac{1}{2}A_xB_{1,-5}$ $\frac{1}{2}A_xB_{1,-3}$	1·032
$f_0 - 4f_p + f_x$ $f_0 - 2f_p - f_x$	0·56	$\frac{1}{2}A_xB_{1,-4}$ $\frac{1}{2}A_xB_{1,-2}$	8·155
		total:	139·266

Table 5-1 Table of analytically computed components of a sinusoï d sampled at a frequency modulated rate $f_p=f_x=0.24$ Hz; $f_0=1.28$ Hz; PFM index $m=0.2$; DC level $A_0=0$. [TenVoorde et al., 1994 Part 1]

spectral component,	Hz	spectral amplitude	V
f_x	0·10	$\frac{1}{2}A_x$	100·000
$f_p - f_x$	0·14	$\frac{1}{2}A_x\frac{1}{2}m_p$	10·000
$f_p + f_x$	0·34	$\frac{1}{2}A_x\frac{1}{2}m_p$	10·000
$-f_0 + 5f_p + f_x$	0·02	$\frac{1}{2}A_xB_{-1,5}$	0·066
$f_0 - 5f_p + f_x$	0·18	$\frac{1}{2}A_xB_{1,-5}$	0·002
$f_0 - 4f_p - f_x$	0·22	$\frac{1}{2}A_xB_{1,-4}$	0·080
$f_0 - 4f_p + f_x$	0·42	$\frac{1}{2}A_xB_{1,-4}$	0·080
$f_0 - 3f_p - f_x$	0·46	$\frac{1}{2}A_xB_{1,-3}$	1·030
		total:	121·258

Table 5-2 Table of analytically computed components of a sinusoï d sampled at an amplitude modulated rate of f_x=0.10 Hz and a frequency modulated rate of f_p=0.24 Hz; f_0=1.28 Hz; PFM index m=0.2; DC level A_0=0. [TenVoorde et al., 1994, Part 1]

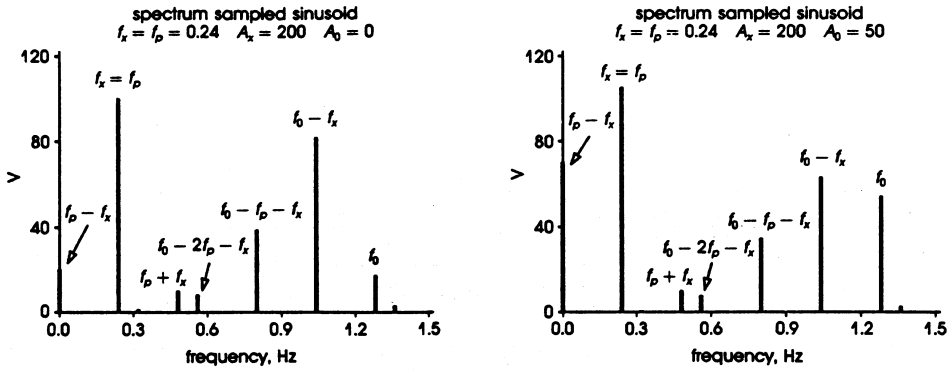

Figure 5-6b Spectral components without (left) and with (right) DC level [TenVoorde et al., 1994, Part 1].

5.3.2 Frequency analysis of non-equidistantly sampled signals

The frequency analysis of the systolic or diastolic blood pressure data can be performed in several ways. The heartbeats can be seen as a series of events, taking place at certain points in time. Rompelman [1982] and De Boer [1985] already published algorithms to estimate the spectra of these heartbeat series and called them respectively the "sparse discrete Fourier Transform (SDFT)" and the "spectrum of counts". TenVoorde [1994] also used these algorithms on blood pressure data. Not only the occurrence times of the systolic (or diastolic) blood pressure values itselves were used, but a "weight" was attributed to them to account for the blood pressure value and/or the interval time. The methods that are described in this section, differ in the way in which these values and interval times are accounted for [TenVoorde, 1994, Part 2].

The first transform is called the Sparse Discrete Fourier Transform and is calculated according to the following definition:

Given a signal described by a sum of Dirac delta pulses,

$$p(t) = \sum_l \delta(t - t_l) \qquad \textbf{(5-19)}$$

the spectral power can be described by

$$P_C(k\Delta f) = \frac{2}{T} X_C(k\Delta f).X_C^*(k\Delta f)$$

with $\Delta f = 1/T$, T being the total record time, and with

$$X_C(k\Delta f) = \int_{-\infty}^{\infty} p(t).e^{-2\pi j k \Delta f t}\,dt = T_0 \sum_{i=1}^{N} e^{-2\pi j k \Delta f t_i} \qquad \textbf{(5-20)}$$

In equation (20) only the times of occurrence t_i of the Dirac delta pulses are used; the transform only estimates the PFM spectrum of the data series (PFT, see figure 5-7a).

In the second method the pulses are weighted by the sample value x_i. The width of every pulse is taken the same, so it is weighted according to its blood pressure value. The actual occurrence times t_i of the pulses are used. The transform is called the equal width Fourier transform (EFT, figure 5-7b):

$$X(k\Delta f) = T_0 \sum_{i=0}^{N-1} x_i e^{-j2\pi k \Delta f t_i} \qquad \textbf{(5-21)}$$

Δf is taken equal to 1/T, the reciprocal of the total record time; T_0 is the mean sampling time interval.
The third method weighs each pulse according to both the sample value and the succeeding interval length $T_i = t_{i+1} - t_i$. The algorithm is called the rectangular integration Fourier transform (RFT, figure 5-7c):

$$X(k\Delta f) = \sum_{i=0}^{N-1} T_i x_i e^{-j2\pi k \Delta f t_i} \qquad \textbf{(5-22)}$$

The mean interval length T_0 is replaced by T_i, the actual interval.
The last method assumes the samples to be equidistantly distributed at time points iT_0, and is known as the normal discrete Fourier transform (DFT/FFT, figure 5-7d):

$$X(k\Delta f) = T_0 \sum_{i=0}^{N-1} x_i e^{-j2\pi k \Delta f i T_0} \qquad \textbf{(5-23)}$$

In this method the non-equidistantly sampled blood pressure values are treated as if they were equidistantly sampled: the interbeat interval variations are simply ignored.

Using the DFT, several approaches are frequently used to assign a value to every equidistant sample point in time:

- clipping: at every equidistantly separated time point the last known value is taken. At every heartbeat this value is "updated"; this corresponds to a zero-order hold circuit, containing systolic (or diastolic) blood pressure values;
- low-pass filtering: at every equidistantly separated time point the filtered output signal of the zero order hold circuit is taken. Often, the cut-off frequency is taken of the same order as the mean heart rate [Jaffe, 1994].

It is obvious, that all three methods introduce changes of the original signal, which may lead to different results.

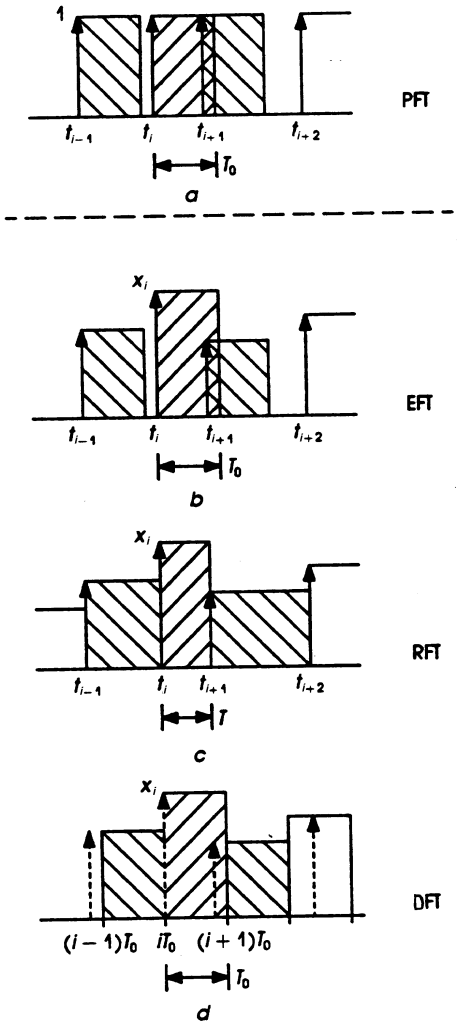

Figure 5-7 Different discrete implementations of the Fourier transform: (a) represents the pulse-modulated event series itself, i.e. the time instants at which the samples are taken; (b)-(d) the other three Fourier transforms EFT, RFT and DFT, respectively.

The Lomb periodogram

A completely different method for the spectral analysis of unevenly spaced data was developed by N. R. Lomb [Lomb, 1976, Press 1988]. The "Lomb method" evaluates data, matching them to sines and cosines, only at the times t_i that they are actually measured. The method was originally developed for use in astronomy, where often missing data occur and the measurement events often cannot be chosen. The Lomb method also enables us to calculate a level of significance related to Gaussian random data.

5.3.3 Direct Blood pressure filtering method (BPF)

In all previously mentioned methods the problem of a relatively low sampling frequency has to be managed. The mean sampling frequency equals the mean heart frequency if only the systolic or diastolic blood pressure values are used in the calculations. The blood pressure signal itself, however, can be sampled equidistantly with a frequency of about one hundred Hertz and contains reliable information up to the cutoff frequency of the Catheter Manometer System (see section 4.1.3). In that case, no problems will occur because of aliasing or the sample points being non-equidistant.
A direct Fourier transform of the complete blood pressure signal requires 100 seconds of that signal to be transformed if a frequency resolution of 0.01 Hz is required. Apart from this, the harmonics of the blood pressure base frequency are 20 to 500 times as intense as the low-frequency power that is sought for. Therefore, the amplitude of the spectral components in the low-frequency part of the spectrum can easily be dominated by spectral leakage of the first harmonic. Although the latter problem can be eliminated by using a carefully chosen window function, it is much more efficient to use a low-pass (digital) filtering of the blood pressure signal immediately after the sampling, leaving only the desired low-frequencies in the resulting signal.

An ideal low-pass filter will have the following form:

$$G(f) = \begin{cases} 1 & if \quad |f| < f_{cut} \\ 0 & if \quad |f| \geq f_{cut} \end{cases} \qquad \textbf{(5-24)}$$

If $f_{respiration} < f_{cut} <$ "heartrate", the influence of respiration on the signal will be unattenuated after filtering. Resampling the filtered signal with a frequency $f_{sampling} > 2 \cdot f_{cut}$ will result in an equidistantly sampled signal with all components up to f_{cut} left in it. The implementation of a filter resembling G(f) to a large extent is described in the next section.

The decision to analyse the full blood pressure signal instead of the beat-to-beat sytolic or diastolic values only, is a fundamental choice. Every value in the blood pressure cycle expresses a characteristic value of the pressure in that particular phase of the cycle. If a blood pressure wave is considered to be a measurement result of one process, it is a complex process. Many underlying physiological variables change during the cycle: the vascular tension, the filling of the heart, the blood flow, and the cross-section of the blood vessels. From that point of view values measured in the same phase of the cycle (e.g., systolic or diastolic pressure) can be compared more straightforwardly, because many of the underlying physiological variables are in the same state. If a frequency analysis of the full blood pressure signal is performed, sum and difference frequencies may show up from processes that have a different influence in different phases of the blood pressure.
A more practical reason for the initial choice to analyse only systolic or diastolic blood pressures was the available calculation power. Nowadays, the computing power is considerably larger, which in principle enables an on-line analysis of the full blood pressure signal.

A preliminary filter design

The implementation of a discrete filter G_n approximating $G(f)$ can be done in several ways. The method we follow is straightforward but not very elegant; in future implementations a more elegant but functionally equivalent method can be chosen [Brigham, 1988; Van den Enden, 1987; Oppenheim and Schafer, 1975; Rabiner and Gold, 1975]. The multiplication of the signal in the frequency domain with G_n corresponds to a discrete convolution in the time domain with the inverse Fourier transform of G_n, denoted by g_j:

$$(g*x)_k = \sum_{j=0}^{N-1} x_{k-j}\, g_j \qquad \textbf{(5-25)}$$

To evaluate the convolution, N samples of the function x_i have to be available that preceed the sample x_k. If that is not the case, 'transient' effects will occur at the beginning of the convolution result. We avoid these effects by using a dataset that is large enough and by limiting N.
The ideal function G_n is a block function (ideal low-pass filter); its inverse Fourier transform is a sinc-function. We limit the sinc function g_j to b points. To do so we multiplied the ideal sinc function with a block function of width b. In the frequency domain this corresponds to a convolution of the desired ideal function G_k with a sinc function with amplitude b at f=0 and zero crossings at $f = m/b$ ($m \in \mathbb{Z}$). The resulting behaviour of the low pass filter G_n is given in figure 5-8. The behaviour at the cut-off frequency is steeper when the sinc function width b is larger. If we use a sinc function with a width of 40 zero-crossings and a cut-off frequency of 1.8 Hz its width has to be $40/1.8 \approx 22$ seconds. With a sample frequency of 100 Hz this corresponds to a number of data points of 2200.

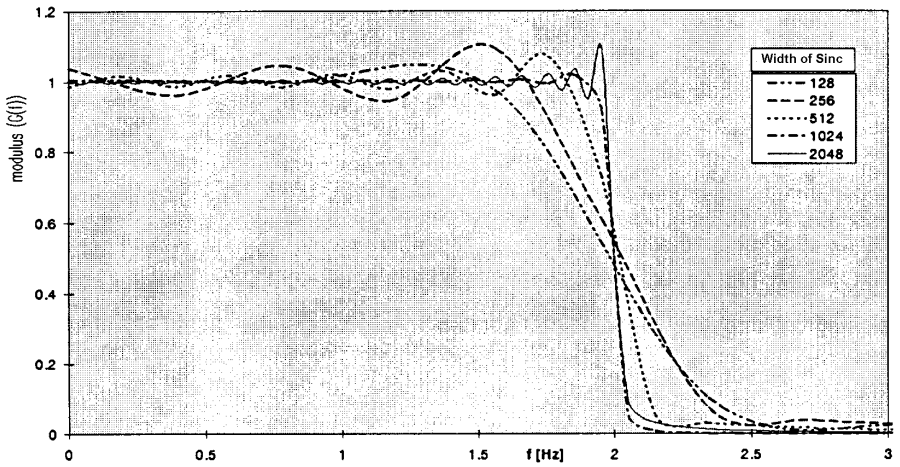

Figure 5-8 Approximation of the block filter for various values of the width of the sinc function in sample points. The sample frequency is 100 Hz and f_{cut} = 2 Hz.

In order to perform the filtering (convolution) operation, the blood pressure signal is split in data segments of 32+b seconds, overlapping a width b/2 with the previous and next segment. This leads to a 32 second filtered blood pressure signal without 'transient' effects.

The filtered signal is now resampled every 0.25 s (4 Hz). This is an equidistant sampling without aliasing if we assume that no substantial power is left above 2 Hz, the Nyquist frequency. The resampled signal can be analysed using the standard DFT procedure described in section 5.2.

If one decides that the filtered signal only has to be available at the instants in time corresponding to the resampling period, the filtering (convolution) only has to be performed for these instants in time. This yields approximately a factor 25 reduction in calculation time.

5.4 Real-time analysis in practice

The theory presented above offers various possibilities to compute the Fourier transform of a typical physiological data set. In this section we will show the differences between the presented algorithms when used on routinely neonatal data series. An important point is the requirement to perform the analysis in real-time. Although all analyses ran off-line during development, they have to perform in real-time when implemented definitively.

5.4.1 Digital Fourier Transforms in practice

The following description gives a summary of the procedure for the frequency domain analysis of the beat-to-beat blood pressure signal, using one of the Fourier Transforms described in section 5.3.2. The Lomb method was applied on the beat-to-beat values without additional processing.

1) raw input of the blood pressure signal, every heartbeat a value
2) smoothing of the instantaneous values with a rectangular moving window
3) resampling of the values equidistantly in time
4) application of a leakage window
5) subtraction of the DC offset
6) suitable spectral analysis (DFT, EFT, RFT)
7) correction for the applied leakage window
8) correction for the applied rectangular moving window
9) inspection of the spectra (take care of aliasing; analyse possible sum and difference frequencies)

1) In the sampled blood pressure signal the set of systolic or diastolic blood pressure values and the times at which they occur are determined. For this purpose, the time corresponding to the sample with the highest or lowest blood pressure during one heartbeat is taken (section 4.1.3). No further curve fitting to increase the accuracy of the systolic or diastolic blood pressure values and their occurrence times is done. Because of the fact that the blood pressure is a relatively slowly varying wave, the resulting increase in accuracy would be of little significance compared to the variability to be measured.

2,3) The raw signal of systolic or diastolic blood pressures is smoothed using a rectangular window having a width of $2/f_s$, where f_s is the frequency at which the signal will be resampled. The window is centered at the sample point. The smoothing is equivalent to a convolution of the raw signal with a rectangular function having a width $2/f_s$ and height 1. The (continuous) frequency spectrum of the signal that will be resampled thus consists of the original spectrum multiplied by the Fourier transform of the rectangular window (a sinc function). The frequency of resampling has to be higher than or equal to the instantaneous heartrate, otherwise aliasing will be introduced.

4) The Discrete Fourier Transform assumes the time signal to be a periodic signal with period T_0. If the frequencies of the signal in the time domain do not fit in the interval T_0, a discontinuity occurs at the end of this interval. This may also be caused by a drift in the signal. The discontinuity causes leakage of power into neighbouring frequency bin(s). To reduce this leakage an appropriate lag window is used.

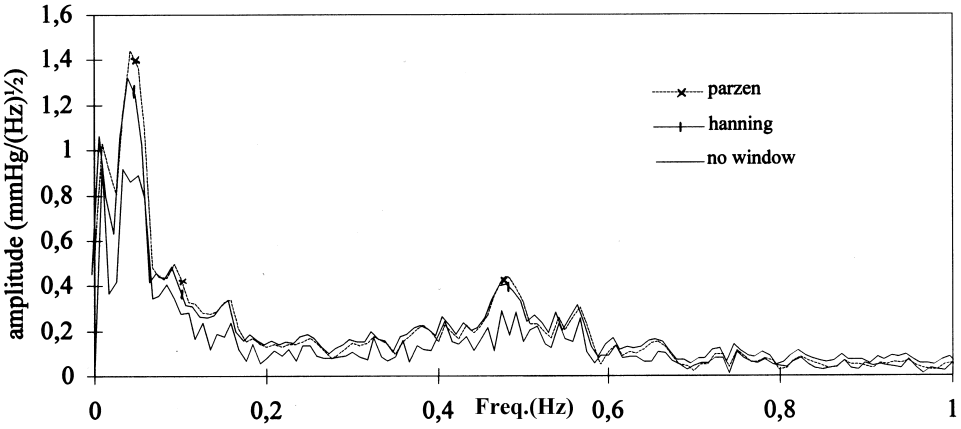

Figure 5-9 Amplitude spectra resulting from the use of different time windows: None (square), Parzen, and Hanning.

We compared the effect of three commonly used windows on a representative series of blood pressure signals. The resulting change in the spectrum is given in figure 5-9. We choose to use the Parzen window, but in our application any other window would do as well. The choice to use a window instead of not using one is more important than the particulare choice for a Parzen window. As figure 5-9 illustrates, the use of any of the mentioned windows reduces the leakage of power to neighbouring frequency bins, which has a large effect at very low frequencies.

5) The mean of the signal is subtracted to eliminate the DC-offset from the signal as good as possible. The DC-offset causes a very high power at frequency zero, which leaks into the neighbouring bin(s) if a non-rectangular lag window is used. When the DC-offset is removed this leakage will be avoided. Some researchers also remove the lowest frequency components and a possible drift by subtraction of a linear trend [DeBoer, 1985].

6) Perform the spectral analysis.

7) The application of a time window reduces the total power of the signal. The correction to be made consists of the division of every frequency component (complex number) by the mean value of the time window. The correction is independent of the frequency.

8) To correct for the rectangular moving window, all frequency components have to be divided by the frequency domain amplitude (Fourier transform) of the rectangular window used for the smoothing. This Fourier transform is a so-called sinc function (see figure 5-1). A reliable correction cannot be made

at frequencies where this function approaches zero. Normally, however, the region of interest is confined to frequencies well below this point. If not, the window has been chosen too large. Note that higher frequency components that might be present in the signal will be suppressed by the moving average filter. If they leak into the signal band (aliasing), at least their magnitude has been reduced.

9) Aliasing can be expected if the respiration frequency approaches the half of the heartrate. If an appreciable amount of energy is present in the spectra near or above half the mean heartrate, aliasing is likely to occur. The real and imaginary spectral components around this frequency and those around the 'mirror' frequency are added, thus resulting in an incorrect estimation of the power.

5.4.2 Evaluation of neonatal data

We will investigate the differences occurring in practice using the different Fourier transform methods (EFT, RFT, and DFT see section 5.3.2), the filtering method BPF (see section 5.3.3), and the Lomb method.
The Fourier algorithms need the beat-to-beat blood pressure values and the corresponding beat-to-beat time stamps of the occurrences of a heart beat. The BPF method uses the full sampled blood pressure signal.

From 55 acquired episodes of neonatal signals (blood pressure, ECG, and thoracic impedance) 7 episodes of 64 seconds were selected to evaluate the algorithms. The criteria for selection were:

- the availability of all three signals,
- lack of artefacts,
- known medication.

The last two episodes are from a patient with a relatively high heartrate variability. They were selected to investigate explicitly the effect of a high modulation of the blood pressure sampling frequency. Also, an episode with a respiratory frequency higher than half the mean heartrate was included to illustrate the effect of aliasing. The characteristics of the patients are summarised in table 5-3.

PIN	episode number	time of acquisition	bed number	age post partum (d)	approx. heartrate (Hz)	approx. respiratory freq. (Hz)	HRV (%)
16049634219	1	960422: 1240	12	6	2.3	0.40	1.7
17039615210	2	960326: 1030	8	9	2.3	1.13	2.2
21039675217	3	960325: 1734	12	4	2.2	0.5	2.4
19049514210	4	950424: 1044	7	5	2.3	1.5	2.3
19129475211	5	941223: 1116	2	4	2.66	0.83	2.0
25059523214	6	950529: 1256	10	4	2.25	0.39	5.1
25059523214	7	950529: 1300	10	4	2.3	0.39	4.0

Table 5-3 The main characteristics of the patient data. The HRV (%) stands for the relative heart rate variability: Ö2 times the quotient of the standard deviation of the heart intervals and the mean heart interval during the episode.

The results of the analyses are shown in figure 5-10 to figure 5-16. In all spectra smoothing was performed using the average of the spectral components with the 3 preceding frequency bins. Inspection of these figures reveals that the spectrum of the BPF signal, the only one certainly not affected by aliasing, often differs from the spectra resulting from the other algorithms. In all the cases the EFT and RFT curves almost coincide. The DFT shows slightly different values, but displays roughly the same maxima and minima as the EFT does. A description of the differences in detail per episode is given below (see table 5-3 for the approximate heartrates and respiratory rates).

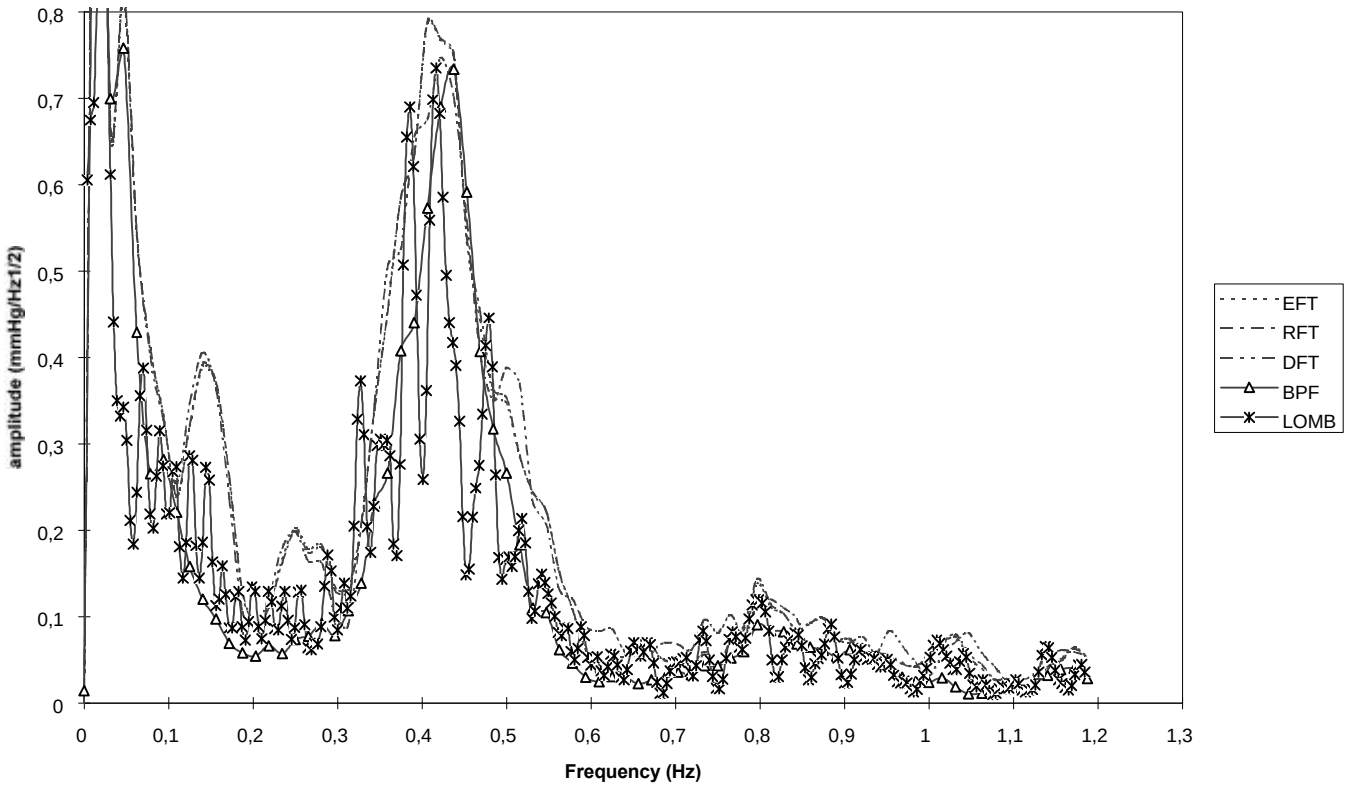

Figure 5-10 Spectrum of the systolic blood pressures of episode 1 using the EFT, RFT, DFT, BPF, and LOMB algorithm; the BPF algorithm (digital filtering) used the full sampled signal.

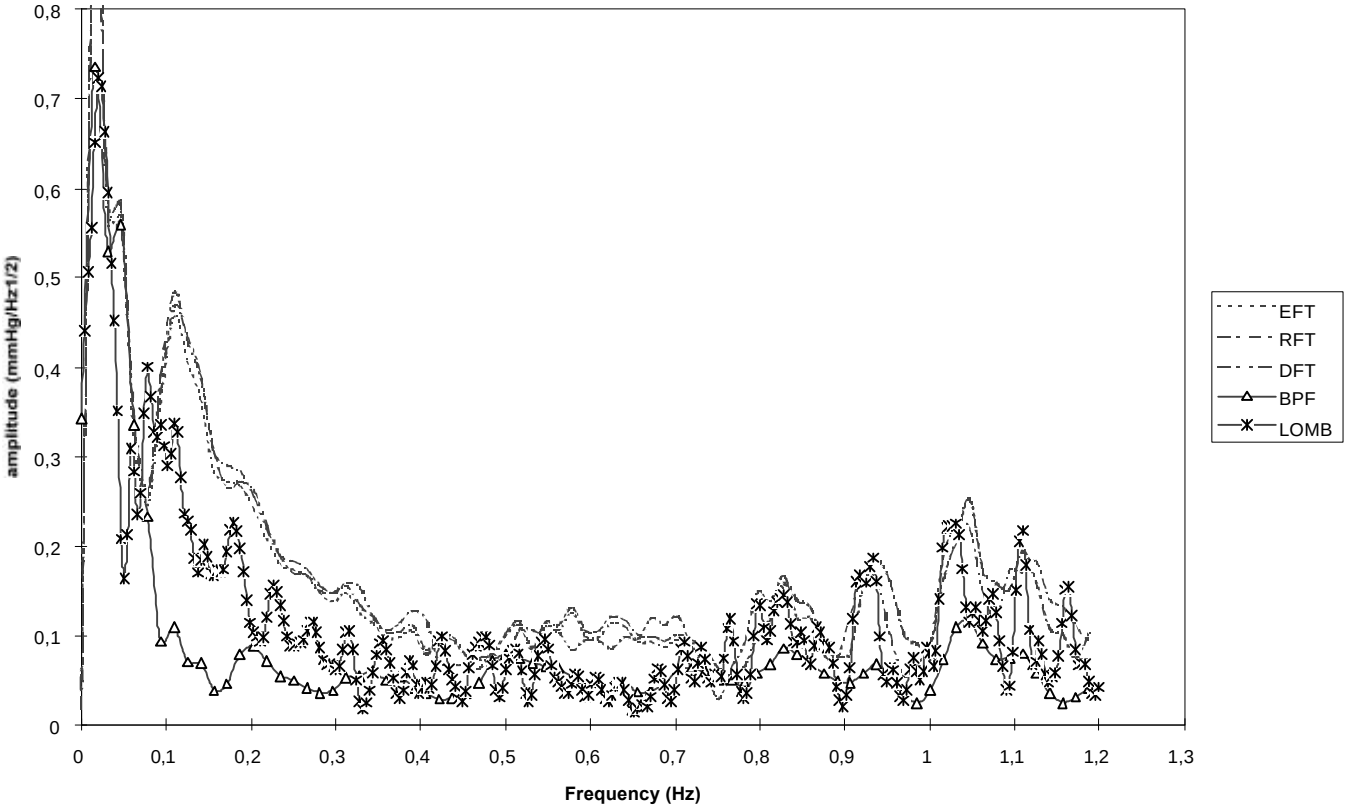

Figure 5-11 Spectrum of the systolic blood pressures of episode 2 using the EFT, RFT, DFT, BPF, and LOMB algorithm; the BPF algorithm (digital filtering) used the full sampled signal.

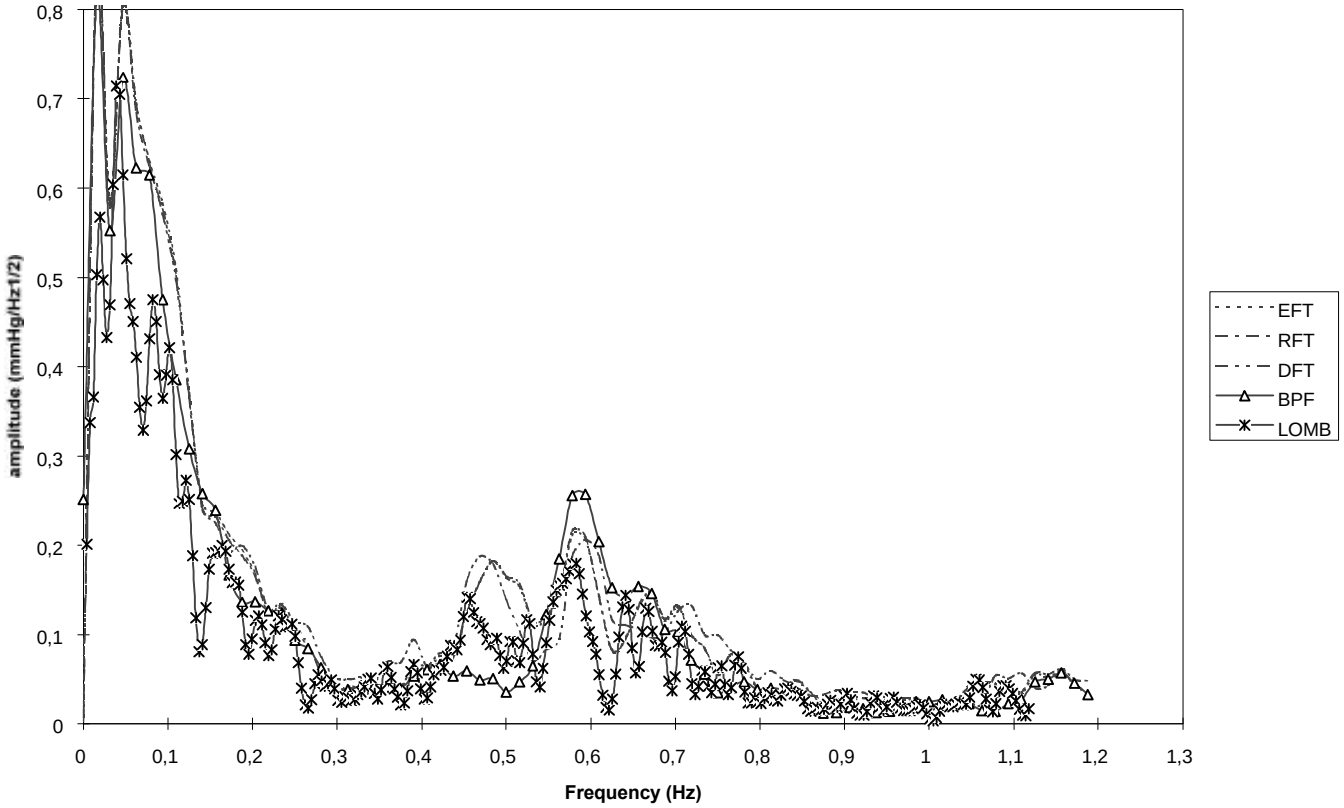

Figure 5-12 Spectrum of the systolic blood pressures of episode 3 using the EFT, RFT, DFT, BPF, and LOMB algorithm; the BPF algorithm (digital filtering) used the full sampled signal.

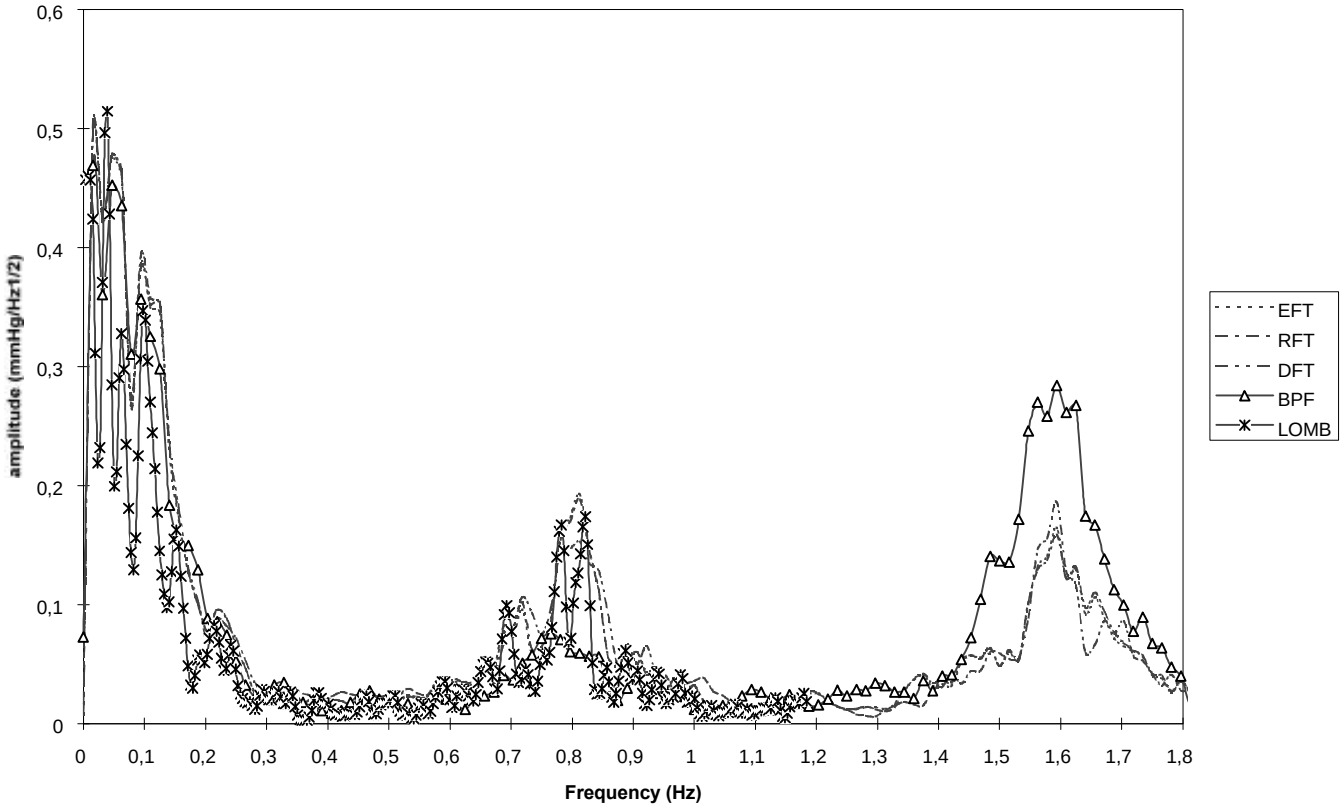

Figure 5-13 Spectrum of the systolic blood pressures of episode 4 using the EFT, RFT, DFT, BPF, and LOMB algorithm; the BPF algorithm (digital filtering) used the full sampled signal.

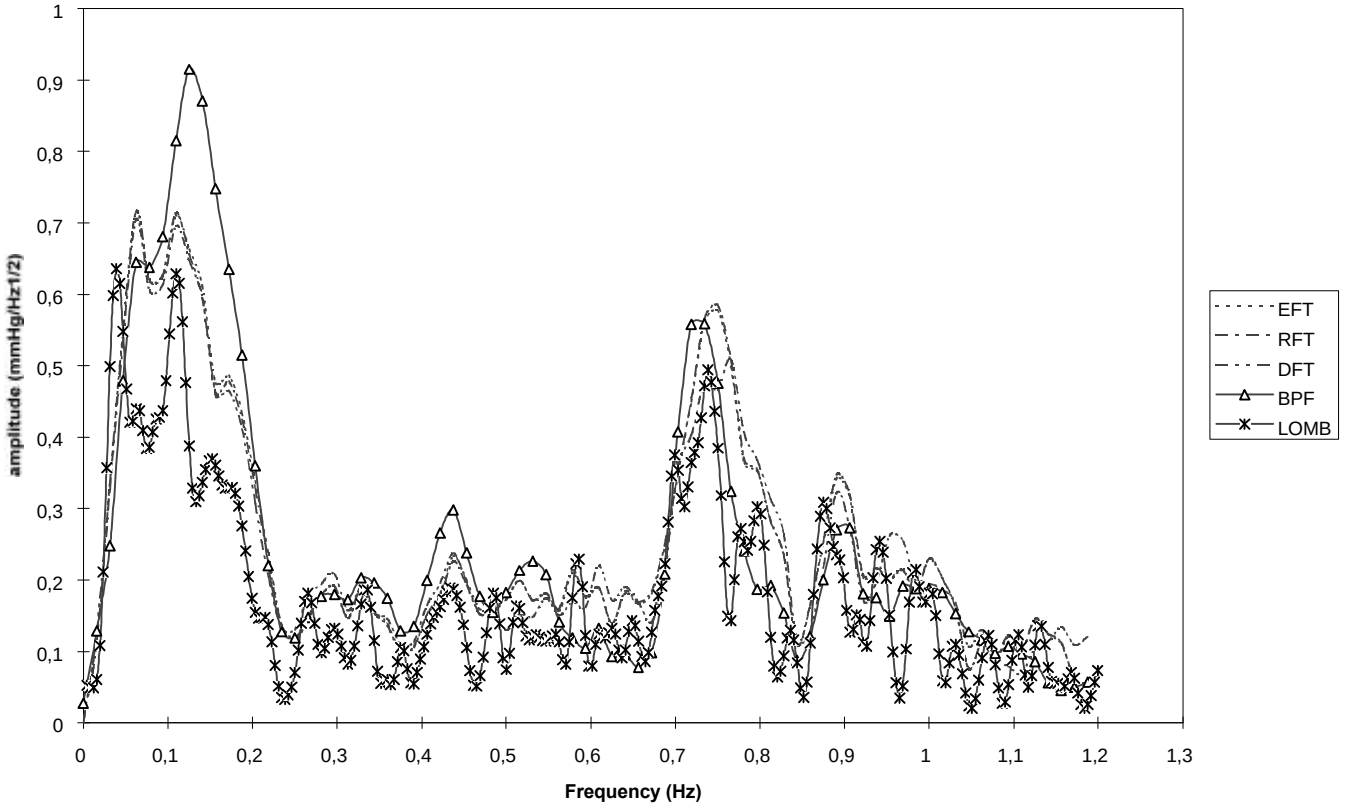

Figure 5-14 Spectrum of the systolic blood pressures of episode 5 using the EFT, RFT, DFT, BPF, and LOMB algorithm; the BPF algorithm (digital filtering) used the full sampled signal.

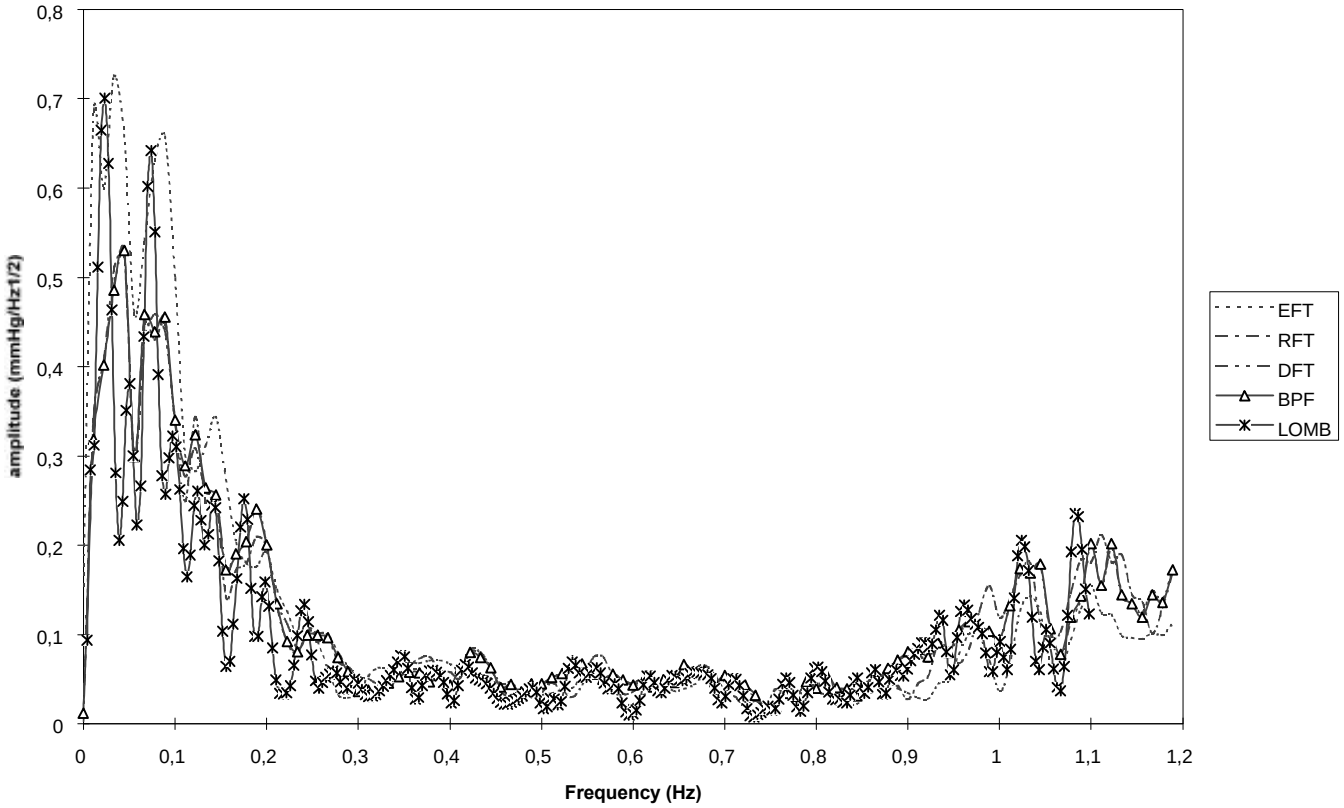

Figure 5-15 Spectrum of the systolic blood pressures of episode 6 using the EFT, RFT, DFT, BPF, and LOMB algorithm; the BPF algorithm (digital filtering) used the full sampled signal.

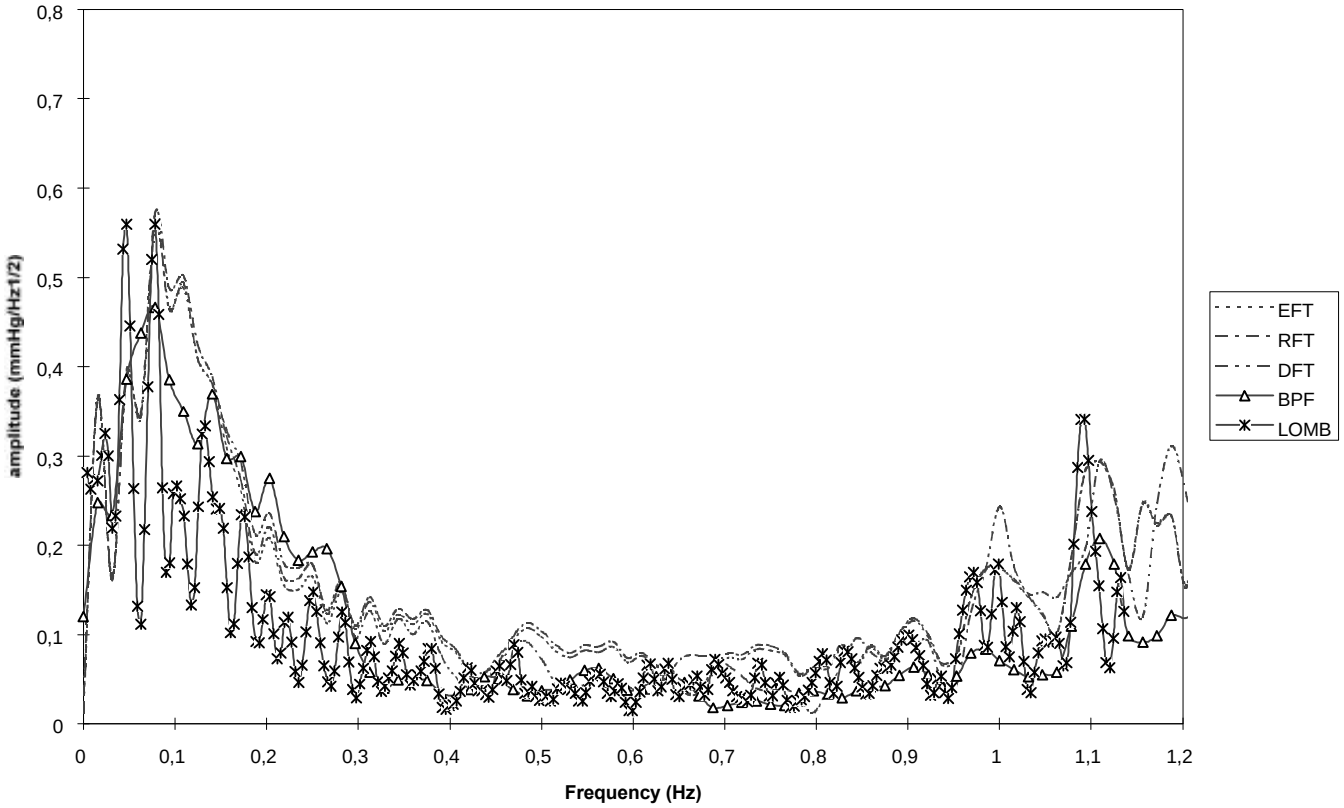

Figure 5-16 Spectrum of the systolic blood pressures of episode 7 using the EFT, RFT, DFT, BPF, and LOMB algorithm; the BPF algorithm (digital filtering) used the full sampled signal.

- In episode 1 the beat-to-beat algorithms, except for the LOMB and BPF methods, have higher values around 0.15 Hz, possibly due to higher order harmonics of the components at about 0.07 Hz.
- In episode 2 the EFT, RFT, and DFT algorithms have higher values over the whole frequency band, probably due to higher order harmonics in the Fourier transforms; note that in the ranges where BPF is significantly lower (0.1-0.4 Hz and 0.55-0.7 Hz), LOMB is also lower.
- All methods roughly show the same behaviour in episode 3.
- In episode 4 it is clear from the BPF that the respiratory influence is located at about 1.6 Hz and not at 0.8 Hz. In fact, at 0.8 Hz the aliased peak is found in the beat-to-beat results, including the LOMB results. The (little) peak at 0.8 Hz in the BPF signal, which cannot be attributed to an aliasing effect, is thought to originate from the fact that the respiration does not equally influence the blood pressure in all its phases. For instance, we know from earlier experiments that the respiratory influence in the systolic phase is higher than in the diastolic phase. Of course, this variation in strength occurs at the heart frequency, which might lead to components at the sum and difference frequencies of heartrate and respiratory frequency. The Fourier algorithms are not hampered by this effect (by aliasing, however, they are): they use beat-to-beat values from the same phase in the cardiac cycle.
- In episode 5 the BPF shows a clear peak at 0.15 Hz, while the other algorithms show a peak at significantly lower frequencies. It suggests an effect that is present in the full blood pressure signal, whereas it is suppressed in the systolic values (beat-to-beat).
- All methods roughly show the same behaviour in episode 6.
- In episode 7 the BPF signal is smaller in the neighbourhood of the Nyquist frequency (1.15 Hz), because the beat-to-beat algorithms add their aliased components to the actual components.
- generally, the LOMB algorithm gives lower values in the LF band than the others. This suggests that higher order harmonics of the low frequency components do not appear in the LOMB spectra. Further computer simulations using the IPFM model might clarify this point.

In cases where the respiratory frequency is high in relation to the heartrate the BPF method avoids aliasing:

- respiratory components are not placed at the incorrect frequency
- variability components higher than half the mean heartrate are not added to the mirror components below half the mean heartrate

It became possible only recently to perform the filtering of the blood pressure signals in real-time. The advantage of that filtering is that the limit of "half the mean heartrate" does no longer apply. A reliable spectrum can be calculated up to the frequency that the Catheter Manometer System can provide.

5.5 Conclusions

In the blood pressure signal spectrum energy in several frequency bands can be observed. Dominant, of course, is the large peak at the heart frequency and its higher order harmonics. They describe the energy neccessary to constitute the blood pressure wave form. At lower frequencies three additional bands, more diffuse, might be observed. They contain implicit information about the respiratory mechanics and about the autonomic nervous system activity of the infant.

Physiologically, the fluctuations *at* the respiratory frequency have their origin in (see chapter 2):
- direct intrathoracal pressure changes;
- changes in arterial preload due to the intrathoracal pressure and volume changes;
- neural activity, during breathing effort.

The frequencies *below* the respiratory frequency have their origin in:
- the vasomotor system (0.05-0.2 Hz);
- fluctuations in the amplitude of the respiration (0.05-0.2 Hz);
- temperature regulation (0.01-0.05 Hz).

The quantification of the power resulting from these processes may lead to more insight in the respiratory mechanics and the function of the autonomic nervous system of the infant. The calculation of the frequency components below the respiratory frequency can be performed in many different ways. The time domain methods require only little computer capacity, but cannot easily be compared with information from other laboratories. The standard frequency domain methods can not be used straightforwardly, due to the fact that the pressure values are not equidistantly sampled. Furthermore, the respiratory frequency is sometimes higher than half the mean heart rate, thus violating the Nyquist criterion.
Other frequency domain methods have serious disadvantages as well. We choose to evaluate the Fourier analysis with respect to a set of representative neonatal data sets. The use of a Fourier spectrum enables us to compare our results easily with results from other laboratories.
One of the problems in the analysis of systolic and diastolic blood pressure series is the fact that they are only available once a heartbeat. To evaluate the error in the calculated spectra a model was taken that describes a system that is both amplitude and frequency modulated. This IPFM model illustrates that - in principle – many sum- and difference frequency components may be present in our data sets.

To evaluate the results in practice, we used several Fourier transform algorithms on representative neonatal data sets. Surprisingly, the results show hardly any significant differences in the spectra from these data, except for the LOMB algorithm. This suggests that the LOMB method does not (or hardly) generate higher order harmonics, e.g., of the large LF components.

Finally, we considered the results of spectral analysis by a direct blood pressure signal filtering method. This method consists of low-pass filtering of the full blood pressure signal, followed by a standard frequency analysis of the filtered signal. The results show that the method is not affected by aliasing of high frequency components and by higher order harmonics at the low frequencies. The full blood pressure signal has been sampled at at least 100 Hz instead of once per heartbeat, like the standard methods, so aliasing does not occur.
A disadvantage of the blood pressure filtering method may be that the system generating the blood pressure is treated as one linear entity, which from a physiologic point of view is not true. Also, of minor importance nowadays, a large number of mathematical operations have to be performed.

A thorough evaluation of results of spectral analysis of simulated data sets generated according to the IPFM model might provide more insight in the performance and validity of the various methods discussed in this chapter. Such an evaluation may be the subject of a future study.

Literature

Akselrod S, Gordon D et al.; Hemodynamic regulation: Investigations by spectral analysis; Am J Physiol 249:H867-H875, 1985;

Baselli G, Cerutti S, Livraghi M, Meneghini; Causal relationship between heart rate and arterial blood pressure variability signals; Med Biol Eng Comput 26:374-378, 1988

Baselli G, Cerutti S; Spectral and cross-spectral analysis of heart rate and arterial blood pressure variability signals; Comp Biomed Res 19:520-534, 1986

Berger RD, Akselrod S, Gordon D, Cohen RJ; An efficient algorithm for spectral analysis of heart rate variability; IEEE Trans Biomed Eng 33:900-904, 1986

Borsevici V, Oleinik W, Mustyatsa A, Tjuteakin A, Silkin D; Mathematical method for a running spectrum analysis; Med Eng Phys 16:301-303, 1994

Brigham EO; The fast Fourier transform and its applications; Englewood Cliffs: Prentice-Hall, 1988

Cerutti S, Alberti M, Baselli G, Rimoldi O, Malliani A, Merri M, Pagani M; Automatic assessment of the interaction between respiration and heart rate variability signal; Med Prog Technol 14:7-19, 1988

Childers, DG; Modern spectrum analysis; New York : IEEE press, 1978

Clayton RH, Bowman AJ, Ford GA, Murray A; Measurement of baroreflex gain from heart rate and blood pressure spectra: a comparison of spectral estimation techniques; Physiol Meas 16:131-139, 1995

Cox DR, Lewis PAW; The statistical analysis of series of events; London, Methuen; 1966

DeBoer RW; Beat-to-beat blood-pressure fluctuations and heart-rate variability in man: physiological relationships, analysis techniques and a simple model; Proefschrift, Universiteit van Amsterdam, 1985

Eckert R, Randall DJ; Animal Physiology; San Fransisco: Freeman, 1983

Enden van den AWM, Verhoeckx NAM; Ontwerpmethoden voor discrete filters; In: Digitale signaalbewerking, Overberg: Delta press BV, 225-245, 1987

Feynmann RP, Leighton RB, Sands M; Lectures on physics; Reading Massachusetts: Addison-Wesley, 1963

Geijn van HP; Studies on fetal and neonatal baseline heart rate variability; Proefschrift Katholieke Universiteit Nijmegen, 1980

Heslegrave RJ, Ogilvie JC, Furedy JJ; Measuring baseline-treatment differences in heart rate variability; variance versus successive difference mean square and beats per minute versus interbeat intervals; Psychophysiology 16:151-157, 1979

Inoue K, Miyake S, Kumashiro M, Ogata H, Ueta T, Akatsu T; Power spectral analysis of blood pressure variability in traumatic quadriplegic humans; Am J Physiol 260:H842-H847, 1991

Jaffe RS, Fung DL; Constructing a heart-rate variability analysis system; J Clin Monit 10:45-58, 1994;

Kalli S, Grönland J, Ihalainen H, Siimes A, Välimäki I, Antila K; Multivariate autoregressive modeling of autonomic cardiovascular control in neonatal lamb; Comp Biomed Res 21:512-530, 1988

Kay SM, Marple SL; Spectrum Analysis - a modern perspective; Proc IEEE 69:1380-1419, 1981

Lomb, NR; Least-squares frequency analysis of unequally spaced data; Astrophysics and Space Science 39, 447-462, 1976

Lossius K, Eriksen M, Walloe; Thermoregulatory fluctuations in heart rate and blood pressure in humans: effect of cooling and parasympathetic blockade; J Auton Nerv Syst 37:245-254, 1994

Malliani A, Pagani M, Lombardi F, Cerutti S; Cardiovascular neural regulation explored in the frequency domain; Circulation 84:482-492, 1991

Oppenheim AV, Schafer RW; Digital filter design techniques; In: Digital signal processing, Englewood Cliffs: Prentice Hall, 236-270, 1975

Parati G, Di Rienzo M, Bertinieri G, Pomidossi G, Casadei R, Groppelli A et al.; Evaluation of the baroreceptor-heart rate reflex by 24-hour intra-arterial blood pressure monitoring in humans; Hypertension 12:214-222, 1988

Parer WJ, Parer JT, Holbrook RH, Block BSB; Validity of mathematical methods of quantitating fetal heart rate variability; Am J Obstet Gynecol 153:402-409, 1985

Press, WH; Numerical recipes; Cambridge: Cambridge university press, 1988

Rabiner LR, Gold B; The theory and approximation of finite duration impulse response digital filters; In: Theory and application of digital signal processing, Englewood Cliffs: Prentice Hall, 75-193, 1975

Ravenswaay-Arts van CMA; Heart rate variability: Physiology and clinical applicability in very preterm infants; Proefschrift Nijmegen, 1993

Ravenswaaij-Arts van C, Hopman J, Kollée L, Stoelinga G, Geijn van H; Spectral analysis of heart rate variability in spontaneously breathing very preterm infants; Acta paediatr 83:473-480, 1994

Ravenswaaij van CMA, Kollée LAA, Hopman JCW, Stoelinga GB, Geijn van HP; Heart rate variability; Ann Intern Med 118:436-447, 1993

Rompelman O; Tutorial review on processing the cardiac event series: a signal analysis approach; Automedica 7:191-212, 1986

Rompelman O, Pijnacker Hordijk WPh; New method for the assessment of neonatal respiratory sinus arrhythmia; Med Biol Eng Comput 25:481-486, 1987

Sabel M; Invloed van respiratie op bloeddruk bij pasgeborenen; Afstudeerverslag, Technische Unversiteit Eindhoven, 1993

Salvaggio A, Antivalle M, Lattuada S; Blood pressure fluctuations, fractional integro-differentiation and spectral analysis; Med Biol Eng Comput 32(4Suppl):S86-S90, 1994

Shin SJ, Tapp WN, Reisman SS, Natelson BH; Assessment of automomic regulation of heart rate variability by the method of complex demodulation; IEEE Trans Biomed Eng 36:274-283, 1989

Steenis van HG, Tulen JHM, Mulder LJM; Heart rate variability spectra based on non-equidistant sampling: the spectrum of counts and the instantaneous heart rate spectrum; Med Eng Phys, 16:355-362, 1994

TenVoorde BJ, Ree ER, Hack WWM, Bergschneider VM, Hoekstra BPT, Faes TJC, Rompelman O; Spectral quantification of respiratory sinus arrhythmia in preterm and fullterm neonates: beyond half the mean haert rate; Automedica 13:15-31, 1990

TenVoorde BJ, Faes ThJC, Rompelman O; Spectra of data sampled at frequency-modulated rates in application to cardiovascular signals: part 1 analytical derivation of the spectra; Med Biol Eng Comput 32:63-70, 1994a

TenVoorde BJ, Faes ThJC, Rompelman O; Spectra of data sampled at frequency-modulated rates in application to cardiovascular signals: part 2 evaluation of fourier transform algorithms; Med Biol Eng Comput 32:71-76, 1994b

Triedman JK, Saul Ph; Blood pressure modulation by central venous pressure and respiration; buffering effects of the heart rate reflexes; Circulation 89:169-179, 1994

Voorhoeve, PE, Walter, WG, Brink, G van den; Physiologie van het centrale zenuwstelsel en de zintuigen; Amsterdam: Agon Elsevier, 1974

West JB; Best and Taylor's physiological basis of medical practice, 12th ed.; Baltimore: Williams & Wilkins, 1990

Yeh S, Forsythe A, Hon EH; Quantification of fetal heart beat-to-beat interval differences; Obstet Gynecol 41:355-363, 1973

6. Clinical Applications

This chapter illustrates the application of the system and the measurement methods described in the preceeding chapters by means of two examples: 1st : the realisation of continuously available spectral estimates of the blood pressure signal; 2nd : a first order quantification of the relation between blood pressure and heartrate.

A continuous presentation of the spectral estimates of the blood pressure signal, discussed in detail in chapter 5, has not been realised yet. The availability of HF and LF spectral amplitude estimates over a longer period of time, however, may present extra information about the internal neuro-cardiovascular state of the patient. A method is worked out to estimate the HF spectral amplitude continuously, using the the blood pressure spectral components at the actual respiratory frequency band. The results from 4 time intervals show that the HF estimates vary significantly in time, although no external actions took place. This suggests that these estimates may contain valuable new information about the internal state. A method for the LF spectral amplitude can be developed in an analogous way.

In the evaluation of a physiological model of the interactions between blood pressure, respiration, and heartrate, quantification of the relation between these variables is necessary. We present a way to calculate the corresponding cross correlation spectra and show how a coherence function between them can be interpreted. Two representative examples show that the interaction is particularly present in the LF and HF regions. The use of this analysis on different patient groups in different physiological states may improve the model description of the cardiovascular system.

6.1 Continuous spectral amplitude estimates

One of the aspects of the spectral analysis of a blood pressure signal has not been worked out yet: the behaviour of spectral estimates as a function of time. To do so, we need larger periods of time than the 64 or 90 second intervals from which spectral estimates were obtained in earlier chapters. Therefore, we measure continuously and calculate spectral estimates every 90 seconds. In this way, the resulting values can be observed over a longer period of time, resulting in new "neuro-vascular" parameter values. An estimate of the HF and LF spectral activity, as explained in section 2.2, may offer valuable extra information about a number of the interactions shown in figure 2-3.

In this section the method for the estimation of the HF amplitude components is worked out; the implementation of the LF amplitude components can be carried out in an analogous way, using the frequency components relevant for LF activity.

6.1.1 Methods

The spectral amplitude in the HF region is caused by both mechanical and neural interactions at the respiratory frequency (see section 2.2). To quantify the effects of these interactions by spectral analysis, it is necessary to determine that frequency accurately. Therefore, the calculation of the HF spectral information consists globally of two parts: 1st the determination of the relevant respiratory frequency band; 2nd the calculation of the spectral components in that band.

patients

We performed the analysis on 4 time intervals (3 neonates), varying from 43.5 to 114 minutes:

patient id. number	**interval reference**	**time interval**	**length (min)**
04089445224	A1	0114-0201	46.5
	A2	0315-0400	45
10039572217	B	1503-1546	43.5
17039543210	C	0032-0226	114

All infants breathed spontaneously and received coffeine as medication against bradycardias.

determination of the HF frequency band

We split the intervals in episodes of 90 s, on which the spectral analysis will be performed. The episode length was chosen as a result of the trade-off between stability and spectral resolution/accuracy. Mean blood pressure level and respiratory patterns often change every minute, requiring a short episode. On the other hand, the error in the estimated spectral amplitudes within a certain frequency band decreases with the increase of the episode length.

We chose to determine the momentary (breath-by-breath) respiratory frequency from the thoracic impedance signal. According to the method outlined in section 4.3.1, every 3 seconds the thoracic impedance signal is analysed to return breath-by-breath the time stamps at which a respiration "occurred". Although the respiratory frequency could be obtained indirectly from the spectrum of the blood pressure signal itself, we did not rely on that because of two serious disadvantages:

- the influence of respiration on the blood pressure signal may be low (e.g., it is damped by the baroreceptor reflex) or the respiratory frequency band may overlap with other frequency bands
- the spectrum does not render breath-by-breath information. If the breath-by-breath respiratory frequency deviates strongly from the frequency band in which

the HF spectral amplitude is located, the reliability of the results is questionable. This check cannot be done using the blood pressure signal alone.

In neonates the breathing patterns show large fluctuations. The analysis of the thoracic impedance signal over a longer period of time, in our case 90 second episodes, may result in a (wide) range of breath-by-breath respiratory frequencies. An example of the distribution of these frequencies during the first 90 second episode of set A1 is given in figure 6-1. The breath-by-breath frequency distributions (may) vary largely from episode to episode. To be able to incorporate these variations in the calculation of the spectral contribution, the median and percentile values of the breath-by-breath respiratory frequency are determined. These values will be used to determine the frequency region of interest.

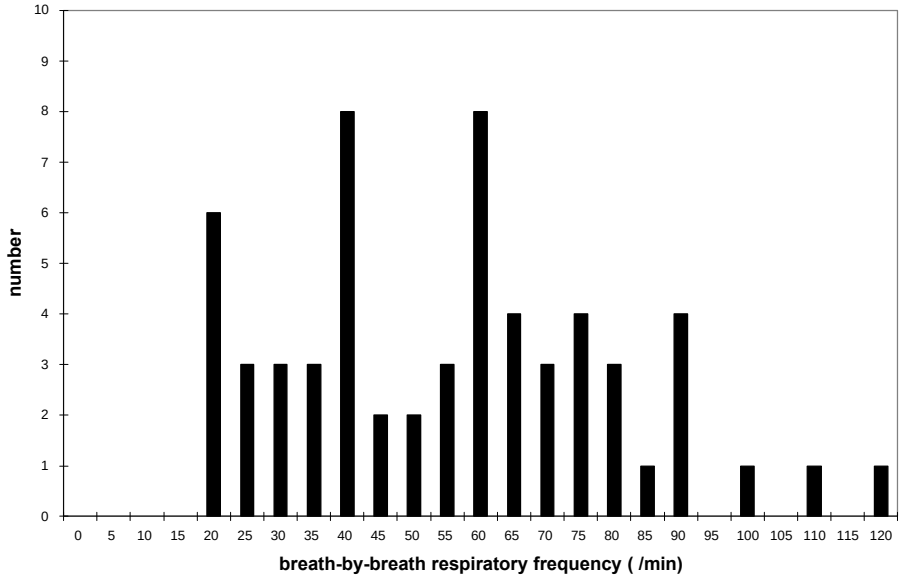

Figure 6-1 Histogram of the breath-by-breath respiratory frequencies found in the first 90 second episode of interval A1.

The respiratory frequency will not only vary between successive 90 second episodes, as shown furtheron in figure 6-3, but may also vary within a 90 second episode. To illustrate the (in)stability of the respiratory signal and the effect of it on the percentile values, we show the breath-by-breath histograms of the first and second half of the first 90 second episode of interval A1 in figure 6-2.

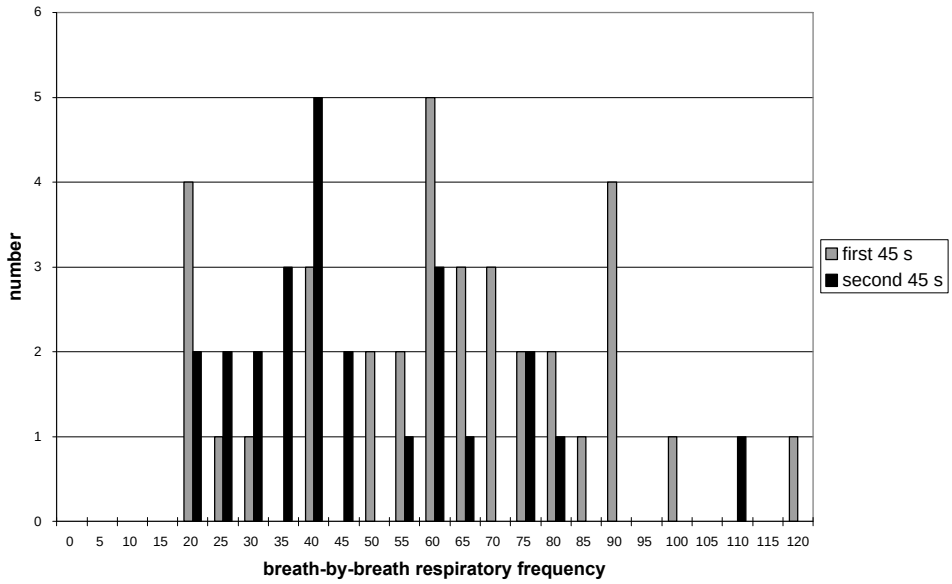

Figure 6-2 Histogram of the breath-by-breath respiratory frequencies found in the first and second 45 seconds of interval A1. The median respiratory frequency in the first 45 seconds is 60/min, p16=34/min, and p84=85/min; in the second 45 seconds the median is 37/min, p16=26/min, and p84=65/min.

As can be seen from this figure and the percentile values given in the caption, the respiratory pattern during the first half of the episode is quite different from the pattern during the second half. In this situation, a broad respiratory frequency band should be chosen to take into account all respiratory contributions in the amplitude spectrum of the blood pressure. The disadvantage of a broad band, however, is that over the whole range a certain noise level is added, and that unwanted contributions from other influences, also present within the same broad band, will be added too. In figure 6-3 the median and percentile values of the respiratory frequency in all 90 second episodes of the total time interval A1 are given. As expected, the (relative) fluctuations are large, especially in the p0 and p100 values. The median and percentile values can be applied for the calculation of the HF spectral amplitude of the blood pressure in roughly two different ways:

1. The spectral amplitudes within a certain percentile range of the respiratory frequencies are added together (variable respiratory bandwidth)
2. The spectral amplitudes in a fixed frequency band around the median respiratory frequency are added together (fixed respiratory bandwidth).

As a consequence of the 90 s episode length, many different breath-by-breath respiratory frequencies will be present in every episode. The advantage of the relatively large time record is the reduction of the error of the spectral amplitude estimates. If one wants to be sure that all respiratory components are included in episodes with a broad respiratory band, the choice for a percentile range will be appropriate. If one merely wants to estimate the maximum amplitude, a choice for a

fixed respiratory bandwidth around the median frequency will do better. The fixed bandwidth, in that case, is merely used to average a number of bins, and as a result reduces the error in the spectral estimates.

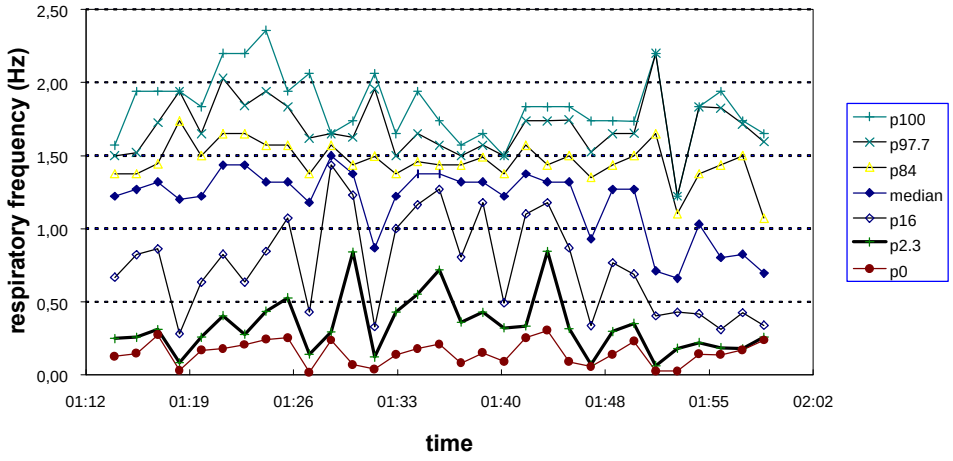

Figure 6-3 The percentile values of the breath-by-breath respiratory frequencies during consecutive 90 second episodes. Note the drop of the p16 and p2.3 values at time 1:31 and 1:47. They cause the respiratory band to be broader and as a consequence may lead to a larger HF-amplitude estimate.

spectral amplitude in the HF band

The HF spectral amplitude of the blood pressure signal is calculated using the respiratory frequency band deduced from the thoracic impedance signal. Three different calculations are made:

- The spectral amplitude components in the range p2.3 - p97.7 are added;
- The spectral amplitude components in the range p16 - p84 are added;
- The spectral amplitude components in the range from 0.2 Hz below to 0.2 Hz above the median respiratory frequency are added.

We did not use the p0 and p100 values because they are very sensitive to artefacts. Almost every misinterpreted breath leads to an inappropriate p0 or p100 value.

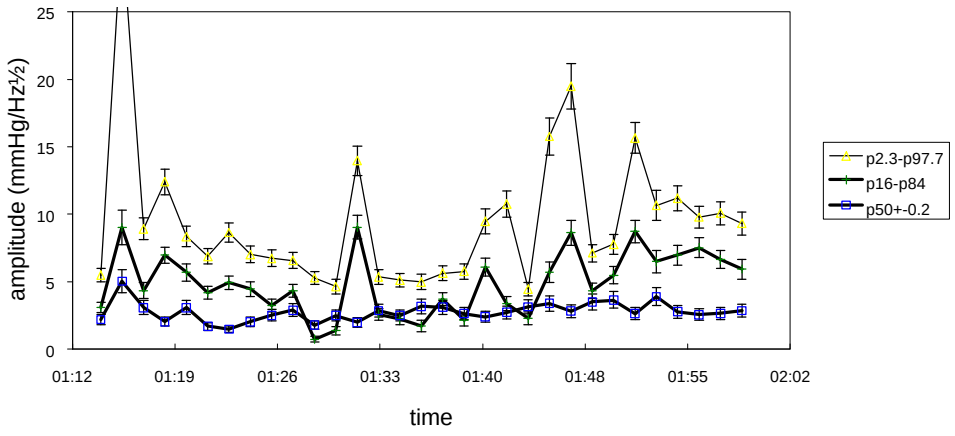

Figure 6-4 The HF spectral amplitude estimates as a function of time for interval A1. The estimates are the sum of the spectral amplitudes in the respective frequency regions p2.3%-p97.7%; p16%-p84%; p50%±0.2Hz.The error bars denote the standard errors of the estimated frequency components. Note that - for instance - at 1:31 and 1:47 the amplitude calculated according to the percentile ranges increases, whereas the amplitude calculated for a fixed width around p50% hardly changes.

estimation of the error in the HF values

The HF values consist of a number of added spectral components from a Fourier transform. Using the Fourier transform on N values sampled during a time episode T results in N/2 independent frequency components with a binwidth of 1/T Hz and a standard deviation of 100%, if the values are the result of a white noise process [Press, 1988]. If we add these components the standard error will be decreased by a factor $1/\sqrt{n}$, with n the number of bins added (see section 5.2.3). If the respiratory bandwidth is 0.4 Hz and T=90 s, this implies that n=36 (0.4/(1/90), and the standard error will be 16.7%. The HF amplitudes and corresponding error bars for the first interval (A1) are given in figure 6-4. Since the relative error levels for the other intervals are comparable, they will not be shown in the corresponding plots; such for reasons of convenience.

6.1.2 Results

In figure 6-4 to figure 6-7 we show the spectral estimates calculated using both a variable and a fixed respiratory bandwidth. The variable bandwidths are often larger than the fixed ones, which of course explains the larger values found for the HF

spectral amplitudes using variable bands. The average bandwidth of the 5 data sets can be found in table 6-1.

Interval	average bandwidth p2.3 - p97.7 (Hz)	average bandwidth p16 - p84 (Hz)	average bandwidth p50 ± 0.2 (Hz)
A1	1.36	0.71	0.4
A2	1.45	0.81	0.4
B	1.21	0.67	0.4
C	1.16	0.65	0.4

Table 6-1 Average respiratory bandwidths of the data sets.

Figure 6-4 shows the HF amplitude values with their corresponding error bars for interval A1. Several variations in these values are clearly much larger than the errors in it, indicating that they can be considered to be significant. Furthermore, these variations were not induced by handling of the patient, which, of course, may lead to large changes in the neuro-cardiovascular state. The upper two signals exhibit large variations, e.g., at times 1:14, 1:31, and 1:47, whereas the fixed interval signal (lowest in the figure) only follows these variations at time 1:14. The variations that are only present in the upper two signals can be explained by the broadening of the respiratory bandwidth at those times. In this respect we like to note the pronounced dips in p2.3 and p16 at 1:31 and 1:47 that can be seen in figure 6-3. The HF values based on the fixed interval merely express the HF amplitude in a small band around the respiratory frequency with highest incidence (modus). If the respiratory frequency shifts during the episode, the spectral components outside the median are not included. On the other hand, many spurious components will affect the HF values based on a variable (i.e., broad, if the respiratory frequency is shifted) respiratory band. A part of the variation of the HF amplitudes at 1:31 and 1:47 can be attributed to that effect.

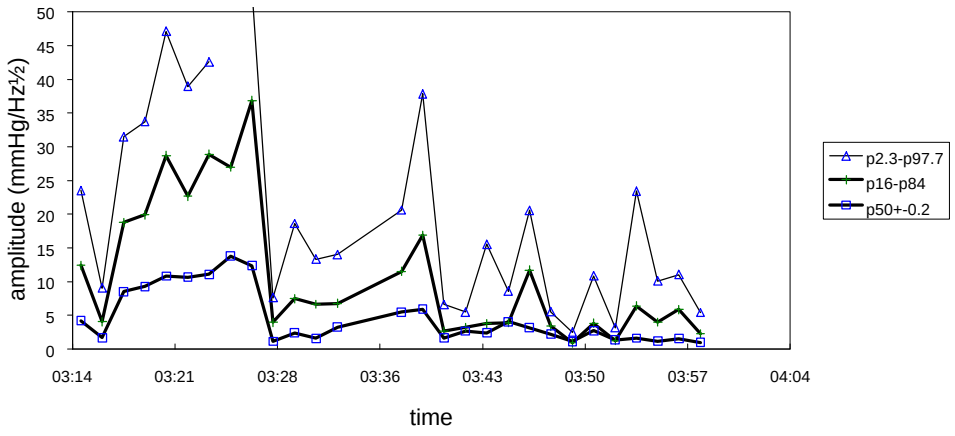

Figure 6-5 The HF spectral estimates as a function of time for interval A2. The estimates are the sum of the spectral amplitudes in the respective frequency regions p2.3%-p97.7%; p16%-p84%; p50%±0.2Hz.

In figure 6-5, showing the spectral amplitudes for interval A2, it is clear that something happened between 3:17 and 3:28. All HF values rise drastically. They all three react in a comparable way upon the pressure changes in the body, although the HF value based on the p50 seems more quiet after 3:43. Furthermore, a repeating peak pattern seems to appear, having a top at 3:26, 3:39, 3:47, and 3:54. This pattern might be related to the temperature regulation of the incubator, or to changes in the behavioural/sleep state of the patient.

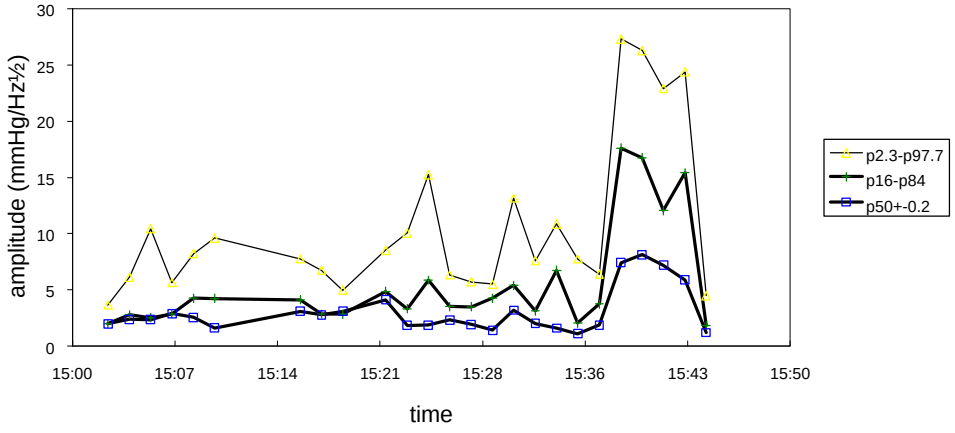

Figure 6-6 The HF spectral estimates as a function of time for interval B. The estimates are the sum of the spectral amplitudes in the respective frequency regions p2.3%-p97.7%; p16%-p84%; p50%±0.2Hz.

The HF values for interval B are plotted in figure 6-6. Significant peaks show up at the end of the interval. The small peaks at 15:24 and 15:34 in the signals based on the variable bandwidth can again be explained by an increase in bandwidth.

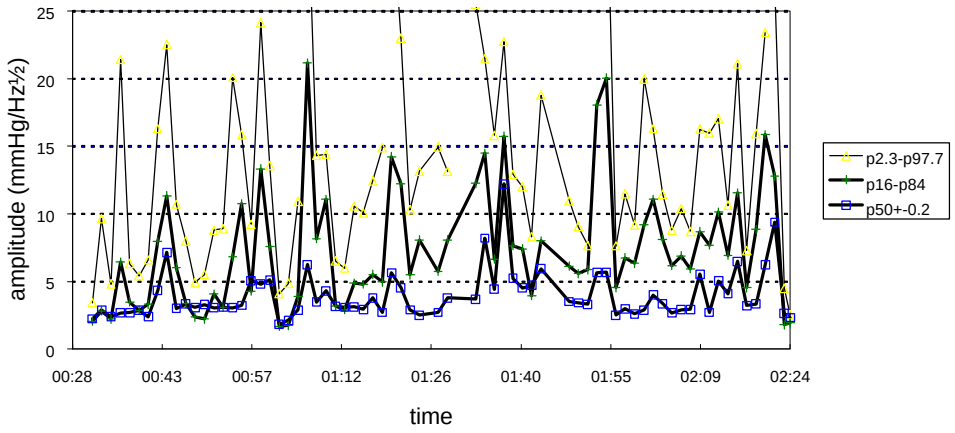

Figure 6-7 The HF spectral estimates as a function of time for interval C. The estimates is the sum of the spectral amplitudes in the respective frequency regions p2.3%-p97.7%; p16%-p84%; p50%±0.2Hz.

The last interval (C) shows a more fluctuating pattern (figure 6-7). Although the lower signal, based on a fixed bandwidth, seems more quiet, the relative standard

deviation of it, 0.45, is comparable to the relative standard deviations of the upper two signals, resp. 0.24 (upper) and 0.55 (middle). Many peaks occur in all three signals; hence it is clear that many variations in the upper two signals are not only caused by a variation in respiratory frequency band, but result from other processes too.

6.1.3 Discussion

The episode length of 90 seconds is one of the choices that may be reconsidered. In view of the required stability of the patient and the fact that respiratory patterns may alter very quickly, a shorter episode might be better. In that case the respiratory band will be smaller too. The bandwidth of 0.4 Hz, used in the previous section, will perhaps be reduced to 0.2 Hz. As mentioned in section 5.2.2, the relative standard error (SE) of 100% will be reduced by a factor $1/\sqrt{n}$, with n the number of bins added together. Generally:

using
$$n = \frac{B_r}{1/T} \qquad \textbf{(6-1)}$$

we obtain
$$T = \frac{1}{B_r \cdot SE^2} \qquad \textbf{(6-2)}$$

with B_r= respiratory bandwidth
T= episode time
SE= standard error in the spectral amplitude estimate.

If we require a maximum SE of 25 % (resp. 33%), and use a bandwidth estimate of 0.2 Hz, equation (6-2) implies that the episode length should be at least 80 (resp. 45) seconds. The use of this smaller episode length leads to a smaller respiratory bandwidth, and hence will also reduce the addition of spurious spectral amplitudes that were not originating from respiratory effort. If a standard error of about 33% can be accepted, it might be worthwhile to reduce the episode length to about 45 seconds. In a real-time implementation the results can then be presented every 45 s, directly after the end of an episode.

All HF spectral amplitude graphs presented above show clear variations in the signals, significantly above the error levels. The neonates were quiet and were not manipulated during the measurements, so the observed variations are likely to result from internal changes in the neonate (behavioural state, neural mechanisms, respiratory patterns). The fact that these 4 examples show quite different fluctuations, which we did not expect before, indicates that they perhaps reveal some extra information about the neonate that could not be made visible up till now.

A real step forward can be expected from the introduction of real time adaptive filtering in the system in the near future. It directly filters the blood pressure signal, with band-pass characteristics that are adapted in real-time to the breath-by-breath respiratory frequency. The signal that results expresses the continuous influence of breathing on the blood pressure around the actual breath-by-breath respiratory frequency. In fact, it will be a nearly perfect Traube-Hering wave from which the amplitude can be taken directly (see section 1.2). In a real-time implementation the estimated amplitude can probably be updated every wavelength period of about 10 s, just as usual with other beat-to-beat parameters.

Future measurements will be necessary to evaluate how the spectral estimates vary with sleep pattern, respiratory pattern, and neural mechanisms. In fact, the quantitative dependence of the spectral estimates on the change in physiological state determines the potential value of their extra information to the clinician.

6.2 Correlations between blood pressure and heartrate

6.2.1 Introduction

From a physiologic point of view, the quantification of the mutual interactions between heartbeat interval (HI) and blood pressure (BP) will give information relevant for the model describing interactions between blood pressure, heartbeat interval, and respiration [Kitney and Rompelman, 1980, Akselrod and Gordon, 1981, 1985, Taylor and Eckberg, 1996]. The linear interactions can be described in the frequency domain by a gain and a phase. The relation of this gain and phase to gestational age, postnatal age, and relations with medication can be investigated. On a shorter timescale the relations with the different states of the autonomic nervous system can be investigated. Different responses can be expected depending on whether a patient is in supine or in standing position, does mental work, or has medication that influences the autonomic state [Saul, Berger et al., 1991; Veldman, Mulder et al., 1993; Akselrod, Gordon et al., 1985; Kitney, Fulton et al., 1985]. These studies consider the signal behaviour under the mentioned different autonomic states. Some of them propose a model describing the interactions between respiration, heartbeat interval, and blood pressure. The results all refer to adults; in neonates the experimental possibilities are restricted compared to adults, both for practical and for ethical reasons.

Several techniques exist to investigate the correlations between two time dependent signals, in the time domain as well as in the frequency domain [Baselli, Cerutti et al., 1986]. We focus on a method that uses the frequency spectra as described in section 5.4.1. This methode has basically also been used by De Boer [Boer RW de, 1985], but

he chose different record lengths and smoothing windows and had a different pre-preparation of the signals. The different approach followed in this thesis is partly caused by the difference in patients (neonates vs. adults).

6.2.2 Methods

The cross spectra between two variables, in our case the systolic arterial blood pressure (SBP) and the heartbeat interval (HI), quantify the linear relationship between them by a gain and a phase in the frequency domain. The gain and phase are evaluated for every frequency bin, analogous to the spectra of the signals themselves.

Cross-spectra

The linear transfer function H(f) between HI and BP is defined as:

$$Y(f) = H(f) \cdot X(f) \qquad \textbf{(6-3)}$$

with $Y(f)$ and $X(f)$ the Fourier spectrum of heartbeat interval and blood pressure, respectively. It can be proven that [Bendat, 1986]:

$$G_{yy}(f) = \left|H(f)\right|^2 G_{xx}(f) \qquad \textbf{(6-4)}$$

$$G_{xy}(f) = H(f) G_{xx}(f) \qquad \textbf{(6-5)}$$

in which G_{xx} and G_{yy} are the one-sided autospectral density functions of the blood pressure and the heartbeat interval, respectively. G_{yy} will be used later on for the calculation of the coherence. G_{xy} is called the one-sided cross spectral density function. The one-sided auto- and cross spectral density functions are defined by:

$$G_{xx}(f) = 2 \lim_{T\to\infty} \frac{1}{T} E[X^*(f,T) X(f,T)] \qquad 0 \le f < \infty \qquad \textbf{(6-6)}$$

$$G_{xy}(f) = 2 \lim_{T\to\infty} \frac{1}{T} E[X^*(f,T) Y(f,T)] \qquad 0 \le f < \infty \qquad \textbf{(6-7)}$$

where $E[X]$ denotes the expected value of X and T the record length in the time domain.

Analogous to the spectral estimates, these density functions have standard deviations that cannot be reduced by an increase of the record length. Therefore, the cross spectral estimate must be smoothed using a spectral window similar to the one used in the calculations of the (auto)spectral estimates. If a discrete Fourier transform of a data segment of finite length T is taken, averaging over n_d segments yields the following estimate for G_{xy}:

$$\hat{G}_{xy}(f) = \frac{2}{n_d T} \sum_{i=1}^{n_d} X_i^*(f,T) Y_i(f,T) \quad \equiv \quad \hat{C}_{xy}(f) - i\,\hat{Q}_{xy}(f) \qquad \textbf{(6-8)}$$

where $C(f)$ denotes the coincidence and $Q(f)$ the quadrature spectral density function. From G_{xx} and the cross spectral density G_{xy} it is now possible to determine $H(f)$:

$$H(f) = \frac{\hat{G}_{xy}(f)}{\hat{G}_{xx}(f)} = \left|\hat{H}(f)\right| \cdot e^{-i\hat{\mathsf{f}}(f)} \qquad \textbf{(6-9)}$$

with: $$\left|H(f)\right| = gain(f) \qquad \mathsf{f}(f) = phase(f) \qquad \textbf{(6-10)}$$

This can be written as:

$$\left|\hat{H}(f_n)\right| = \sqrt{\frac{\hat{C}_{xy}^2(f_n) + \hat{Q}_{xy}^2(f_n)}{\hat{G}_{xx}^2(f_n)^2}} \qquad \textbf{(6-11)}$$

$$\hat{\mathsf{f}}(f_n) = \arctan\frac{\hat{Q}_{xy}(f_n)}{\hat{C}_{xy}(f_n)} \qquad \textbf{(6-12)}$$

These equations show that the transfer function can be calculated directly from the auto and cross spectral densities. These densities can be calculated for consecutive episodes, after which the respective frequency components can be averaged to decrease the measurement error.

Error determination

The degree of linear correlation between two stationary signals can be expressed by the so-called coherence function γ_{xy}^2. A smoothed estimate of this function, the smoothed coherence estimate, is defined analogous to the correlation function used in linear regression analysis by:

$$\hat{\mathsf{g}}_{xy}^2(f) \equiv \frac{\left|\hat{G}_{xy}(f)\right|^2}{\hat{G}_{xx}(f)\hat{G}_{yy}(f)} \qquad , \qquad 0 \le \hat{\mathsf{g}}_{xy}^2(f) < 1 \qquad \textbf{(6-13)}$$

In the ideal case of a linear system with constant parameters, the coherence function will have the value 1 and the relation between *X(f)* and *Y(f)* will be described perfectly well by *H(f)*. If the data are linearly fully unrelated, the value will be 0. The following cases lead to a coherence between 0 and 1:

- the measurements contain external noise;
- the system relating blood pressure and heartbeat interval is not linear;
- heartbeat interval and blood pressure do not only depend on each other, but also on other input parameters.

The coherence estimate is used in the calculations of the standard error of gain and phase. In case of Gaussian random data the standard error can be expressed by the coherence function and a factor accounting for the way of smoothing. The reduction of the error by smoothing depends on the way of smoothing:

- If *m* neighbouring frequency bins (in frequency domain) are averaged the reduction is $1/\sqrt{m}$.
- If a convolution with a window *w* is taken the reduction is given by the integral given in Equation (5-15). Taking the average over *m* frequency bins in fact

corresponds to the application of a rectangular window *w* with width *m*. The error reduction can be written in the form K/√*m*, with K a constant depending on the kind of window.

– Smoothing can also be performed in the time domain, by averaging the frequency estimates of *i* consecutive time segments. If the segments are half overlapping an optimal reduction in error is achieved. The reduction of the error can be expressed by: $\alpha = \sqrt{\frac{8i^2}{9i-1}}$ (see equation (5-17)).

Writing the smoothing reduction factor as α, the following expressions can be derived for the standard error $\varepsilon(f)$ in $H(f)$, $\gamma_{xy}(f)$, and the standard error in $\varphi(f)$ [Jenkins and Watts, 1968, Bendat, 1986]:

$$\varepsilon[\hat{H}(f_n)] = \frac{1}{\alpha}\frac{\sqrt{1-\gamma_{xy}^2(f_n)}}{\gamma_{xy}(f_n)\sqrt{2}} \qquad \textbf{(6-14)}$$

$$\varepsilon[\gamma_{xy}^2(f_n)] = \frac{\sqrt{2}}{\alpha}\frac{\sqrt{1-\gamma_{xy}^2(f_n)}}{\gamma_{xy}(f_n)} \qquad \textbf{(6-15)}$$

$$\varepsilon[\hat{\varphi}(f_n)] = \frac{1}{\alpha}\frac{\sqrt{1-\gamma_{xy}^2(f_n)}}{\gamma_{xy}(f_n)\sqrt{2}} \qquad \textbf{(6-16)}$$

Our time series were 192 s, and were split in 11 half overlapping episodes of 32 s. This results in a standard error in:

– spectral amplitudes: 16 %
– gain: <33%, if the coherence >0.5

The absolute error in the phase is smaller than 13°, if the coherence >0.5.

Interpretation

In the present analysis, the gain denotes the ratio between the variation of the heartbeat interval and the variation of the blood pressure (s/mmHg). The phase reflects the delay between a blood pressure change and a change in heartbeat interval. The phase is a periodic function with a period of 360°. So, without further information one cannot decide from the phase which signal precedes the other. If the delay is longer than one period, an integer times 360° should be added or subtracted. However, the phase as a function of frequency (modulo 360°) will be continuous and will go to 0 if the frequency goes to 0. Phase shift φ (°) and time delay τ are related as follows:

$$t(f) = \frac{1}{360} \cdot \frac{f(f)}{f} \qquad \textbf{(6-17)}$$

A positive phase in our analysis means that the blood pressure precedes the heartbeat interval.
The coherence spectrum can be compared to the correlation coefficient r, as used in linear regression analysis. A high value of the coherence spectrum at a certain frequency indicates a clear linear relation between the heartbeat interval and (part of the) blood pressure spectrum, and hence the phase can be estimated reliably.

Implementation

The analysis was implemented under the name CorrelaX. It uses the software described in section 5.4.1, to determine the amplitude spectra of the blood pressure and the heartbeat interval. The analysis methods of these signals are totally identical, preventing a possible bias due to differences in the calculations preceding the calculation of the cross spectra.

6.2.3 Results

Spontaneous breathing

An illustration of the analysis of 192 s (instantaneous) heartbeat interval and systolic arterial blood pressure signal is shown in figure 6-8.

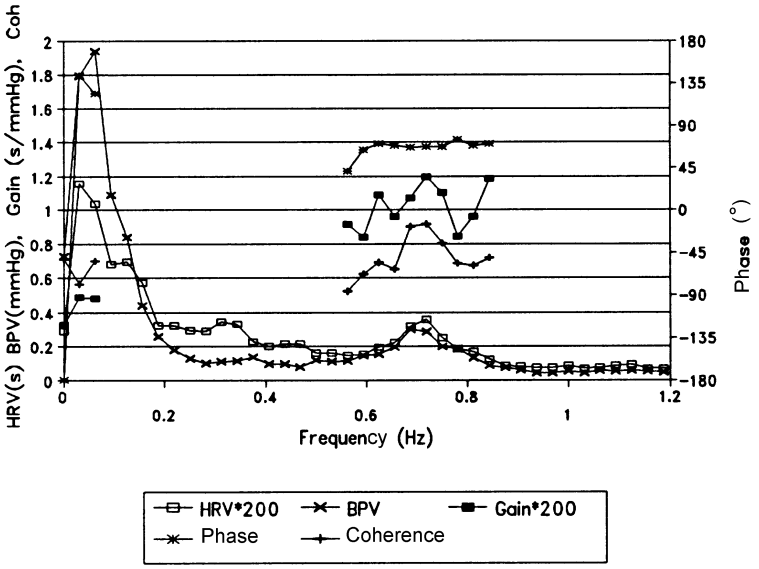

Figure 6-8 Example of a correlation spectrum of a spontaneous breathing neonate. The spectral amplitudes of heartbeat interval (HRV) and systolic blood pressure (BPV) are shown; gain, phase, and coherence between them are also plotted.

In figure 6-8 the amplitude spectra of the heartbeat interval and the blood pressure are shown. Also the gain, phase, and coherence are shown for all frequencies where the coherence function was higher than 0.5. Note that precisely two frequency bands, the HF (Traube-Hering) and LF bands (Mayer), meet the requirement of a "high" coherence. The gain in the HF band is about 0.005 s/mmHg, which means that a variation of 4 mmHg with respiration corresponds to a variation in heartbeat interval of 20 ms, which is within expectation [Koolen et al., in press]. The phase is about 70°, which implies that the blood pressure changes precede the heartbeat interval changes (given that the phase needs not be shifted by an integer times 360°) by about 70/360 times the respiratory interval. As can be seen from the figure, the respiratory frequency is about 0.7 Hz, giving an average respiratory interval of 1.4 s. Hence, the lag of the heartbeat interval changes with respect to the blood pressure changes amounts to about 0.28 s. In the LF band the gain is about 0,0025 s/mmHg and the phase about 135°. This phase refers to approximately 0.05 Hz waves, so the lag of the heartbeat interval with respect to the blood pressure changes amounts to about 7.5 s.

Mechanical ventilation

When a neonate is ventilated, a different characteristic pattern of interactions between blood pressure and heartbeat interval can be expected. A correlation spectrum of a ventilated neonate is plotted in figure 6-9. The width of the HF band, of course, is significantly smaller than in the spontaneous breathing case. The spectral amplitudes of the heartbeat interval and blood pressure in this patient in principle cannot be compared to those of the spontaneously breathing patient. The HRV turns out to be much lower than in the spontaneous breathing patient, certainly in the HF band. In the LF band no coherences larger than 0.7 were seen. The gain in the HF band is approximately 0,001 s/mmHg; the phase equals 0°. The fact that no lag seems to be present supports the assumption of a central and/or mechanical origin of the variations.

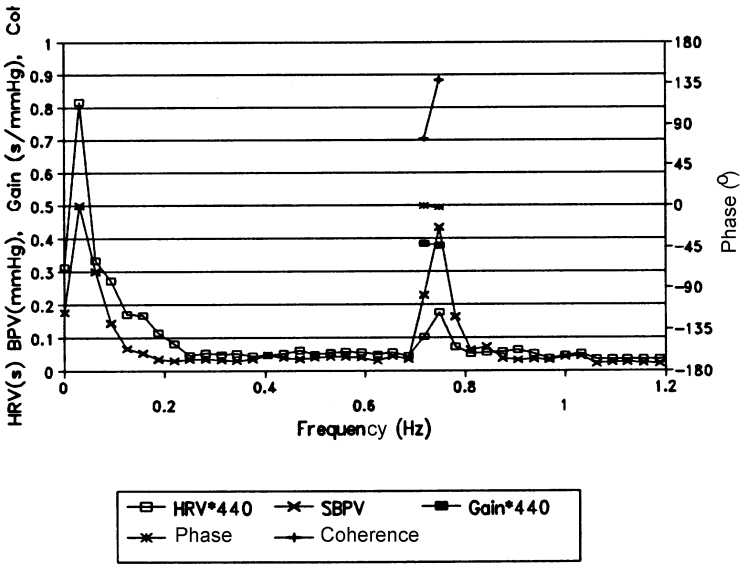

Figure 6-9 Example of a correlation spectrum of a ventilated neonate. The spectral amplitudes of the heartbeat interval (HRV) and the systolic blood pressure (SBPV) are shown; gain, phase and coherence between systolic blood pressure and heartbeat interval were also determined .

6.2.4 Discussion

The above data give an illustration of the cross spectral analysis of the heartbeat interval and the systolic blood pressure signals.

The results of the spontaneously breathing patient in figure 6-8 support the model in which the respiratory sinus arrythmia (RSA) is explained by the vagally mediated

baroreceptor reflex (see Section 2.2.1). At the respiratory frequency the coherence was high and a phase of 70°, corresponding to a delay of 0.3 s, was present. Blood pressure variability changes influence the heartbeat interval right after their occurrences (± 0.3 s delay). As the heartbeat interval is not a continuous variable, one can conclude that the time of occurrence of the next heartbeat is influenced by the blood pressure. Central vagal nerve activity to the SA-node, in relation to the phrenic nerve activity driving the respiration, can influence even more instantaneously the moment of occurrence of the (next) heartbeat. It is influenced then just before the respiratory activity takes place. The respiratory activity on its turn leads to mechanically induced blood pressure changes. This coincidence, also supported by Saul et al. [1991] and DeBoer et al. [1987], is nicely illustrated by the data of a ventilated patient in figure 6-9. It shows a phase of about 0° at the respiratory frequency. In adult volonteers Saul et al. found that above 0.25 Hz the mechanical influence of respiration on arterial blood pressure dominates the influence of RSA. From other investigations, however, it is clear that other interactions may occur. Taylor and Eckberg [1996], for example, found that RSA in adults can contribute to arterial blood pressure fluctuations, which is against the "current" expectations that RSA is caused by arterial blood pressure fluctuations.

In the LF band (Mayer) of the spontaneously breathing infant a phase of about 135° was found (0.05 Hz), corresponding to a lag of the heartbeat interval of 7.5 s with respect to the blood pressure changes. In the interpretation of this effect we have to be careful because of the fact that the phase value is based on only 2 frequency bins. DeBoer [1985] found in a young adult subject a phase of 70° at 0.1 Hz, which corresponds to a lag of the heartbeat interval of 2.0 s. The disagreement between this value and the 7.5 s we found might be attributed to the immature sympathetic nervous system of the neonate. The example is in agreement with the generally proposed model in which the fluctuations at the Mayer frequency are mediated by the (slow) sympathetic nervous system. The coherence of the spectra of the ventilated patient in this band was considered too low to draw definite conclusions.

Further investigations may contribute to the development and improvement of a model of the cardiovascular system and the neural mechanisms that apply. We can support the investigations in particular with data from (ill) neonates and "healthy" premature infants, that are - if required - measured over long time intervals.

Literature

Akselrod S; Power spectrum analysis of heart rate fluctuation: a quantitative probe of beat-to-beat cardiovascular control; Science 213:220-222, 1981

Akselrod S, Gordon D et al.; Hemodynamic regulation: Investigations by spectral analysis; Am J Physiol 249:H867-H875, 1985

Baselli G, Cerutti S ; Spectral and cross-spectral analysis of heart rate and arterial blood pressure variability signals; Comp Biomed Res 19:520-534, 1986

Bendat JS, Piersol AG; Random data, analysis and measurement procedures; New York: John Wiley, 1986

Boer de RW; Beat-to-beat blood-pressure fluctuations and heart-rate variability in man: physiological relationships, analysis techniques and a simple model; PhD thesis; University Amsterdam, 1985

Boer de RW, Karemaker JM, Strackee J; Hemodynamic fluctuations and baroreflex sensitivity in humans: a beat-to-beat model; Am J Physiol 253:680-689, 1987

Jenkins GM, Watts DG; Spectral analysis and its applications; San Fransisco: Holden-Day, 1968

Kitney RI, Rompelman O; The study of heart-rate variability. Oxford: Clarendon Press, 1980

Kitney RI, Fulton T, McDonald AH, Linkens DA; Transient interactions between blood pressure, respiration and heart rate in man; J Biomed Eng 7:217-224, 1985

Koolen AMP, Van den Aker JHL, Bartels LW, Bastin FH; Cardiovascular fluctuations and transfer function analysis of the circulation in healthy preterm infants; in press

Press, WH; Numerical recipes; Cambridge university press, 1988

Saul JP, Berger RD, Albrechts P, Stein SP, Chen MH, Cohen RJ; Transfer function analysis of the circulation: unique insights into cardiovascular regulation; Am J Physiol 261(4pt2):H1231-1245, 1991

Taylor JA, Eckberg, DL; Fundamental relations between short-term RR interval and arterial pressure oscillations in humans; Circulation 93:1527-1532, 1996

Veldman JBP, Mulder LJM, Mulder G, Heide van der D; Short-term coherence between blood pressure and heart-rate during mental loading: an exploration in the time- and frequency domain; Psychophysiology of cardiovascular control, 391-405

7. Final discussion

7.1 Data acquisition system

A data acquisition system has been developed to be able to eliminate the present restrictions on data exchange with the patient's monitors. In the young discipline of neonatology, systematic logging of normal values and systematic evaluation of medical treatment are common practice. These require an adequate infrastructure with respect to the patient measurement data. Furthermore, the vulnerability of the neonates prevents the medical staff from the measurement of many signals. So the need is felt to handle the available data as efficiently as possible.

Vendors of the monitor systems put more and more effort into the development of so called Patient Data Management Systems (PDMS), which allow not only the logging of all nursery, pharmaceutical, and other medical activities, but also logistic and order management functions. The benefit of these systems is evident, but the demand for them is still moderate, because of the investment that has to be made. Generally, these systems only acquire and review the bedside data; they hardly perform any additional analysis on the signals acquired from the patients. Many of the signals are not even stored at all.

More difficult is the development of a system that is able to analyse the signals and parameters that are continuously measured by the patient's monitor. The implementations of these functions are still subject of research. At the moment, some systems have become available, mainly in the field of cardiac monitoring. In this respect, it is important to know that the market of neonatal intensive care monitoring is much smaller than the market of general cardiac monitoring.

Another way of analysis of the measured signals is the acquisition by a Personal Computer. Nowadays, the power of PCs has grown to a sufficient level to be able to perform analysis on signals while they are acquired and stored. Many hospitals use such a stand alone "data-acquisition PC" to be able to acquire and analyse signals of one bed at a time. These PCs can also be connected to a network, enabling the use of the signals at other places.

We choose to set up a general data-acquisition system in co-operation with the Eindhoven University of Technology. Our development strategy combines the user friendly analysis possibilities of PCs and the scalability of a large modular general system. The combination of a general data-acquisition system and a standard PC network proves to combine the advantages of flexibility and scalability. The most important advantages of the system are the future possibilities to perform self-configured front-end processing and data reduction. Recently, the system has

been extended with another parallel sampler, combined with possibilities of real-time digital signal processing at the front end. These functions enable us to analyse all available signals measured from the neonates, while the huge data-flow of all the sampled values is restricted to the front end. Most of the computations will be performed at the dedicated PhyDAS system and only the results are put on the LAN. The set up of the system, and many of the measurements presented in this thesis were performed several years ago. The opportunity is present yet to evaluate the strategy and development of the system. The scalability and the modularity were obviously important: the number of parallel samplers has been doubled and a start has been made with the implementation of preprocessing using digital signal processors. With the implementation of a graphical user interface one of the "difficulties" of the system will be left behind. The available processing power and the use of memory have followed the market developments.
Steps in the direction of an expert system have not been taken yet. In my opinion, the connection with a broader oriented patient data management system (PDMS or an electronic patient record system), will be of more clinical importance in the near future.

7.2 Measurement of the signals

The measurement of blood pressure in neonates normally is done using a CMS. As we showed, this instrument has several disadvantages with respect to the blood pressure measurements, but is primarily used to take blood samples. A measurement using a tip catheter has a better dynamic performance (a transfer function close to 1, up to several hundred Hz). However, the very small catheters necessary in neonatal care are still very expensive. A clinical indication for them is not available: in most cases the blood pressure information of a CMS satisfies clinically.
As Van Langen [Van Langen, 1993] showed, many of the CMSs in clinical use have a resonance frequency below 30 Hz, and therefore give an inaccurate blood pressure wave form. The fairly bad condition of the CMSs was striking. Gevers [Gevers, 1994] determined by simulations the deformation of a sample blood pressure waveform, acquired under optimal conditions. From these results the conclusion can be drawn that systolic blood pressure values often will deviate by more than 5 % from the real values. If one wants to register accurate blood pressure values, the CMS should be checked at least every 6 hours, e.g., after each blood sampling procedure. The flush pulse method (see section 4.1.3) has been developed for this purpose, and the resulting natural frequency f_n and damping ζ can be calculated automatically. If desired, a deconvolution of the signal can be performed to reconstruct the signal to its form before entering the CMS. If one wants to use the blood pressure waveform, it is very important at what place in the body the measurement took place. An umbilical artery measurement will always be insufficient if frequencies above a few Hertz should be analysed. The initial filling procedure of the CMS can be adapted to obtain a better condition of the infusion fluid, giving a higher f_n and a lower ζ in the first hours of use. The flushing with alcohol and CO_2 and filling with specially

degassed infusion fluid is a time consuming procedure. Along with the fact that after several hours the blood sampling procedure may reduce the performance of the CMS to its usual level, we expect it is only worth to take this extra effort if one really needs the transfer of components above the 10 to 15 Hz commonly achieved. Because the characteristics of the CMS in clinical practice differ much from the ones in laboratory practice, the conclusions drawn from investigations of the CMSs in laboratory situations should be considered with reserve. An in situ check of the CMS is necessary to determine its transfer characteristics, and it can be performed using the flush-pulse method described in Section 4.1.3.

The artefact reduction algorithms that were developed for the different signals perform satisfactorily. However, as was described in chapter 4, some signal artefacts presently cannot be detected automatically. Hence, the signals usually are inspected visually before using them for further analysis. If real-time cross correlations on all measured signals can be performed, a significant better performance could be achieved as soon as we are able to develop an algorithm which is capable of detecting almost every artefact. It must always be taken into account, however, that it depends on what is expected or measured, whether or not a signal component will be labeled as an artefact. For example, thoracic pressure variations can be seen as an artefact or as extra information in the invasive arterial blood pressure signal. Just as with movement artefacts: they are present in the signal, and therefore truly present, but may disturb the clinically relevant information one wants to measure.

Measuring the beat-to-beat heartrate, one is concerned about the reliability and the accuracy of the heart intervals found from the analysis of the ECG available for the monitoring of the neonate. We use the heart beat information to investigate the variation in heart intervals resulting from nervous influences. These influences cause variations both in the interval between the onset of cardiac atrial depolarisation and the ventrical depolarisation and in the interval between the latter and the onset of the next heartbeat: P-R and R-P interval times. For practical reasons we choose the R-wave as the starting-point in the determination of the occurrence time of a heart beat.

The sampling error in the occurrence time of the R-wave has been reduced to $1/3^{th}$ of the original error using parabolic interpolation using 3 points around the maximum or minimum closest to the R-wave extreme. It was found that a higher order interpolation does not lead to a significant better estimate. We expect the use of a matched filter to give a slightly better result, because such a filter will optimally use the waveform of the QRS-complex. The disadvantage of the use of a matched filter is the large calculation capacity that is needed - in the near future this is no serious problem if parallel samplers with dedicated DSP utilities are used - and the continuous adaptation of the filter template to the current QRS-complex waveform that is required. Eventually, it depends on the accuracy with which one wants to assess the variability in heart rate whether the sampling error is within acceptable limits. Using 512 Hz sampling frequency our mean absolute sampling error will be

about ½* 0,98/3 = 0,16 ms. This is 0.04% of a mean heartrate of 150 beats/min. Related to the normal physiologic changes of several percents in a minute this is quite satisfactory.

7.3 Frequency domain analysis of the invasive arterial blood pressure signal

The frequency analysis of neonatal blood pressure signals differs in many respects from the analysis of signals from adults. In neonates:
- the frequencies of heartrate and respiration are normally much higher,
- the heartrate variability turns out to be less pronounced,
- the number of artefacts in the signals is higher than in adults.

Many studies have been done on heartrate variability in adults and neonates, some on blood pressure variability, but only a few on blood pressure variability in neonates.

The analysis methods used, mainly Fourier transform or a modification of it, and autoregressive model estimates, lead to a variety of representations of the results. All methods have their own characteristics, constraints, and assumptions. In time domain analysis many different indices have been proposed, often only to be used in specific circumstances.

The frequency domain methods seem more general; the autoregressive methods require certain model assumptions, like the order of the system. The main problems of the Fourier methods will be discussed in the next sections.

7.3.1 Aliasing

In our analysis the problem of aliasing occurs if the momentary respiratory frequency is higher than half the heartrate. In neonates this situation will occur regularly. The ratio of the respiratory frequency and heartrate in neonates is often higher than in adults. All Fourier techniques are hindered by a relatively high respiratory frequency. The Lomb method, which is able to handle non-equidistantly sampled signals, shows better results if the major part of the momentary sampling frequencies is larger than half the heartrate.
We found a more fundamental alternative in using the blood pressure filtering (BPF) technique. Using the full blood pressure signal, aliasing will occur only above 32 Hz (half the sampling frequency), which is far beyond our region of interest. The BPF technique is not a final solution. It introduces a problem that is related to the complexity of a physiological signal like the blood pressure signal. The blood pressure signal consists of pulses that result from different states of heart contraction under strongly changing internal physiological states. These physiological states vary with the heart frequency, and, as a result, they modulate the other variations in the blood pressure signal. Sum and difference frequencies will be present; the difference

frequencies being at the same frequency as the aliased frequencies from above half the heartrate when a Fourier technique is used. Using the BPF method, however, they can be explained by a real physical variation. Using one of the other methods, one should always check separately on the respiratory frequency to be attentive to possible spectral aliasing.

7.3.2 Spectral leakage

Spectral leakage implies the leakage of spectral power to neighbouring frequency bins, due to the (generally) non periodicity of the signal in the time domain. In most cases, the application of one of the standard lag-windows gives acceptable results. The HF frequency components we are interested in contain variations, which lead to a broadening of the concerned frequency components. The effect of leakage to the neighbouring bins in that case only marginally affects the result. The LF and VLF components, however, sometimes extend over only a few bins. In that situation one should be aware that the accuracy of the spectral components may decrease considerably.

7.3.3 Spectral equidistancy

A signal built of beat-by-beat parameters (a set of consecutive beat-by-beat values) is inevitably non-equidistant in time. In most of the neonatal signals, the consequences will not be dramatic. The 30% distortion of spectral components mentioned by TenVoorde [TenVoorde, 1994] does not apply to neonates because of their small respiratory sinus arrythmia (see section 5.4), and thus small frequency modulation of the sampling intervals of the beat-to-beat values. If the heartrate variability is larger, the error increases. We used neonatal data to evaluate the impact of the heartrate variability on the spectral components, using several different Fourier algorithms. Our conclusion is that the algorithms that specifically take into account the heart interval (EFT, RFT) give (slightly) different results, compared to the standard DFT/FFT algorithm. The standard DFT/FFT was applied such that the non-equidistancy was ignored. Many institutions follow that method; the boxcar integration *we* apply in the standard procedure introduces an extra filtering and resampling. The extra filtering reduces the aliasing of higher frequencies and enables us to resample equidistantly. The neonatal data we examined show only small differences with respect to the particular Fourier method chosen. Important is that the respiratory sinus arrhythmia, the main cause of the non-equidistancy of the beat-to-beat values, is much smaller in neonates than in adults.

7.3.4 Stationarity

Stationarity is an important item. If one wants to characterise certain spectral components, resulting from physiological processes in the body. If the underlying physiological processes change during the registration, qualitative characterisation will

sometimes be impossible, and quantitative characterisation will only be possible in proportion. Given the fact that all physiological processes in the body change in time, it is desired to limit the registration time to a period in which the body processes hardly change. A trade-off has to be made is between the accuracy of the measurement and the stability of the underlying processes. Physiological changes that we want to exclude from the measurements are, for instance,

- changes in the heartrate base level, e.g., caused by labour or mental stress
- changes in behavioural state or sleep state
- changes in the chemical state of the blood (e.g., pCO_2 level changes that drive many central processes)

Tools that check the data on stability should be developed. The clinician could then be informed automatically if the observed variations were the result of a changing process during the measurement. We suggest to use correlations between the signals to detect artefacts, but did not work out procedures by now.

7.3.5 beat-to-beat values versus the full sampled signal

Usually, beat-by-beat values are used in spectral analysis of the blood pressure variations. Originally, the main reason for this approach was that no calculation power was available to handle the frequency analysis of a full sampled signal, consisting of approximately 30 to 100 times as much data as the beat-by-beat values in a certain time interval. We showed that nowadays the limited calculation power no longer impedes the analysis of the full sampled signal. In that case, problems concerning aliasing and non-equidistancy do not exist any more. The graphs in chapter 5 show such results, and a comparison with the results of the analysis of a beat-to-beat signal. Theoretically, a significant improvement of the results should be obtained, if neither aliasing nor non-equidistant sampling would occur. Part of the improvement, however, is spoiled by the modulations expressed in the full sampled signal at sum and difference frequencies of the heartrate and respiratory rate. It will strongly depend on the application and signal characteristics which method will satisfy most.

7.4 Clinical applications

In chapter 6 three different calculations were carried out to determine the HF spectral amplitude in the invasive blood pressure signal every 90 seconds of a larger time interval. According to these three calculations, signals were formed by the resulting consecutive HF values in time. In many circumstances, these three signals show the same significant fluctuations. If the fluctuations in these signals did not correspond, in almost all cases an explanation could be found in a change of the respiratory band width. Therefore the hypothesis can be sustained that all three methods used to calculate the HF spectral components can be applied successfully. A choice can be made whether or not to emphasise respiratory fluctuations. Of course, this hypothesis

should be tested on more neonatal data sets. A relation between the spectral amplitudes and gestational age, age after birth, and behavioural state can be investigated in the future.

The assessment of the autonomic nervous system activity by the HF values is hampered by fluctuations of the respiratory frequency and the respiratory amplitude (depth). The future developments, that allow for real-time filtering with adaptive bandwidth filters, will resolve the problem of the fluctuating respiratory frequency: the actual respiratory frequency can be followed by an adaptation of the filter coefficients. The fluctuations of respiratory amplitude, however, will still influence the HF spectral amplitude, suggesting changes in the autonomic nervous system that do not exist. Part of the fluctuations in the HF signals, e.g., in the figures 6-4, 6-6 and 6-7 could be attributed to variations in the respiratory frequency. The impact of respiratory amplitude variations on the HF values should be investigated to be able to estimate their influence on the spectral amplitudes.

The determination of cross spectra between blood pressure and heart interval as presented in section 6.2 looks promising. The quantification of mutual interactions between blood pressure and heart interval will give us more insight in the origin of the interactions and may refine the underlying physiological model. Further measurements involving large and different patient groups will be required to be able to draw more definite conclusions on the physiological model.

Literature

Gevers, M; Arterial pressure wave forms in newborn infants; Thesis, Free University of Amsterdam, 1994

Langen van H, Brienesse P, Kopinga K, Wijn P; Dynamic response of a neonatal catheter-manometer system in situ; J Clin Monit 9:335-340, 1993

Summary

In a neonatal intensive care unit, care is given to very ill neonates, most of whom are prematures. In the prognosis and treatment of such neonates, both lung and brain conditions play an important role. The treatment of immature lungs has been significantly improved by a routine use of surfactant. The assessment of the brain function remains an important issue.
The patients are continuously monitored. Treatment is evaluated using data recordings from the monitors (vital signs) and intermittently obtained values (blood gases, weight, and defecation). The vital signs, however, are often disturbed by movement artefacts and cannot be measured as easily as in adult intensive care conditions. The evaluation of the condition of the patient and his or her treatment needs a reliable vital signs data set and effective use of the small number of signals measured. A physiological-data acquisition system, capable of real-time artefact reduction and analysis, combining data, and archiving of the measurements, is necessary to optimise the information on the condition of the patient.
Such an acquisition system would allow - for example - the assessment of additional information present in the invasive arterial blood pressure signal. In this thesis a strategy to quantify the low frequency blood pressure components, related to lung mechanics, brain and nervous functions, is described. Two applications, built on this strategy and made for use in neonatal practice, are presented and evaluated.

Physiology

The origin of the blood pressure signal, and the variations on it, can be found in the physiology of the cardiovascular system. The understanding of basic physiological interactions is necessary to be able to develop derivated parameters with clinical importance. In this thesis we focussed on the interactions in which the nervous system is involved; the humoral influence was not a part of the investigations. The nervous system can be divided into the voluntary nervous system and the involuntary nervous system, also called the autonomic nervous system. The latter again consists of 2 parts, generally responsible for an opposite effect: the sympathetic and the parasympathetic system. They are essential in the regulation of the blood pressure: the sympathetic system influences the heart contractility, heart frequency, and peripheral blood vessel constriction, while the parasympathetic system influences the heart frequency almost directly. The neural interaction is driven by baroreceptors at several locations in the cardiovascular system and by the activity of the central respiratory centre. Apart from the neural respiratory influences, a direct interaction exists which results from the intrathoracic pressure variations related to the respiration.

Data acquisition system

A physiological information system, capable of acquisition of all data from the patient's monitors, processing and analysis of that data, and providing a user-friendly output of the results, is required to fulfil the objectives of section 1.3. For the acquisition of the signals it was basically chosen to take the signals of the patient's monitors. They are available continuously and can be taken without interfering with the patient care. The PhyDAS system, a real-time data acquisition system developed at the Eindhoven University of Technology, was used for the continuous processing of the incoming signals. It is connected to a PC-LAN, where further off-line analysis takes place, and data can be graphically displayed. The off-line analysis was distributed to an arbitrary number of PCs connected to the LAN segment in order to increase the computer capacity to a desired level. The next step in the development strategy will be the implementation of pre-processing and real-time filtering at the front end of the parallel sampling units. All data is archived automatically using a cyclic buffer with capacity of 3 days in case of signals and 50 days in case of parameters.

Measurement of the signals

The main signals needed for the monitoring of the neonatal patient have been described: the blood pressure, the electrocardiogram (ECG), and the respirogram. Except for the blood pressure signal, they are recorded from every patient. The catheter manometer system, through which the invasive blood pressure measurements take place, is discussed. The flush pulse method was made applicable to the real-time measurements to determine the frequency characteristics of the catheter manometer system. Also, the automatic detection of the individual blood pressure waves is described.
The acquisition of the ECG signal and the way it is used are described. The determination of the occurrence time of a heartbeat is discussed and a way of fitting the sampled signal enabling a better determination of the maximum or minimum of the ECG signal.
The thoracic impedance signal used for standard monitoring was analysed together with the ECG signal to be able to detect (central) apnea periods properly. It was demonstrated that the current algorithm to deduce the respiratory frequency was not sufficient to detect apnea periods properly. A thermistor measuring nasal air flow was used to evaluate the algorithm we developed.

Frequency domain analysis of the invasive blood pressure signal

The analysis of the invasive blood pressure is useful because of the high amount of information it contains: not only the beat-to-beat blood pressure values, but also natural lower frequency fluctuations that occur in these values. These fluctuations are related to the respiratory mechanics and to interactions mediated by the autonomic nervous system.

The quantification of these fluctuations in a series of systolic or diastolic blood pressure values by spectral analysis is more complicated than in the case of standard sampled signals, because of modulation by the heart rate. A model exists in which the non-equidistant sampling has been taken into account, but conclusions drawn from the model only apply to adults. It was shown, as a result of the little respiratory sinus arrythmia in neonates, that the impact of the frequency modulation component on neonatal data was less strong than in the adult case. The analysis results of the algorthms that take into account the frequency modulation differ little from the normal DFT algorithm results.
Finally, the presented model was compared to a direct frequency analysis method, starting from the full blood pressure signal instead of systolic or diastolic values. After low-pass filtering of the signal, Fourier analysis is performed on a true equidistantly sampled signal.The differences compared to the filtered signal and compared to the Lomb algorithm are significant. Using the filtered signal, the Nyquist limit of "half the mean heartrate" no longer applies. The Lomb algorithm seems to give a better spectral amplitude estimate at frequencies where higher order harmonics would occur.

Clinical applications

On the basis of two examples, the application of the system and the measurement methods are illustrated:

1. the realisation of continuously available spectral estimates;
2. a first order quantification of the relationship between blood pressure and heartrate.

A continuous presentation of the spectral estimates, discussed in detail in chapter 5, has not been realised yet. The availability of HF and LF spectral amplitude estimates over a longer period of time, however, may present extra information about the "internal" neuro-cardiovascular state of the patient. A method is worked out to estimate the HF spectral amplitude continuously, using the the blood pressure spectral components at the actual respiratory frequency band. The results of five time intervals show that the HF estimates vary significantly in time, although no external actions or disruptions took place. This suggests that the values may contain valuable new information about the internal state. A method for the LF spectral amplitude can be developed in an analogous way.

In the evaluation of a physiological model of the interactions between blood pressure, respiration, and heartrate, quantification of the relation between them is needed. We present a way to calculate the corresponding cross spectra and show how a coherence function between them can be interpreted. Two representative examples show that the interaction is particularly present in the LF and HF regions. The use of this analysis on different patient groups in different physiological states may improve the model description of the cardiovascular system.

Samenvatting

Op de Neonatale Intensive Care Unit (NICU) van het Sint Joseph Ziekenhuis, Veldhoven worden ernstig zieke en premature pasgeborenen behandeld en verzorgd. Voor het bepalen en evalueren van een optimale behandeling is o.a. het volgen van long- en hersenfuncties van grote betekenis. Impliciet zijn resultanten van long- en hersenfuncties traceerbaar in enkele standaard beschikbare bewakingssignalen zoals het arteriële bloeddruksignaal, het elektrocardiogram en het respirogram. De kennis van de onderliggende overdrachtsfuncties en de beschikbaarheid van deze impliciete informatie kunnen echter nog sterk worden verbeterd.

Alvorens onderzoek kon worden verricht naar de potentiële bruikbaarheid van deze impliciete informatie is een systeem opgezet waarmee de fysiologische signalen van de bewakingsmonitoren continu konden worden ingelezen en verwerkt en waarmee tevens, naar behoefte, extra signalen of parameters konden worden toegevoegd. De kern van dit systeem wordt gevormd door PhyDAS: een real-time data-acquisitie en -verwerkings unit, ontwikkeld door de Technische Universiteit Eindhoven. PhyDAS heeft een gebruikersvriendelijke user interface en is enerzijds gekoppeld aan alle bewakingsmonitoren op de NICU en anderzijds aan een PC-netwerk voor databeheer en verdere data-analyse. Vanwege de modulaire opzet is het systeem flexibel toepasbaar en/of uitbreidbaar.

De onderliggende fysiologie en de signaaleigenschappen van de standaard bewakingssignalen worden uitgebreid besproken. Voor elk signaal wordt een beschrijving gegeven van de wijze waarop het signaal wordt verkregen, op artefacten gescreend en geanalyseerd. Bij de meting van het respirogram wordt tevens een eigen nasale luchtflowmeting geï ntroduceerd, waarmee met name de betrouwbaarheid van de detectie van apnoea perioden aantoonbaar kon worden verbeterd.

Het onderzoek spitst zich toe op het invasieve bloeddruksignaal, waarin effecten van de ademhaling en interacties van het autonome zenuwstelsel zijn terug te vinden. Als methode voor quantificatie van deze effecten wordt uitgegaan van de beat-to-beat systolische bloeddrukwaarden welke aan een frequentie-analyse worden onderworpen. Complicerende factoren zijn daarbij het feit dat de betref-fende beat-to-beat waarden geen equidistant gesamplede dataset opleveren (vanwege de hartritme-variabiliteit) en dat bij een hoge respiratiefrequentie het Nyquist criterium wordt geschonden. Een aantal alternatieve methoden, waaronder de filtering van het volledige gesamplede signaal, worden uitgewerkt en de resultaten van verschillende toepasbare methoden van frequentieanalyse worden op een aantal neonatale datasets geëvalueerd. Geconcludeerd kan worden dat bij hoge respiratiefrequen-ties filtering van het volledige gesamplede signaal de voorkeur verdient boven beat-to-beat analyse en dat bij prematuren de mogelijke afwijkingen ten gevolge van het niet equidistant zijn van de beat-to-beat waarden relatief gering zijn.

Afsluitend worden twee klinische toepassingen uitgewerkt. De eerste betreft het continu toepassen van de bovengenoemde analysemethode op voor langere tijd geacquireerde signalen. De spectrale inhoud van verschillende van belang zijnde frequentiebanden (HF en LF gebieden) kan zo continu als functie van de tijd worden weergegeven. De resultaten hiervan worden getoond op een aantal neonatale meetsets. Zij laten een grote verscheidenheid aan variaties zien, waarnaar nader onderzoek gewenst is. Als tweede onderdeel wordt met behulp van kruisspectra en de coherentiefunctie de relatie tussen bloeddrukvariabiliteit en hartritmevariabiliteit onderzocht. Twee representatieve voorbeelden laten zien dat juist in de HF en LF gebieden van het spectrum een significante interactie tussen de variabiliteit van beide signalen bestaat.

Dankwoord

Dit proefschrift is het resultaat van een aantal jaren ontwerpen, meten en onderzoeken van meetgegevens die worden verzameld rondom pasgeborenen op de neonatale intensive care afdeling van het Sint Joseph Ziekenhuis Veldhoven. Het zal duidelijk zijn dat bij een dergelijk proces zeer velen betrokken zijn en het ondoenlijk is ieder die eraan heeft bijgedragen persoonlijk te noemen. Ik kijk in elk geval terug op een heel plezierige samenwerking met de vele verpleegkundigen, artsen, assistenten in opleiding en studenten voor de kleine (en grote) werkzaamheden die in het kader van dit onderzoek zijn uitgevoerd. Iedereen wil ik hierbij bedanken voor de goede samenwerking.
Een aantal mensen wil ik hierna toch in het bijzonder bedanken.

Pieter Wijn, 1ste promotor en voor mij toch vooral opleider tot klinisch fysicus. Pieter, jij was het die tijdens mijn opleiding suggereerde de vele lopende stage- en afstudeerprojecten te gebruiken als basis voor een promotie-onderwerp. Ondanks de moeilijkheden die ik regelmatig had om de grote hoeveelheid beschikbare meetgegevens binnen een zinvol kader te interpreteren en de neiging om keer op keer zijpaden in te slaan die het beeld nog completer moesten maken, heb je mij ervan overtuigd dat de kracht meer ligt in de beperking dan in het reeds invullen van mogelijk vervolgonderzoek.

Klaas Kopinga, 2de promotor, ben ik veel dank verschuldigd. Klaas, als er iemand is die zowel op detail niveau als op structuur niveau veel heeft bijgedragen dan ben jij het wel. Jouw gestructureerde benadering en duidelijke bijdrage om ook de vager geformuleerde klinische onderzoeken van een degelijke wetenschappelijke basis te kunnen voorzien heb ik zeer gewaardeerd. Op het gebied van data-acquisitie, digitale filtering en signaalanalyse hebben we uitgebreide discussies gevoerd over de mitsen en maaren van het toepassen van niet-standaard methoden. Dat het proefschrift door die inbreng flink is "opgehard", wil overigens niet zeggen dat je daarbij weinig oog had voor de klinische vraagstelling en fysiologische achtergronden. Integendeel. Ook je vele suggesties m.b.t. de formulering hebben de leesbaarheid zeer positief beï nvloed.

Martin de Voigt en Geert-Jan Tangelder wil ik bedanken voor het lezen en beoordelen van het manuscript en Geert-Jan tevens voor zijn inbreng in een eerder stadium op het gebied van de fysiologische achtergronden van de invloed van ademhaling en/of beademing op de bloeddruk. Ook Carlos Blanco wil ik bedanken voor de oriënterende contacten die er vooral in de eerste fase van dit onderzoek zijn geweest.

Binnen het ziekenhuis wil ik met name mijn collega's van de afdeling Klinische Fysica bedanken. Tenslotte was dat de afdeling waar ik toe behoorde en de meeste tijd doorbracht. Naast Pieter Wijn heeft Herman van Langen in de eerste jaren dat ik

als klinisch fysicus in opleiding werkzaam was veel aan het neonatologie project gewerkt. Herman, vele van de keuzes die de eerste jaren gemaakt moesten worden voor de ontwikkeling van het meetsysteem en de klinische toepassingen hebben we toen intensief besproken. Jouw inbreng heeft voor een belangrijk deel bepaald wat in dit proefschift is beschreven. Verder wil ik graag Fred Benning bedanken, met wie ik vooral veel samenwerkte voor de andere onderdelen van de opleiding. We waren goed op elkaar ingespeeld en we kregen veel voor elkaar. Met Frank Bastin, opvolger van mij in het NICU project heb ik vanuit Tilburg nog intensief contact gehad over alles in de ruimste zin van het woord. Frank, bedankt voor de vele dingen (van meedenken over filterkarakteristieken tot files met meetgegevens) die je me aanreikte ten behoeve van dit werk. Het maakte voor mij de afstand tussen Tilburg en Veldhoven toch een stuk kleiner. Rian, secretaresse van de afdeling, wist naast het werk altijd de nodige afleiding te bieden. Afwisselend mokkend en mopperend, maar meestal de vrolijke en trotse moeder van Björn en Britt, die als geen ander leek te begrijpen hoe ik als persoon in elkaar zat. Onze gezamenlijke "roots" in Tilburg hebben daar misschien ook toe bijgedragen.

De afdeling Neonatologie was natuurlijk een afdeling waar ik vaak vertoefde. Ik wil daar met name André Koolen bedanken. André, na een periode waarin het enigszins onduidelijk was hoe Klinische Fysica en Neonatologie invulling zouden geven aan de onderzoeksmogelijkheden op de NICU, ben jij daarin een steeds belangrijker rol gaan spelen. Ik wil je graag bedanken voor de medische inbreng in de lopende projecten, het meedenken over onderzoeksvragen en het uitvoeren van vele metingen/registraties. Je altijd kritische benadering heeft ons bij de interpretatie van meetgegevens en statistiek scherp gehouden. Mede dankzij jouw inbreng is de onderzoekslijn steeds verder uitgekristalliseerd. Ook de andere neonatologen, Martin de Kleine, Jan Buijs en Germa van de Kamp wil ik bedanken voor de goede samenwerking. Dat geldt ook voor de vele assistenten die delen voor hun rekening hebben genomen met specifiek klinische vraagstelling, maar waarvan de metingen ook ten behoeve van dit werk zijn gebruikt. Met name wil ik daar noemen Monique Trijbos-Smeulders, Rachel Agbeko, Rene van Gent en Janet van den Aker. Ook de verpleegkundigen die altijd behulpzaam waren als rond het bed iets moest gebeuren of juist niet!

Op de Technische Universiteit Eindhoven viel ik vaak terug op bestaande contacten met de Werkgroep Laboratoriumautomatisering, vooral als het ging om het implementeren van nieuwe componenten binnen het PhyDAS. Ik wil daar speciaal Fred van Nijmweegen, Roel Smeets, Leon van Houten en Huib Schouten bedanken. De vele gesprekken over de gebruikerseisen en de terugkoppeling na ingebruikname van onderdelen hebben ons uiteindelijk op het punt gebracht dat het systeem goed bruikbaar was en voldeed aan de mooie theoretische uitgangspunten. Hoewel ik soms het niveau, waarbij een paar maal zelfs stukjes assembler geï ncludeerd moesten worden, wel erg 'dicht bij de machine' vond komen was ook die ervaring een nuttige

waar ik met plezier op terugkijk (evenals trouwens de bij jullie gebruikelijke kerstborrel waarover ik hier niet verder zal uitwijden).

Verder wil ik de vele stagiares en afstudeerders bedanken die een steen(tje) hebben bijgedragen aan dit proefschrift. Het feit dat gemiddeld vaak meer studenten aanwezig waren dan medewerkers binnen de afdeling schiep veel ruimte voor wetenschap en nieuwe ontwikkelingen. Vele studenten hogere informatica hebben hun bijdrage geleverd aan de user interface en besturing van het PhyDAS, vele studenten van de TU hebben aan een meer klinische vraagstelling gewerkt. Een aantal van hen wil ik met name noemen: Hugo Spruijt (een van de eersten die vol enthousiasme de respiratie-specifieke methode-nul ontwikkelde; moeilijk, adaptief en sterk niet lineair); Patrick Brienesse (bloeddrukmetingen en het Catheter Manometer Systeem); Jan Schellekens (bloeddruk metingen en ademhalingsinvloed daarop); Mark Sabel (jouw inbreng leidde tot beter beschrijfbare methoden om ademhaling uit de bloeddruk te filteren; je ontwikkelde de eerste filters voor het druksignaal als geheel, je bouwde de schakeling waarmee we succesvol ademhaling konden registreren met een thermistor. Ik zal ook nooit vergeten hoe we samen frustraties over de voortgang uitleefden door de eerste analoge kabel over het plafond vanuit de care-ruimte naar onze meetruimte te leggen. Eenmaal op het matje geroepen heb ik moeten benadrukken dat het hier toch alleen om een tijdelijke oplossing ging, die achteraf overigens meer dan een jaar zou duren); Bernard van Vlimmeren (project PhyDAS weer op schema en de eerste analoge signalen parallel in real-time…); Guido D'hert (mechanisme doorgifte ademhaling op de bloeddruk, monitorsignalen bij een apnoea); Peter de Munck (variabiliteit in bloeddruk en hartritme); Hans Stoorvogel (implementeren automatische check met flush pulse methode, Fourier algoritmen en ontwerp directe filtering van het gehele bloeddruksignaal. Hans, jouw inbreng bij het toepassen van de verschillende algoritmen en filtertechnieken had ik niet willen missen); Sigrid Horsten; Marc Roelands; Marco van Uden; Guido ter Horst; Judith Bastiaanssen en Mark Manders.

Verder wil ik graag de medewerkers van de afdeling Medische Techniek bedanken voor de goede samenwerking. Paul Rieter die als hoofd zeer betrokken was en er altijd voor open stond om mee te denken en een oplossing te zoeken. Noud Heuvelmans, die veel uren beschikbaar was voor dit project en behalve voor de techniek bij nieuwe ontwikkelingen ook een steeds grotere rol kreeg t.b.v. de continuï teit. Frank Bayens, die op het gebied van software ontwikkeling de nodige bijdragen heeft geleverd. En tenslotte Rini Brok, bij wie ik altijd terecht kon voor afstemming en planning.

Op het gebied van werkgroepen wil ik nog graag de Werkgroep Klinische polygrafie bij kinderen bedanken. Aan de discussies binnen die groep heb ik veel gehad. In dit verband wil ik ook Lennie Gevers bedanken voor de uitwisseling van ervaringen op het gebied van arteriele bloeddrukmeting en bloeddrukgolfvormen.

Voor de ondersteuning op het gebied van 'rust', stimulerende woorden en niet op de laatste plaats literatuur heb ik veel waardering voor de medewerkers van de medische bibliotheken in het St. Joseph en in het St. Elisabeth: Marion Heijmans en Henriëtte van de Griendt, bedankt voor het opzoeken van zo vele artikelen en voor jullie belangstelling; Nora Mathilda en Godelieve Engbersen, ook jullie bedankt voor het vele speurwerk, de opbeurende woorden die ik wel eens kon gebruiken en voor het doorspitten van mijn literatuuropgaven.

Ook de andere medewerkers binnen het St. Elisabeth Ziekenhuis die hulp aanboden en belangstelling toonden hebben me geholpen vol te houden op de moeilijke momenten (Mariëtte Vonk, bedankt). Speciaal wil ik daar noemen Gerrit Gielen, die altijd paraat was als de tekstverwerker, scanner of ander aan Windows gekoppeld product weer eens niet deed wat een normaal mens ervan verwachtte. De medewerkers van de functieafdeling en van de afdeling KNF (jullie zagen me de laatste tijd steeds minder en minder). Nico Meijer en wijlen Henk van Erp wil ik bedanken voor de gesprekken over wetenschap, niet-wetenschap, gezin en de (onmogelijke) combinatie van dat alles.

Naast deze zakelijke contacten wil ik graag de vrienden, vriendinnen en kennissen bedanken die mogelijk tegen hun wil (in elk geval tegen de mijne) de frequentie van onze contacten sterk hebben zien teruglopen. Ik ga ervan uit dat ik hier in de komende tijd weer wat goed kan maken. Judith, Herman, Evelyne, Hanneke, Marloes, Herman en vele anderen: Bedankt voor het initiatief dat jullie soms moesten nemen om contact te houden. Ook de gastouders Brigitta Feijen en Carla van Kessel wil ik bedanken voor de uitstekende opvang van onze kinderen.

Mijn ouders wil ik bedanken voor hun ondersteuning, zowel materieel als immaterieel. Het was en is belangrijk jullie waardering voor mijn werk en ons gezin te voelen, ongeacht de eventuele prestaties op dat gebied. Gerben, je hebt me de laatste tijd niet veel gezien. We zullen snel weer eens een weekend afspreken.

Tjitske en Joris, ook jullie hebben me de laatste tijd wat teveel moeten missen. Op de dagen dat ik er als papa voor jullie was kon ik de waarde daarvan goed merken. Tjitske, samen de appie in met jou blijft een genot. Joris, jouw kopjes blijven een prachtig fenomeen.

Lieve Joke, zonder jouw inzet om voor mij ruimte te maken voor dit werk was het nu niet zover geweest. De laatste paar jaar waren niet gemakkelijk. Ik kon aan alles merken dat ik eigenlijk vaker thuis nodig was dan een combinatie van werk en promotie toeliet. Ik hoop dat we nu, na de promotie en met steeds minder luiers, weer meer tijd voor elkaar krijgen.

Curriculum vitae

Wim de Jong werd geboren op 4 januari 1962 te Rotterdam. Hij deed in 1980 eindexamen gymnasium β aan het St. Joriscollege te Eindhoven, waarna hij natuur-, wis- en sterrenkunde ging studeren aan de Katholieke Universiteit Nijmegen. In 1983 behaalde hij kandidaatsexamens in deze vakken; in 1989 is hij afgestudeerd in de experimentele natuurkunde in de richting medische fysica en biofysica. Aansluitend heeft hij als medisch fysicus aan de Faculteit Geneeskunde van de KU-Nijmegen een onderwijsmodule op het gebied van computersimulaties ontwikkeld ten behoeve van het curriculum Gezondheidswetenschappen.
In 1990 begon hij de opleiding tot klinisch fysicus binnen een samenwerkingsverband tussen het Sint Joseph Ziekenhuis Veldhoven en de Technische Universiteit Eindhoven. In 1992 sloot hij de korte onderzoekersopleiding klinische fysica af (TU-gedeelte van de opleiding) en in 1994 verkreeg hij de registratie als klinisch fysicus. Aansluitend heeft hij een tijdelijke aanstelling binnen het St. Joseph Ziekenhuis gehad ten behoeve van dit promotieonderzoek. Sinds 1995 werkt hij als algemeen klinisch fysicus in het St. Elisabeth Ziekenhuis Tilburg.